

**OXIDATIVE CYCLIZATION OF
PHENOLIC *N*-ACYL SULFONAMIDES**

by

Xueqing Wang

B.Sc., The University of British Columbia, 2015

A THESIS SUBMITTED IN PARTIAL FULFILLMENT OF
THE REQUIREMENTS FOR THE DEGREE OF

MASTER OF SCIENCE

in

THE FACULTY OF GRADUATE AND POSTDOCTORAL STUDIES
(Chemistry)

THE UNIVERSITY OF BRITISH COLUMBIA
(Vancouver)

April 2017

© Xueqing Wang, 2017

Abstract

The oxidative activation of appropriately substituted phenols with a hypervalent iodine reagent, in the presence of suitable nitrogen nucleophiles, results in formation of 2- or 4-amidodienones. The process is described as the oxidative amidation of phenols. The dienones thus produced are useful building blocks for the synthesis of alkaloids. The nitrogen nucleophile may be an oxazoline, a sulfonamide or phosphoramidate (intramolecular reactions), or a nitrile (bimolecular reaction), but not a carboxamide. This is because carboxamides express O-nucleophilicity toward oxidatively activated phenols, resulting in formation of iminolactones, which are readily hydrolyzed to lactones upon workup.

This present thesis describes efforts to extend oxidative amidation chemistry to carboxamides. The behavior of phenolic *N*-acyl sulfonamides was thus explored. The product obtained upon oxidative cyclization of these substrates proved to be dependent upon their structure. In many cases, *N*-sulfonyl iminolactones were thus obtained. These heretofore undocumented products proved to be surprisingly stable and resistant to hydrolysis.

Preface

The present thesis was written by X. Wang, as a result of the research conducted in the laboratories of Professor M. A. Ciufolini.

Prof. M. A. Ciufolini also provided the project design and recommendations through the course of the studies, carried out the Molecular Mechanics calculation using MM+ program provided with the HyperChem® software, and thoroughly edited the current manuscript. X. Wang was responsible for all experiments and analysis of research data unless otherwise specified.

The preparation of compound **2.29** was described in: Mendelsohn, B. A.; Lee, S.; Kim, S.; Teyssier, F.; Aulakh, V. S.; Ciufolini, M. A. *Org. Lett.* **2009**, *11*, 1539, and was previously prepared by S. Xu in our laboratory. D. Tang conducted preliminary study on the formation of compound **3.13d** using a different procedure illustrated in Chapter 3.1.

Table of Contents

| | |
|---|-------------|
| Abstract..... | ii |
| Preface..... | iii |
| Table of Contents | iv |
| List of Tables | vi |
| List of Figures..... | vii |
| List of Schemes..... | viii |
| List of Abbreviations | x |
| Acknowledgements | xiv |
| Dedication | xvi |
| Chapter 1 Introduction | 1 |
| 1.1 Oxidative amidation of phenols | 1 |
| Chapter 2 Background | 8 |
| 2.1 Tetrodotoxin via the bimolecular oxidative amidation of a phenol | 8 |
| 2.2 Logic behind the present investigation and objectives thereof | 11 |
| 2.3 Early examples of oxidative cyclization of phenolic <i>N</i> -acyl sulfonamides | 15 |
| Chapter 3 Discussion | 17 |
| 3.1 Preperation of phenolic <i>N</i> -acyl sulfonamides | 17 |
| 3.2 Oxidative cyclization of phenolic <i>N</i> -acyl sulfonamides | 20 |
| 3.3 Determination of the maximum allowable reaction concentration | 23 |
| 3.4 Cyclization of a tyrosine-derivative substrate and rearrangement of the product | 25 |
| 3.5 Spectral properties of presumed 3.14 vs. those of other spirocyclic compounds | 28 |
| Conclusion | 35 |

| | |
|--|------------|
| References..... | 36 |
| Appendices..... | 39 |
| Appendix A: Experimental Sections..... | 39 |
| A.1 Sequence to various sulfonyl-iminolactones from 3.1 | 41 |
| A.2 Sequence to various sulfonyl-iminolactones from 2.29 | 42 |
| A.3 Preparation of compound 3.7 | 43 |
| A.4 Preparation of compound 3.8 | 43 |
| A.5 Preparation of compound 3.9a - 3.9f | 44 |
| A.6 Preparation of compound 3.10a - 3.10f | 44 |
| A.7 Preparation of compound 3.13a - 3.13f | 45 |
| A.8 Preparation of compound 3.15 | 45 |
| A.9 Preparation of compound 3.16 | 45 |
| A.10 Preparation of compound 3.17 | 46 |
| A.11 Preparation of compound 2.30 | 46 |
| A.12 Preparation of compound 3.19 | 47 |
| A.13 Preparation of compound <i>rac</i> - 3.18 | 47 |
| Appendix B: Experimental Data and NMR Spectra | 48 |
| B.1 Experimental data of various intermediates to sulfonyl-iminolactones 3.13 | 48 |
| B.2 Experimental data of tyrosine-derivatives for rearrangement | 102 |
| Appendix C: X-ray Diffractory Data | 120 |
| C.1 X-ray data for compound 3.18 | 120 |
| C.2 X-ray data for compound 3.13a | 123 |

List of Tables

| | |
|---|----|
| Table 3.1 Yields of compounds shwon in Scheme 3.3 | 19 |
| Table 3.2 Oxidative cyclization of phenolic <i>N</i> -acyl sulfonamides | 21 |
| Table 3.3 Oxidative cyclization of <i>N</i> -acyl sulfonamide 3.10a at variable concentrations | 24 |
| Table 3.4 Comparison of ¹³ C chemical shifts of the products of oxidative cyclization obtained in this study with those of authentic spirolactams | 30 |

List of Figures

| | |
|--|----|
| Figure 2.1 Structure of tetrodotoxin, 2.1 | 8 |
| Figure 2.2 X-ray structure of compound 2.43 | 16 |
| Figure 3.1 X-ray structure of compound 3.18 | 27 |
| Figure 3.2 NOESY spectrum of the product of oxidative cyclization of 2.30 | 28 |
| Figure 3.3 Determination of carbon atoms <i>a</i> and <i>b</i> in the products of oxidative cyclization..... | 29 |
| Figure 3.4 X-ray structure of compound 3.13a | 31 |
| Figure 3.5 Probable structure of compound 3.19 | 32 |
| Figure 3.6 Calculated (MM+) steric energies of diastereomers 3.24 and 3.25 | 34 |

List of Schemes

| | |
|--|----|
| Scheme 1.1 General mechanism of oxidative amidation of phenols | 1 |
| Scheme 1.2 An example of first-generation oxidative amidation reaction..... | 2 |
| Scheme 1.3 Retrosynthesis of FR-901483..... | 3 |
| Scheme 1.4 Kita's attempt on oxidative activation of phenolic amide | 3 |
| Scheme 1.5 Similar difficulties in Knapp's alkene iodolactamization study | 4 |
| Scheme 1.6 Resonance interactions within the carboxamide and the imide | 4 |
| Scheme 1.7 An example of <i>para</i> -oxidative amidation reactions: Synthesis of (-)-cylindricine C. | 5 |
| Scheme 1.8 Examples of <i>ortho</i> -oxidative amidation reactions | 6 |
| Scheme 1.9 An example of oxidative amidation reactions in a bimolecular mode..... | 6 |
| Scheme 2.1 Xu's Synthesis of <i>rac</i> -TTX: preparation of advanced intermediate 2.8 | 8 |
| Scheme 2.2 Inverted transformations in the desymmetrization of the diene | 9 |
| Scheme 2.3 Stereoselective assembly of the DuBois TTX precursor | 10 |
| Scheme 2.4 Possible diastereoselective cyclizations | 11 |
| Scheme 2.5 Proposed synthesis of an enantioenriched form of TTX precursor 2.6 | 12 |
| Scheme 2.6 Proposed cyclization and desymmetrization from <i>N</i> -acyl sulfonamide 2.24 | 12 |
| Scheme 2.7 Retrosynthesis of an appropriate <i>N</i> -acyl sulfonamide..... | 13 |
| Scheme 2.8 Two possible diastereomers of cyclization products from 2.31 | 13 |
| Scheme 2.9 Conversion of lactone 2.33 to TTX intermediate 2.8 | 14 |
| Scheme 2.10 Formal formation of a carboxamide via excision of the sulfonyl group | 14 |
| Scheme 2.11 Attempted oxidative cyclization of <i>N</i> -acyl sulfonamide 2.38 | 15 |
| Scheme 2.12 An example of oxidative cyclization of naphthalic sulfonamides | 15 |
| Scheme 3.1 Tang's procedure for the preparation of <i>N</i> -acyl sulfonamide 3.5 | 17 |

| | |
|--|----|
| Scheme 3.2 Preparation of mono-TBDMS protected acid 3.8 | 18 |
| Scheme 3.3 Preparation of phenolic <i>N</i> -acyl sulfonamides 3.10 | 18 |
| Scheme 3.4 Undesired formation of spirolactone 1.16 | 20 |
| Scheme 3.5 Attempted oxidative cyclization of phenolic <i>N</i> -acyl sulfonamide | 21 |
| Scheme 3.6 A possible mechanistic pathway for the formation of spirolactone 1.16 | 22 |
| Scheme 3.7 Anticipated hydrolysis of <i>N</i> -sulfonyl iminolactone 3.13 | 22 |
| Scheme 3.8 Proposed diastereoselective rearrangement of presumed spirolactam 3.14 | 25 |
| Scheme 3.9 Synthesis of presumed tyrosine-derived spirolactam 3.14 | 26 |
| Scheme 3.10 Attempts to induce the transposition of 3.14 to 2.32 | 27 |
| Scheme 3.11 Possible structure of the product of oxidative cyclization of 2.30 | 28 |
| Scheme 3.12 Interpretation of oxidative cyclization revisit | 31 |
| Scheme 3.13 Proposed mechanistic pathway for the formation of <i>rac</i> - 3.19 | 32 |
| Scheme 3.14 Proposed mechanistic pathway for the formation of <i>rac</i> - 3.18 | 33 |
| Scheme 3.15 A possible mechanism for the rearrangement of <i>rac</i> - 3.19 | 34 |

List of Abbreviations

| | |
|--------|------------------------------------|
| Ac | acetyl |
| addn. | addition |
| anh. | anhydrous |
| app | apparent |
| aq. | aqueous |
| Ar | generic aryl group |
| Bn | benzyl |
| BOC | <i>t</i> -butyloxycarbonyl |
| BOM | benzyloxymethyl acetal |
| br | broad |
| ca. | approximate |
| calcd. | calculated |
| cat. | catalytic |
| COSY | correlation spectroscopy |
| d | doublet |
| dd | doublet of doublet |
| DCM | dichloromethane |
| DIB | <i>I,I</i> -(diacetoxyiodo)benzene |
| DIBAL | diisobutylaluminum hydride |
| DMAP | 4-dimethylaminopyridine |
| DMF | <i>N,N</i> -dimethylformamide |

| | |
|----------|---|
| DMSO | dimethyl sulfoxide |
| EAS | electrophilic aromatic substitution |
| EDCI·HCl | 1-ethyl-3-(3-dimethylaminopropyl) carbodiimide hydrochloride |
| EtOAc | ethyl acetate |
| EI | electron impact |
| ESI | electrospray ionization |
| equiv | equivalent |
| Et | ethyl |
| G | a substituent of appropriate steric demand |
| Hex | hexanes |
| HFIP | 1,1,1,3,3,3-hexafluoro-2-propanol |
| HF·pyr | pyridine hydrogenfluoride |
| HMBC | heteronuclear multiple bond correlation |
| HMDS | hexamethyldisilazide |
| hr | hour |
| HRMS | high resolution mass spectrometry |
| HSQC | heteronuclear single quantum coherence |
| imid. | imidazole |
| INOC | intramolecular nitrile oxide cycloaddition |
| IR | infrared spectroscopy |
| LDA | lithium diisopropylamide |
| m | multiplet |

| | |
|------------|---|
| min | minute |
| mp | melting point |
| Me | methyl |
| MS | mass spectrometry |
| Ms | methanesulfonyl |
| NMO | <i>N</i> -methylmorpholine- <i>N</i> -oxide |
| NMR | nuclear magnetic resonance |
| NOESY | nuclear overhauser effect spectroscopy |
| Ns | nosyl |
| OA | oxidative amidation |
| OTf | triflate |
| P | generic protecting group |
| prot. grp. | protecting group |
| PAN | <i>p</i> -anisyl |
| Ph | phenyl |
| PIFA | phenyliodine bis(trifluoroacetate) |
| ppm | part per million |
| PPTS | pyridinium <i>p</i> -toluenesulfonate |
| pyr | pyridine |
| q | quartet |
| quant. | quantitative |
| R | generic alkyl group |
| rac | racemic |

| | |
|-------|--|
| r.t. | room temperature |
| s | singlet |
| sat. | saturated |
| SM | starting material |
| t | triplet |
| TBAF | tetra- <i>n</i> -butylammonium fluoride |
| TBDMS | <i>tert</i> -butyldimethylsilyl |
| TBDPS | <i>tert</i> -butyldiphenylsilyl |
| TBSCl | <i>tert</i> -Butyldimethylsilyl chloride |
| tBu | <i>tert</i> -butyl |
| TFA | trifluoroacetic acid |
| TFE | trifluoroethanol |
| THF | tetrahydrofuran |
| TLC | thin-layer chromatography |
| TMS | trimethylsilyl |
| TPAP | tetrapropylammonium perruthenate |
| Ts | <i>p</i> -toluenesulfonyl |
| TTX | tetrodotoxin |
| UV | ultraviolet |
| XRD | X-ray diffraction |

Acknowledgments

I would like to thank Dr. Marco A. Ciufolini for his guidance. As a supervisor, he has been consistently sharing his vast knowledge of organic chemistry and providing guidance to the best he can. Recalling my undergraduate study at UBC, his stunning delivery of my two favourite courses, heavily influenced my decision about grad school and the area of research – simple, or maybe naïve, but that was how the whole story began. He is a chemist with big ego, about which I had gazillions of “heartbroken moments” and “character-building experiences”, but I do believe I will benefit from it later on in my life. Thanks to Drs. Ciufolini, Sammis and Tanner for being my examination committee.

I would also like to thank the great chemistry departmental faculties: Paul and Maria from NMR, Brian and Anita from X-ray, Emily, Felix and Yurou from the SIF, and also the MS lab for my arrays of HRMS submissions.

And of course there is gratitude towards my lab mates as well as former group members. Thanks Jason Hwang for preparing me for working on the total synthesis of Nosiheptide, Nikita Jain for valuable experience on methodology, Dimitrios Panagopoulos for being my big brother and Hero 6, Dr. Josh Zaifman, Dr. Sanjia Xu, Dr. Taka Kasahara and Dr. Leanne Racicot for always being there in the main lab available for help. And many many people came and left: Mara, Emma, Audrey, Hojung, Andy, Yiming, and Chirag.

My gratitude towards my family goes without saying, especially towards my parents for their love and support since the day I arrived at UBC Chemistry as a first-year undergraduate. Apologies are given to my grandparents, who have both passed away when I was away in

Canada. Finally I want to thank my boyfriend/lab mate Marco Paladino. Thank you for always being my closest consultant at research, thank you for understanding that frustration has been so often a by-product of our lab work (and you know I always bring it back home). I feel grateful that beyond research, I have you in my grad school. Grazie per tutto.

<A smiling face to all the friends and people I encountered in this lovely department>

January 17th, 2017

written on Flight MU598 from Vancouver to Shanghai

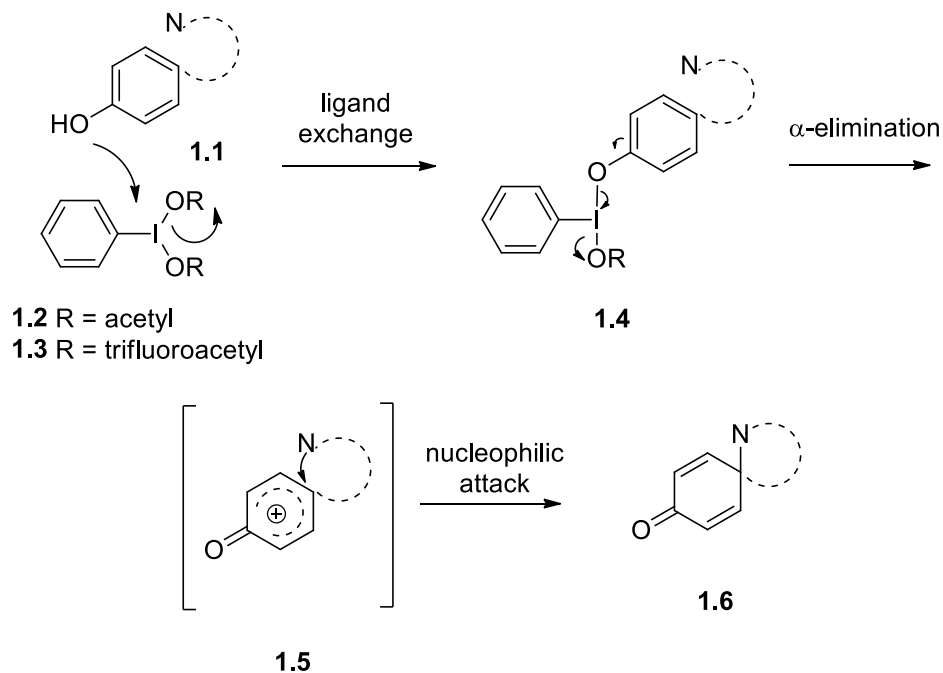
Dedication

致我的祖父母
与外祖父母

Chapter 1 Introduction

1.1 The oxidative amidation of phenols

The oxidative activation of a phenol such as **1.1** (Scheme 1.1) with a hypervalent iodine reagent, e.g., *I,I*-bis(acetoxy)iodobenzene (DIB) or *I,I*-bis(trifluoroacetoxy)iodobenzene (PIFA), in the presence of a suitable nitrogen nucleophile, N, results in formation of a dienone such as **1.6**. The dashed line in **1.1-1.6** indicates that the nucleophile may be tethered to the phenolic nucleus (intramolecular reaction) or it may be independent (bimolecular reaction). In all cases, the N atom in **1.6** emerges as part of an amide group. For that reason, the overall process is described as the oxidative amidation of phenols.¹

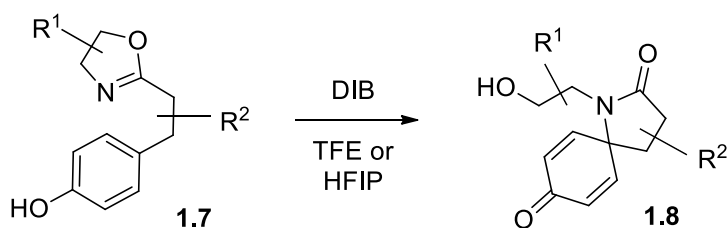


Scheme 1.1 General mechanism of oxidative amidation of phenols

Mechanistically, the reaction is believed to start with an initial ligand exchange at the iodine atom, leading to intermediate **1.4**. This complex then fragments to liberate cationic intermediate **1.5**, which is intercepted by the nitrogen nucleophile to give the product. Both the

ligand-exchange and the fragmentation steps are strongly proton-catalyzed. Therefore, the reaction is best carried out in a Brønsted acidic medium. The acidic strength of the latter must be adjusted to provide effective catalysis of the above steps without inducing protonation of the nitrogen nucleophile to such an extent that the rate of capture of electrophilic species **1.5** becomes excessively slow. As indicated below, this is generally accomplished through the judicious choice of a protic, non-nucleophilic solvent.

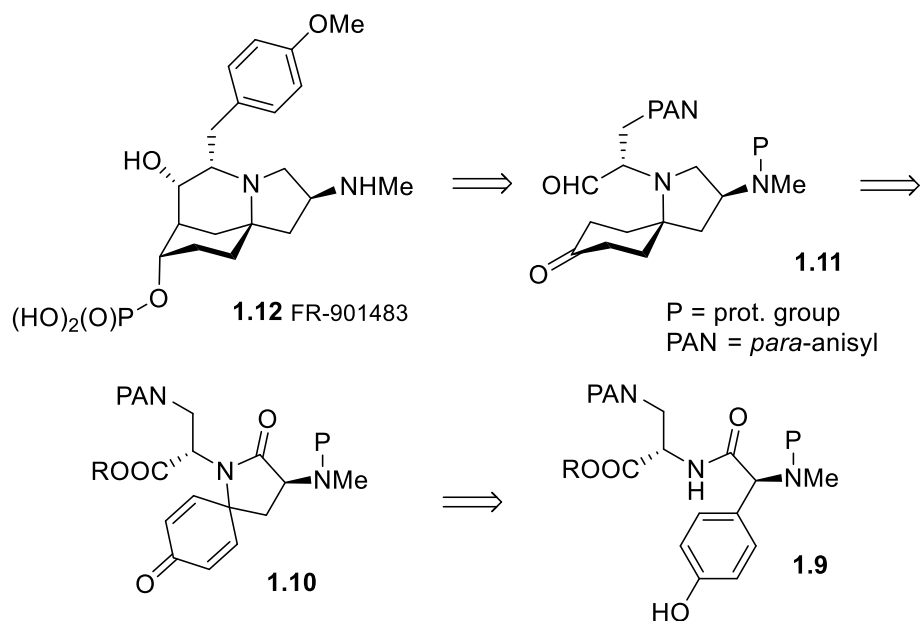
Three modes – or generations – of oxidative amidation have been developed to date. These differ for the nature of the nitrogen nucleophile, and each was devised in response to specific synthetic problems. Especially relevant to the present study is the first-generation reaction, which employs an oxazoline as the nitrogen nucleophile (Scheme 1.2). The transformation is best carried out in moderately acidic fluoroalcohol solvents² such as 2,2,2-trifluoroethanol (TFE, pKa = 12.4)³ or 1,1,1,3,3,3-hexafluoroisopropanol (HFIP, pKa = 9.3).⁴ These solvents are effective promoters of the mechanistic steps shown in Scheme 1.1, but they are insufficiently acidic to protonate oxazolines (pKa of protonated form = 5-6)⁵ to a significant extent.



Scheme 1.2 An example of first-generation oxidative amidation reaction

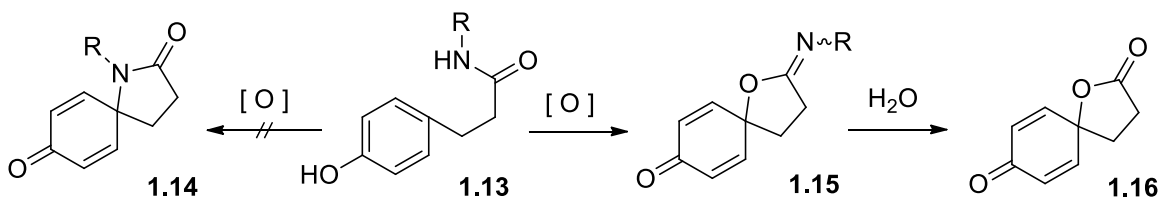
A brief historical overview is in order at this juncture. Oxazoline methodology was initially developed in connection with the synthesis of FR-901483, **1.12**.⁶ As shown in Scheme 1.3, a hypothetical oxidative cyclization of tyrosinyltyrosine derivative **1.9** to spirocyclic lactam **1.10**

would provide an expeditious route to the target molecule. However, such a transformation is problematic. For instance, Kita and collaborators reported in 1987, that oxidative activation of a



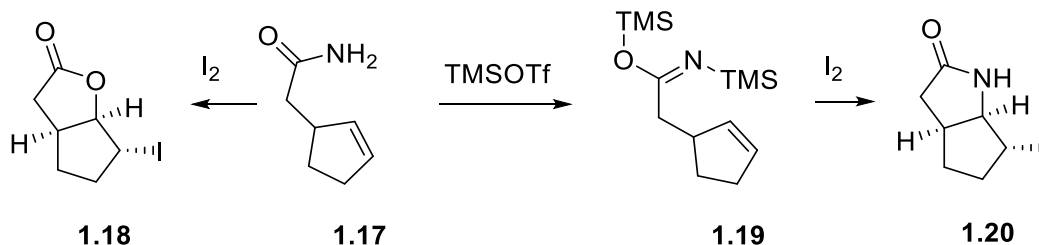
Scheme 1.3 Retrosynthesis of FR-901483

phenolic amide such as **1.13** affords not lactam **1.14**, but lactone **1.16**, arguably through iminolactone **1.15**, which is rapidly hydrolyzed during aqueous workup (Scheme 1.4). The carboxamide function thus expresses nucleophilic character at the oxygen atom, not at the nitrogen center.



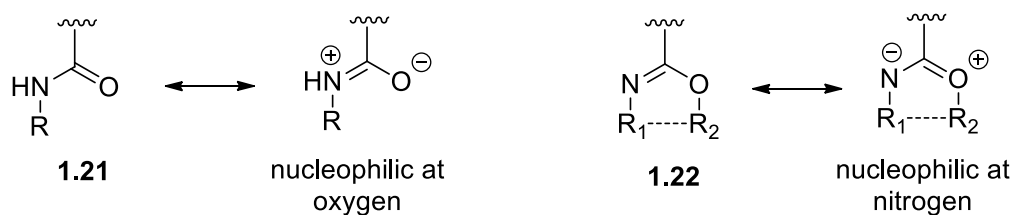
Scheme 1.4 Kita's attempted oxidative cyclization of phenolic amides

Knapp and coworkers experienced similar difficulties during their study of alkene iodolactamization.⁷ Indeed, treatment of **1.17** with I₂ afforded lactone **1.18** instead of the desired



Scheme 1.5 Similar difficulties in Knapp's alkene iodolactamization study

lactam **1.20** (Scheme 1.5). The problem was corrected by converting the amide into silyl imide **1.19**, which upon exposure to molecular iodine successfully cyclized to **1.20**. Evidently, resonance interactions within the carboxamide unit render this functional group nucleophilic at oxygen, but they promote *N*-nucleophilicity within an imide (Scheme 1.6).

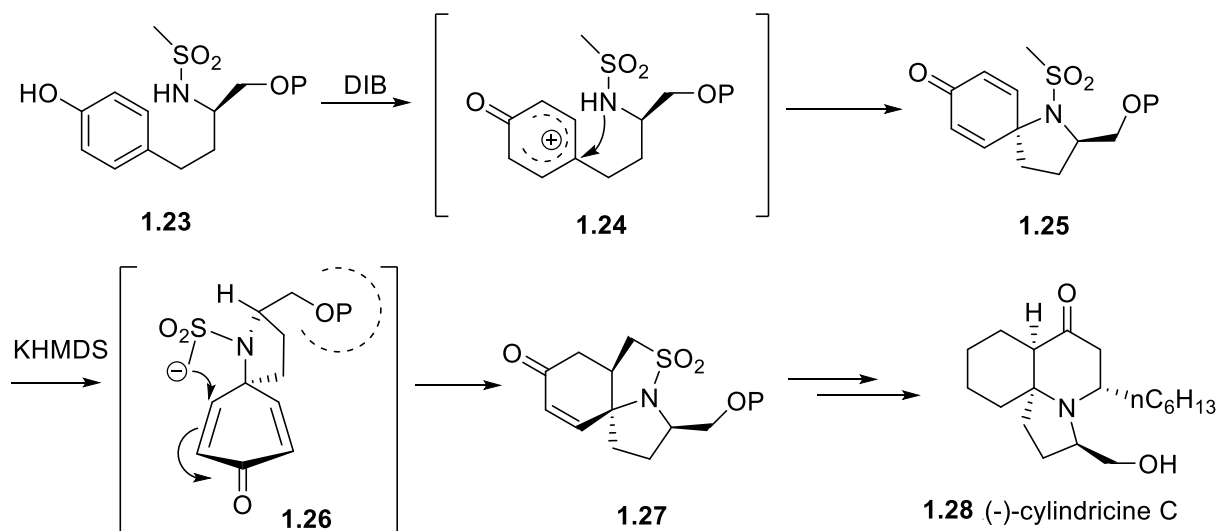


Scheme 1.6 Resonance interactions within a carboxamide and an imide

Imidates proved to be poor substrates for oxidative amidation chemistry, but their cyclic analogs, i.e., oxazolines, were satisfactory.⁸ A recent development in this area is the application of oxazoline technology to the synthesis of *Erythrina* alkaloids.⁹

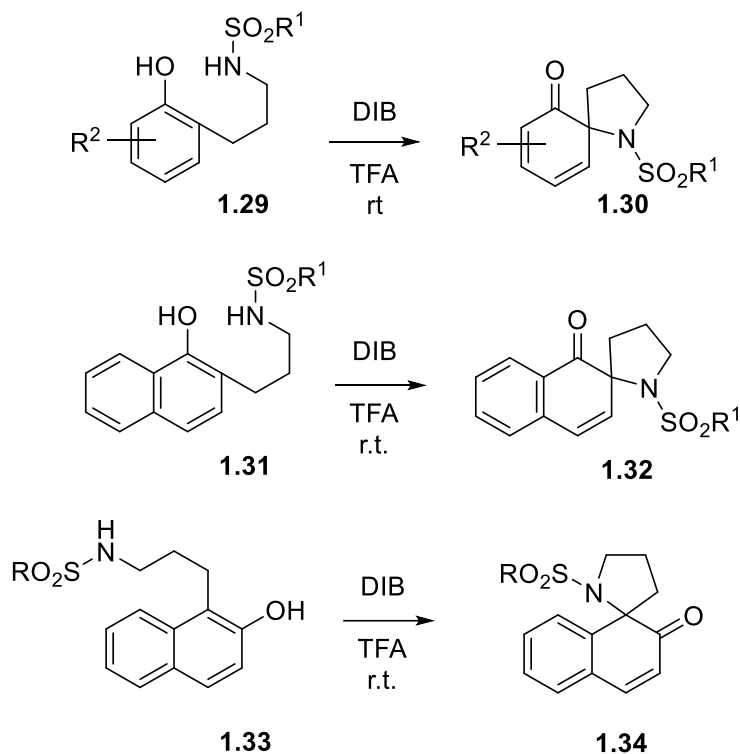
Efforts toward cylindricine and congeners¹⁰ unveiled the desirability of a method for the oxidative *amination* of phenols. Only one example of such a reaction was known at the onset of our investigations,¹¹ and very few examples have since been recorded.¹² This transformation is exceedingly problematic because ordinary amines are protonated to a significant extent in the acidic media that are required for the reaction. Indeed, the sparse examples of oxidative amination recorded in the literature involve weakly basic amines. In the event, sulfonamides proved to be outstanding surrogates of free amines for the reaction in question (Scheme 1.7). We

describe the oxidative cyclization of sulfonamides as the second-generation oxidative amidation. The nonbasic character of sulfonamides permits the conduct of the reaction in neat trifluoroacetic acid (TFA),¹³ a reaction medium that affords the desired products in generally excellent yield. Fukuyama nitrosulfonamides¹⁴ can be easily cleaved after oxidative cyclization to afford formal products of oxidative amination. Phosphoramides may be employed in lieu of sulfonamides.¹⁵ It will shortly be seen that second-generation technology is also quite relevant to the present study.



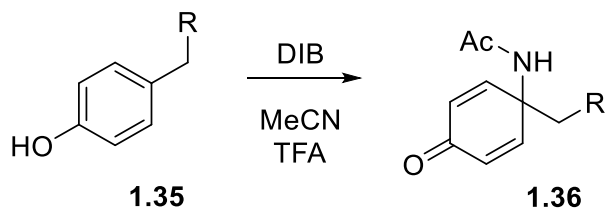
Scheme 1.7 An example of *para*-oxidative amidation reaction: synthesis of (-)-cyclindricine C

The transformations depicted in Schemes 1.3 and 1.7 are examples of *para*-oxidative amidation reactions. An *ortho*-oxidative amidation reaction ensues when a 2-substituted phenol such as **1.29** is subjected to the same conditions (Scheme 1.8). Substituent(s) R^2 in **1.29** should preferably be a heavier halogen (Br, I) or an alkyl group. This minimizes the tendency of dienones of the type **1.30** to undergo Diels-Alder dimerization. Naphthol-derived substrates **1.31** and **1.33** are also amenable to oxidative cyclization.¹⁶



Scheme 1.8 Examples of *ortho*-oxidative amidation reactions

First- and second-generation reactions are intramolecular processes. A bimolecular mode of oxidative amidation became desirable in connection with a number of synthetic efforts; notably one that led to a formal synthesis of tetrodotoxin (TTX).¹⁷ In response to such a need, a third-generation oxidative amidation was devised in the form of a Ritter-like¹⁸ reaction that ensues when a 4-substituted phenol such as **1.35** is treated with DIB in acetonitrile containing some TFA (Scheme 1.9).¹⁹



Scheme 1.9 An example of oxidative amidation reactions in a bimolecular mode

The relevance of this transformation to the synthesis of TTX is illustrated in the next section, which also outlines the hypotheses that motivated the present study.

Chapter 2 Background

2.1 Tetrodotoxin via the bimolecular oxidative amidation of a phenol

Tetrodotoxin, **2.1** (Figure 2.1), is a potent neurotoxin of marine origin and an ambitious target for total synthesis.²⁰

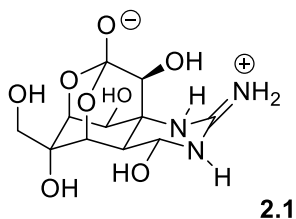
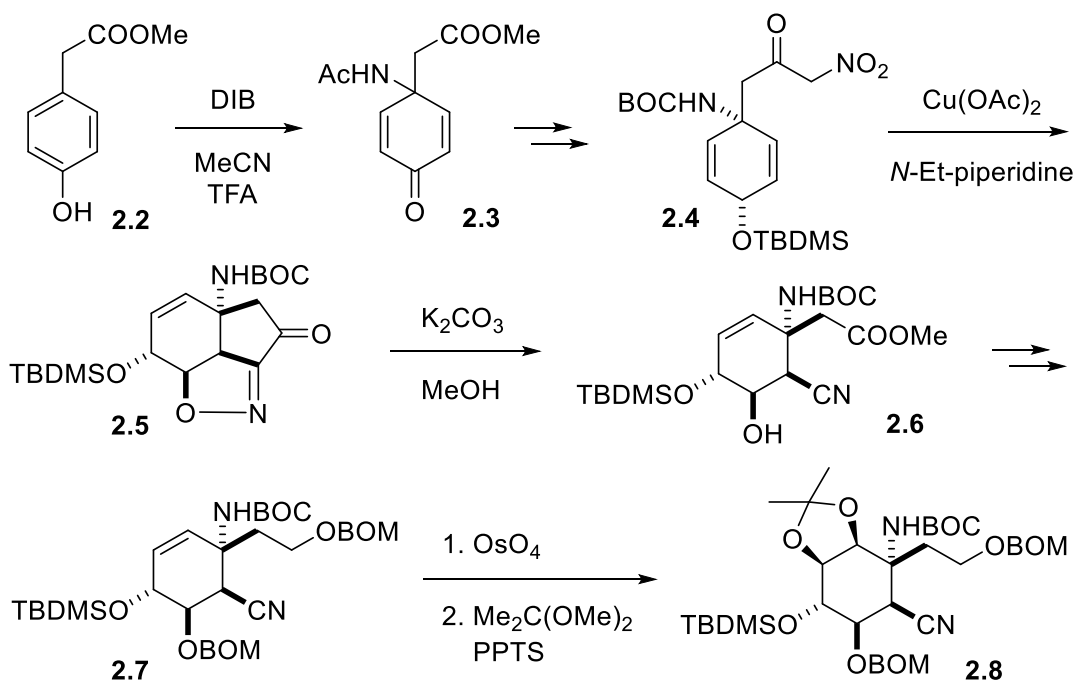


Figure 2.1 Structure of tetrodotoxin, **2.1**

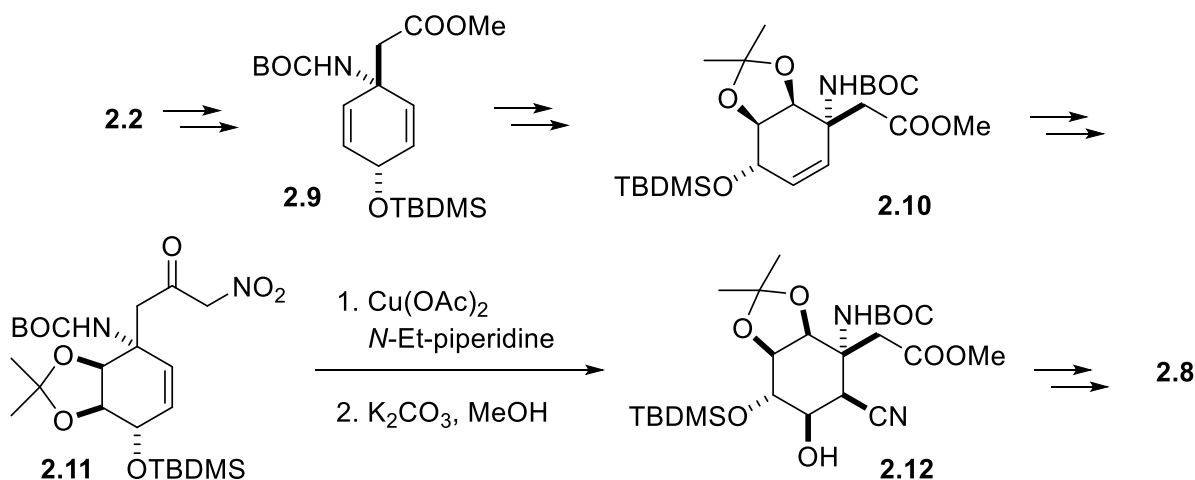
A recently disclosed formal synthesis of *rac*-**2.1**¹⁷ starts with a bimolecular oxidative amidation of phenol **2.2** (Scheme 2.1). The resultant **2.3** is elaborated to advanced intermediate **2.8** by a sequence that involves two key transformations. First, compound **2.3** is elaborated to



Scheme 2.1 Xu's Synthesis of *rac*-TTX: preparation of advanced intermediate **2.8**

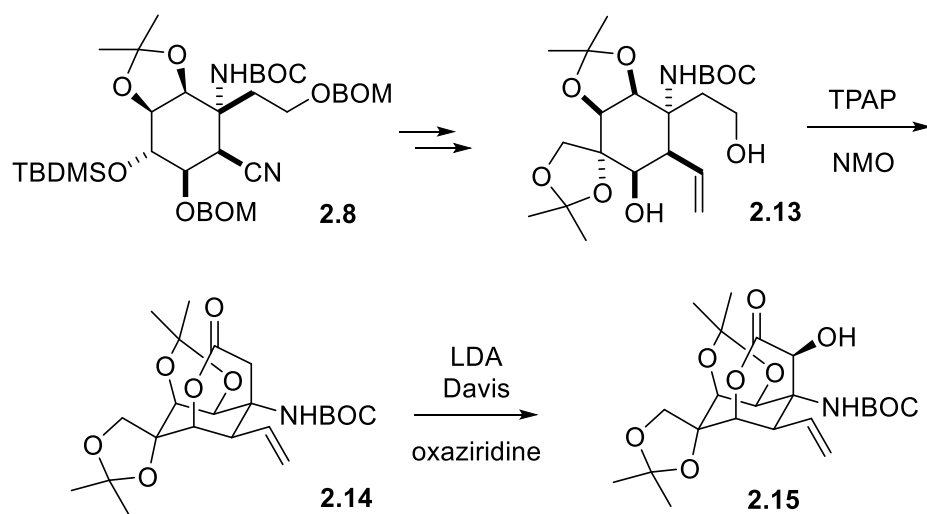
nitroketone **2.4**, which then undergoes a Cu(II)-mediated cyclization to isoxazoline **2.5** (Machetti-De Sarlo reaction).²¹ This step induces the desymmetrization of diene **2.4**, and as a consequence, the NHBOC-bearing carbon becomes stereogenic. In its present form, the reaction cannot differentiate between the two enantiotopic double bonds of the diene. Therefore, isoxazoline **2.5** and all derived compounds are obtained as racemates. Exposure to methanolic K₂CO₃ induces nucleophilic fragmentation of **2.5** to cyanoester **2.6**. The latter is converted into **2.7** in preparation for a second crucial transformation: a highly diastereoselective dihydroxylation of the double bond followed by protection of the diol to afford acetonide **2.8**.

It is important to note that order of the above steps can be inverted.²² Thus, dienone **2.9** may be converted into **2.10** through a key dihydroxylation reaction (Scheme 2.2). The emerging **2.11** can then be advanced to **2.12** via a tandem Machetti-De Sarlo cycloaddition / isoxazoline



Scheme 2.2 Inverted transformations in the desymmetrization of the diene

fragmentation, and the resultant **2.12** elaborated to intermediate **2.8**. Finally, the latter is advanced in a highly stereoselective manner to the DuBois TTX precursor, **2.15** (Scheme 2.3),²³ which can be converted into TTX in 4 steps.

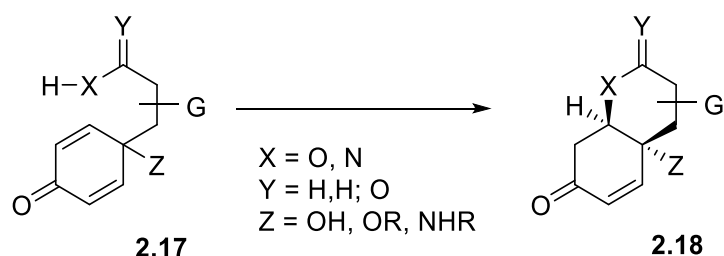


Scheme 2.3 Stereoselective assembly of the DuBois TTX precursor

2.2 Logic behind the present investigation and objectives thereof

It is apparent from the foregoing that the configuration of the NHBOC-bearing carbon atom in **2.8** (or **2.5**) can be relayed to all other stereogenic centers of TTX. Therefore, a method that might desymmetrize diene **2.3** or dienone **2.9** in a stereochemically controlled manner, i.e., one able to produce the correct configuration of the NHBOC-bearing atom, would enable an enantiocontrolled synthesis of the target.

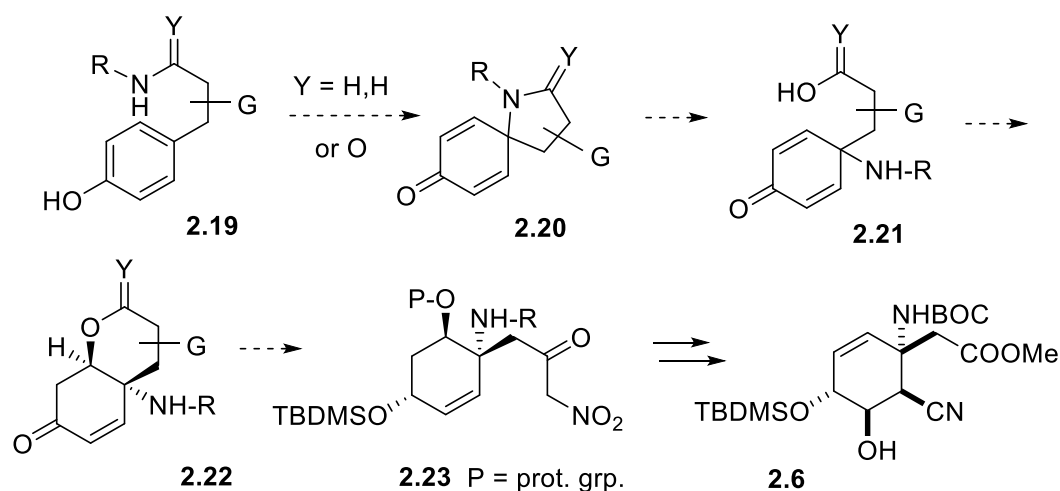
A possible solution was envisaged based on the propensity of dienones such as **2.17**, wherein G is a substituent of appropriate steric demand, to cyclize to **2.18** in a highly



Scheme 2.4 Possible diastereoselective cyclizations

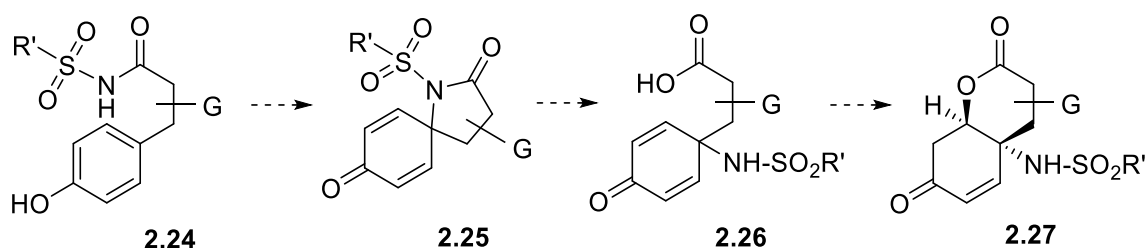
distereoselective manner (Scheme 2.4).²⁴ Thus, the configuration of the atom bearing G can be relayed to that of the atom bearing Z.

In the context of a TTX synthesis, the above principle could be harnessed as indicated in Scheme 2.5. The hypothetical oxidative cyclization of **2.19**, followed by opening of the azacycle, would reveal **2.21**, which may stereoselectively cyclize to **2.22**. The latter could be advanced to an enantioenriched form of TTX precursor **2.6**, perhaps via **2.23**, thereby achieving the desired objective.



Scheme 2.5 Proposed synthesis of an enantioenriched form of TTX precursor **2.6**

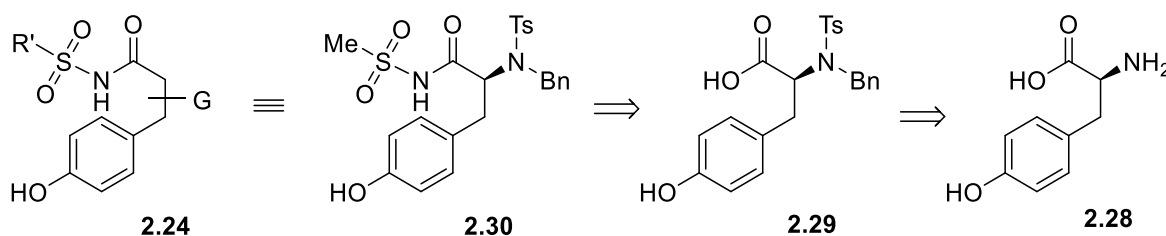
The cleavage of the nitrogenous ring would be especially facile if Y were an oxygen atom; i.e., if the nitrogen atom were part of a carboxamide-type functionality, or – equivalently – if Y in the diagram above were an oxygen atom. Furthermore, amide cleavage would be facilitated if R were a suitable electron-withdrawing group, such as a sulfonyl residue.²⁵ It will be recalled that phenolic sulfonamides undergo efficient oxidative cyclization. This led us to wonder whether an *N*-acyl sulfonamide such as **2.24** (Scheme 2.6) might also successfully cyclize to **2.25**, which could then be advanced to the desired **2.27**.



Scheme 2.6 Proposed cyclization and desymmetrization from *N*-acyl sulfonamide **2.24**

Group G in the above molecules had to satisfy two requirements. First, it was to be of sufficiently great steric demand as to promote a highly diastereoselective cyclization of intermediate **2.27**. Second, it had to enable the conversion of **2.27** into nitroketone **2.23**; an

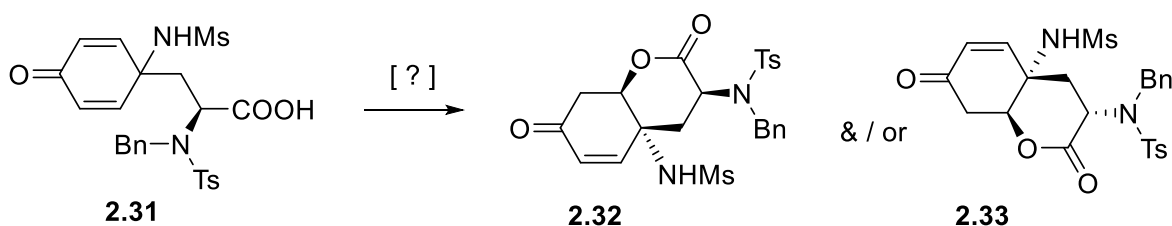
operation that requires the excision of the lactone carbonyl carbon from **2.27**. Such an objective could be best achieved if G were a heteratomic functionality located at the α -position of the lactone carbonyl. That being the case, substrate **2.29** could be a derivative of readily available L-tyrosine, **2.28** (Scheme 2.7). The modest steric demand of the NH₂ unit in the parent aminoacid



Scheme 2.7 Retrosynthesis of an appropriate *N*-acyl sulfonamide

may be increased significantly by conversion into an *N*-benzyl tosylamide (*cf.* **2.29**).²⁶ Because compound **2.29** was already available in our laboratory,²⁷ our choice fell on acylsulfonamide **2.30** as a substrate for the planned investigation.

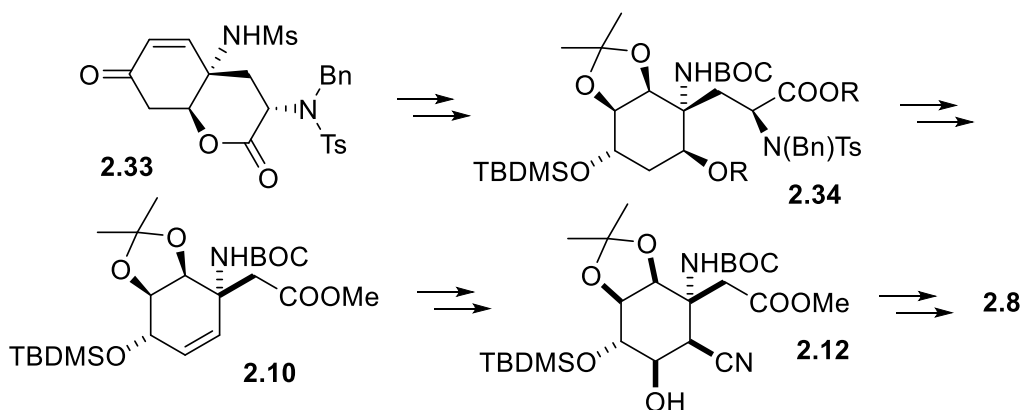
A molecular mechanics study of the cyclization of **2.31** failed to reveal a clear preference for the formation of one of the two possible diastereomers of the product, **2.32** and **2.33** (Scheme 2.8).²⁸ It is noted, however, that either **2.32** or **2.33** are serviceable for our objectives. It will be



Scheme 2.8 Two possible diastereomers of cyclization products from **2.31**

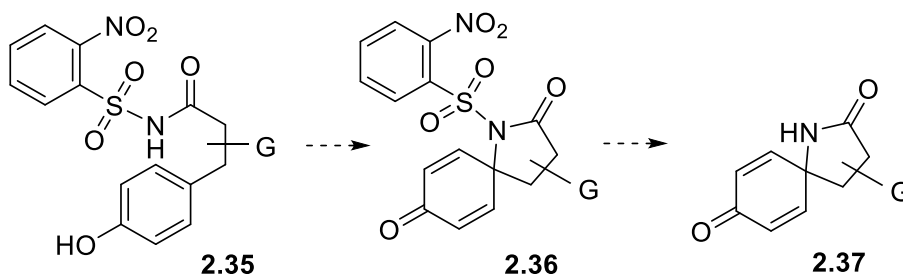
recalled that the order of the key steps in the sequence leading to advanced TTX intermediate **2.8** (Machetti-De Sarlo and dihydroxylation reactions), can be inverted (Scheme 2.2, p. 9). Thus, **2.32** would be converted into as seen earlier in Scheme 2.5 (p. 12), while **2.33** could be advanced

to **2.8** as per Scheme 2.9. Therefore, what matters here is that the cyclization of **2.31** proceeds with a satisfactory degree of stereoselectivity.



Scheme 2.9 Conversion of lactone **2.33** to TTX intermediate **2.8**

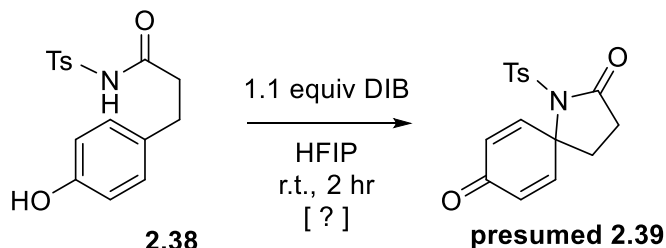
The goal of the present investigation was thus to explore the scope of the oxidative cyclization of phenolic *N*-acyl sulfonamides and to achieve the conversion of spirocycles **2.25** into lactones **2.27**. If successful, the new reaction would enable access to products formally arising through oxidative cyclization of carboxamides, thereby circumventing the limitations discussed on p. 3 above. Indeed, cyclization of a Fukuyama-type *N*-acyl nitrosulfonamide¹⁴ such as **2.35** would afford **2.36**. Excision of the sulfonyl group should then afford the formal product **2.37** of oxidative cyclization of a carboxamide (Scheme 2.10).



Scheme 2.10 Formal formation of a carboxamide via excision of the sulfonyl group

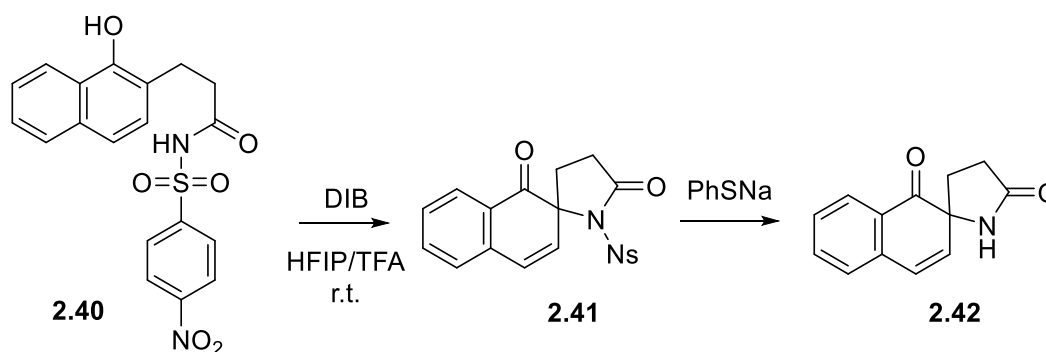
2.3 Early examples of oxidative cyclization of phenolic *N*-acyl sulfonamides

A former undergraduate member of our group, Doris Tang, briefly explored the oxidative cyclization of *N*-acyl sulfonamide **2.38** with DIB (1.1 equiv of DIB in HFIP, r.t., 2 hr).²⁹ The product thus obtained was not thoroughly characterized, but its spectra were not inconsistent with structure **2.39** (Scheme 2.11).



Scheme 2.11 Attempted oxidative cyclization of *N*-acylsulfonamide **2.38**

More recently, Nikita Jain, a graduate student in our group, extended the oxidative cyclization of sulfonamides to the naphthalene series (Scheme 2.12). In the course of that endeavor, she demonstrated that treatment of acylsulfonamide **2.40** with DIB in hexafluoroisopropanol induces conversion into **2.41**, which can be readily desulfonylated to furnish lactam **2.42**.¹⁶ The structure of the mesyl variant of spirocyclic acylsulfonamide **2.43** was ascertained by X-ray diffractometry (Figure 2.2).³⁰



Scheme 2.12 An example of oxidative cyclization of naphthalic sulfonamides

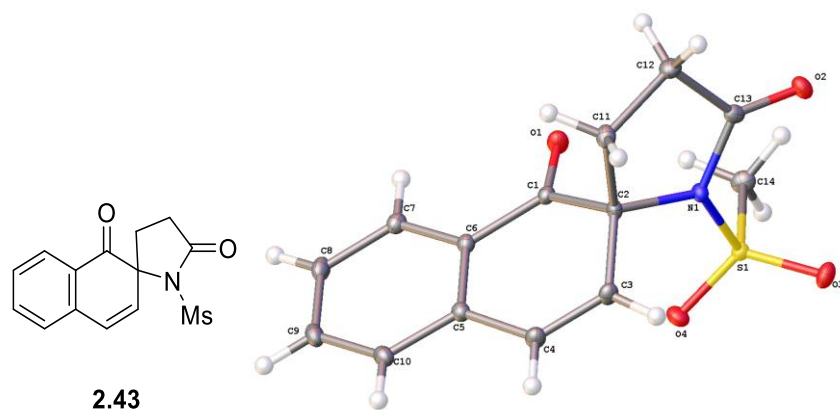


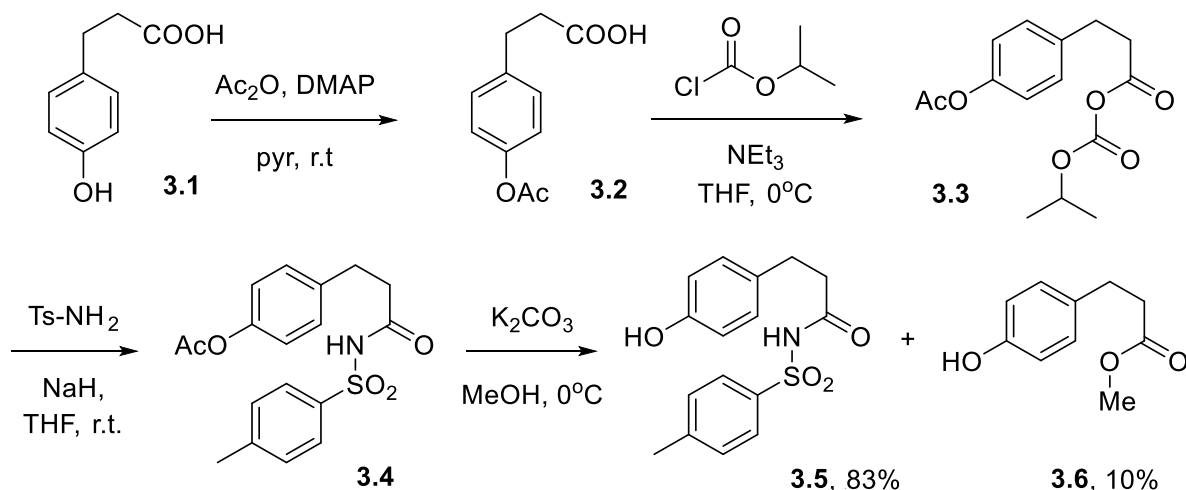
Figure 2.2. X-ray structure of compound **2.43**

This was the extent of precedent at the onset of the investigations described in this thesis.

Chapter 3 Discussion

3.1 Preparation of phenolic *N*-acyl sulfonamides

The Tang²⁹ procedure for the synthesis of *N*-acyl sulfonamide **3.5** entails the formation of mixed anhydride **3.3**, which is then condensed *in situ* with sodiated tosylamide (Scheme 3.1). Deprotection of the emerging **3.4** affords a mixture of desired **3.5** plus ester **3.6**, which is

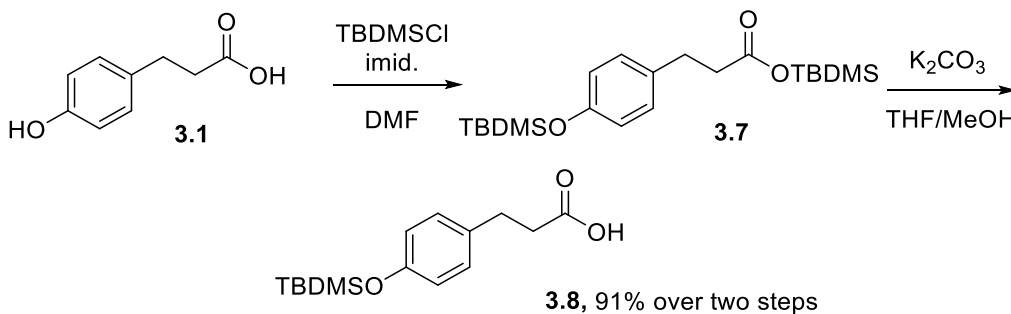


Scheme 3.1 Tang's procedure for the preparation of *N*-acylsulfonamide **3.5**

removed by column chromatography and may be recycled. However, the polarity of substance **3.5** complicates chromatographic operations. An alternative that proved to be more practical was developed by Jain¹⁶ in the form of EDCI-mediated coupling of acid **3.8** with a sulfonamide. Purification of the final product **3.10** was significantly facilitated because no byproducts are formed upon deprotection of **3.9** with HF.

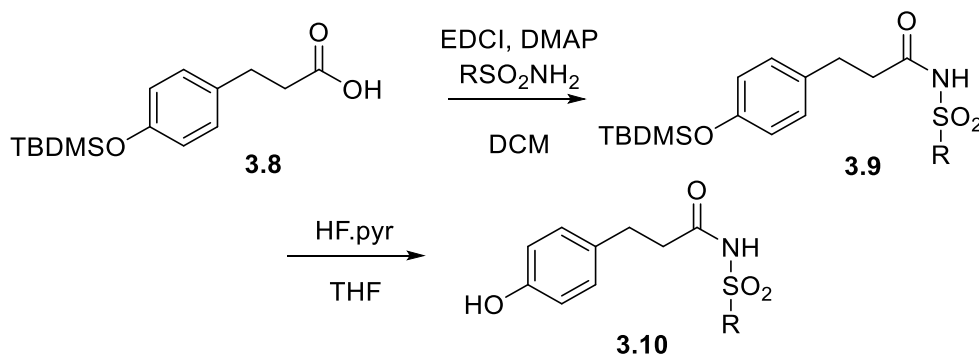
It should be noted that the EDCI coupling reaction performed poorly if the phenol was left unprotected. However, selective protection of the phenolic OH in commercial 3-(4-hydroxyphenyl)propionic acid, **3.1**, was not successful; at least not with TBDMSCl and imidazole. Thus, the reaction of **3.1** with TBDMSCl and imidazole furnished **3.7**, which was selectively deblocked upon treatment of potassium carbonate in methanol/THF to afford acid **3.8**

(Scheme 3.2). As a side note, various intermediates are very polar, rendering chromatography rather difficult. For ease of chromatographic purification, a TBDPS group can be used instead of TBDMS.



Scheme 3.2 Preparation of mono-TBDMS protected acid **3.8**

The mono-TBDMS protected acid **3.8** is joined with a sulfonamide, R-SO₂NH₂, via an EDCI-mediated coupling reaction (Scheme 3.3). The sulfonamide is used in excess (1.5 equiv) to ensure the complete consumption of compound **3.8**. The coupling reaction generates *N*-acyl sulfonamide in good to moderate yields, depending on the nature of the R group. These reactions are also generally clean, with only excess sulfonamide and reagents to remove. The subsequent deprotection of the OTBDMS group was best done with HF·pyridine in THF. Other deprotecting reagents such as tetrabutylammonium fluoride (TBAF) and Amberlyst®-15(H⁺) ion-exchange resin would also work for robust sulfonamides, such as methyl sulfonamide. Yet, HF·pyridine



Scheme 3.3 Preparation of phenolic *N*-acyl sulfonamides **3.10**

gives the best result. This reagent cleaved the OTBDMS without harming the *N*-acyl sulfonamide moiety, resulting in clean reaction mixtures that are easier to purify. As indicated in Table 3.1, the desired compounds **3.10** emerge in moderate to excellent yields.

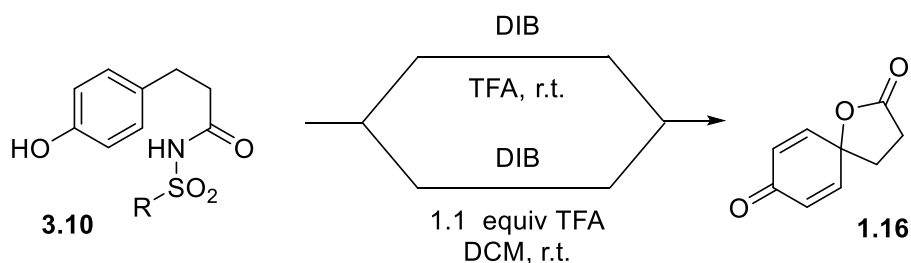
| Entry | R | Yield (%) of compounds 3.9 ¹ | Yield (%) of compounds 3.10 ¹ |
|----------|--|--|---|
| a | Me | 85 | 77 |
| b | tBu | 51 | 99 |
| c | 4-Me-C₆H₄ | 83 | 87 |
| d | 4-O₂N-C₆H₄ | 75 | 80 |
| e | 4-MeO-C₆H₄ | 92 | 84 |
| f | 2,4,6-triisopropyl | 79 | 91 |

¹ Yield of chromatographically purified product.

Table 3.1 Yields of compounds shown in Scheme 3.3

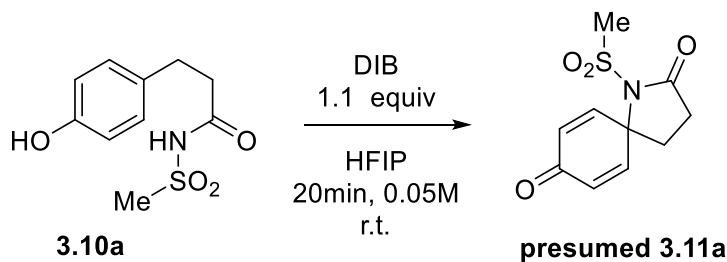
3.2 Oxidative cyclization of phenolic *N*-acyl sulfonamides

It will be recalled that TFA is the solvent of choice for the cyclization of ordinary sulfonamides (e.g., Scheme 1.8, p. 6). This was not so in the case of *N*-acyl sulfonamides. Thus, addition of a substrate of the type **3.10** to a solution of DIB in TFA resulted in formation of spiro lactone **1.16** as the major product. A similar result was obtained upon addition of **3.10** to a solution of DIB in DCM containing only 1.1 equiv of TFA (Scheme 3.4). Other solvents such as plain DCM or MeCN were found to be inappropriate for this reaction, because of the poor solubility of the substrates in these media.



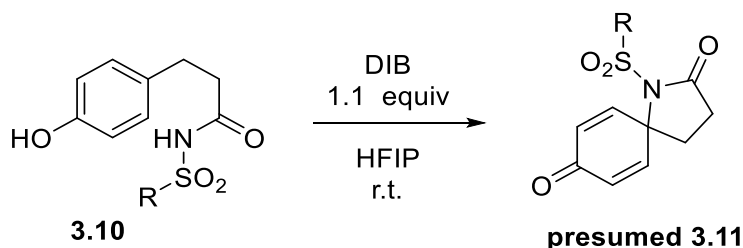
Scheme 3.4 Undesired formation of spiro lactone **1.16**

Tang had presumably achieved the oxidative cyclization of phenolic *N*-acyl sulfonamide **2.38** using DIB in HFIP (Scheme 2.11, p. 15).²⁹ Accordingly, the cyclization of **3.10** was attempted under Tang conditions. Dropwise addition of an HFIP solution of **3.10a** (18 mg / mL) into a solution of DIB in HFIP (33 mg / mL) at room temperature (final concentration equal to 0.05 M) resulted in conversion into a product, the spectra of which seemed in accord with



Scheme 3.5 Attempted oxidative cyclization of phenolic *N*-acyl sulfonamide

structure **3.11a** (Scheme 3.5). This material was obtained in 84% yield after chromatography. Oxidative cyclization of other *N*-acyl sulfonamides under the same conditions proceeded efficiently to afford presumed **3.11** in yields ranging from 57% to 90% (Table 3.2).

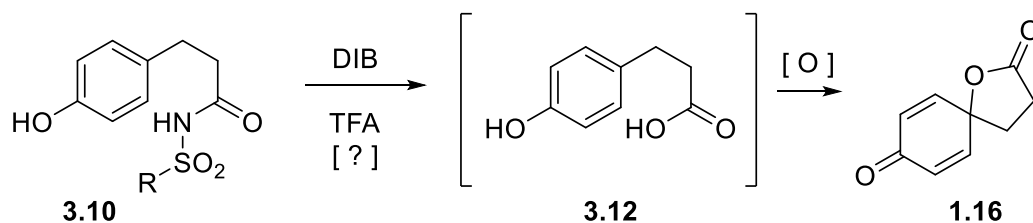


| Entry | R | Yield (%) ¹ |
|----------|--|------------------------|
| a | Me | 83 |
| b | tBu | 86 |
| c | 4-Me-C₆H₄ | 90 |
| d | 4-O₂N-C₆H₄ | 57 |
| e | 4-MeO-C₆H₄ | 81 |
| f | 2,4,6-triisopropyl | 59 |

¹ Yield of chromatographically purified product.

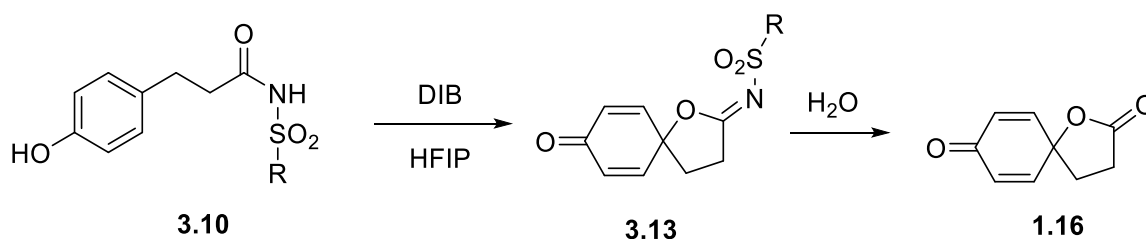
Table 3.2 Oxidative cyclization of phenolic *N*-acyl sulfonamides

At the present stage, the above results was interpreted as implying that TFA must promote an undesired, rapid conversion of the *N*-acyl sulfonamide into acid **3.12**, which then cyclizes to **1.16** (Scheme 3.6). The hypothetical formation of an *N*-sulfonyl-iminolactone **3.13** was regarded as less likely, because iminolactones of similar structure, wherein an *N*-alkyl group is present in lieu of an *N*-sulfonyl one, are known to undergo rapid hydrolysis to **1.16** upon



Scheme 3.6 A possible mechanistic pathway for the formation of spiro lactone **1.16**

aqueous workup and definitely would not survive column chromatography.³¹ Substances of structure **3.13** were anticipated to behave similarly. Subsequent observations (*vide infra*) forced us to revisit this interpretation.

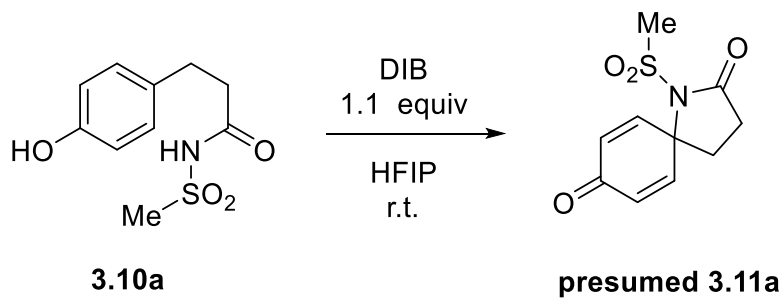


Scheme 3.7 Anticipated hydrolysis of *N*-sulfonyl iminolactone **3.13**

3.3 Determination of the maximum allowable reaction concentration

The reason that the above reactions were run at a final formal concentration of substrate of only 0.05 M is that the oxidative cyclization of phenolic sulfonamides in HFIP performed best when run under dilute conditions. At higher concentrations, competitive reactions promoted formation of polymeric by-products. Thus, formal final concentration of substrate were typically in the neighborhood of 10 mM.³² Such dilute conditions are by no means appropriate for preparative work, especially when costly solvents such as HFIP are employed. The subsequent discovery that the reaction was best carried out in neat TFA completely suppressed the need for HFIP as a co-solvent and enabled operation at a formal final concentration of substrate of up to 0.3 M.

As with the oxidative cyclization of *N*-acyl sulfonamides, in an effort to minimize the use of HFIP, the cyclization of **3.10** was studied at increasingly higher final concentrations of substrate. It was pleasing to observe that concentration had virtually no effect on outcome in the present case. With some substrates, the yields actually became higher with increasing concentration. This was the case, for instance, for mesylamide **3.10a** (Table 3.3). With most *N*-acyl sulfonamides, operation at a concentration greater than 1.0 M was problematic because of the limited solubility of the substrates. Indeed, a special procedure was developed to ensure that the substrate dissolved properly when operating at higher concentrations. Thus, an HFIP solution of substrate was injected into a vial containing solid DIB, followed by immediate sonication to promote rapid dissolution and mixing. This is different from the typical procedure for oxidative cyclization, in which separate solutions of substrate and DIB are mixed. In the case of *N*-acyl sulfonamides, the two procedures returned the same product in equally good to excellent yields.



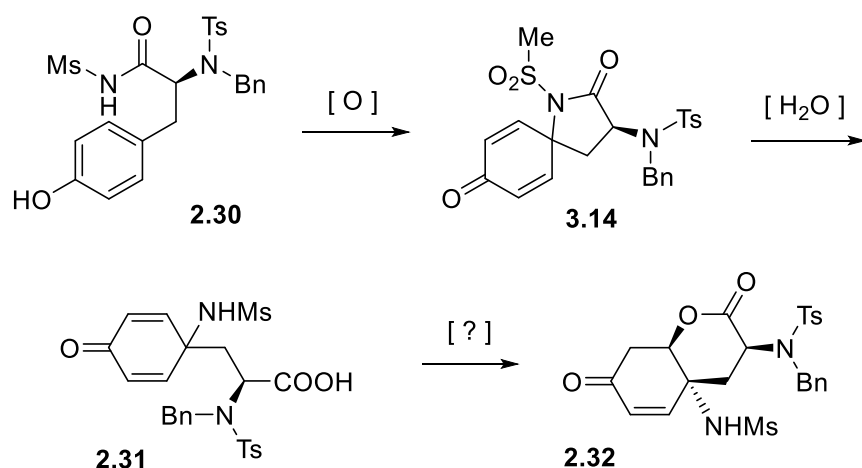
| Entry | Concentration (M) | Yield (%) ¹ |
|----------|-------------------|------------------------|
| a | 0.05 | 83 |
| b | 0.5 | 85 |
| c | 1.0 | 93 |

¹ Yield of chromatographically purified product.

Table 3.3 Oxidative cyclization of *N*-acyl sulfonamide **3.10a** at variable concentrations

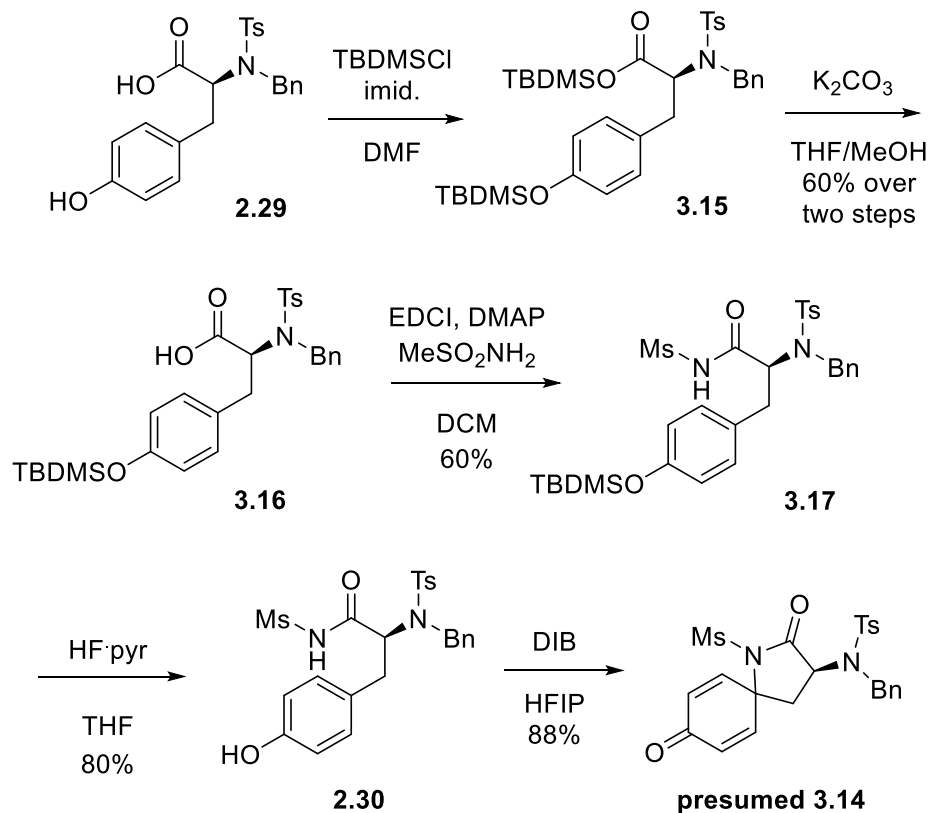
3.4 Cyclization of a tyrosine-derived substrate and rearrangement of the product

The discussion in Section 2.2 (p. 11) indicated that an important objective of the present work was to determine whether the product **3.14** of cyclization of tyrosine derivative **2.30** could be selectively rearranged to substance **2.32** or to its diastereomer (Scheme 3.8). Fortunately, a former group member, Dr. S. Xu, had had been prepared quantities of substance **2.29** by a literature method in connection with another project. We are very grateful to Dr. Xu for kindly agreeing to provide several grams of this compound for the present effort.



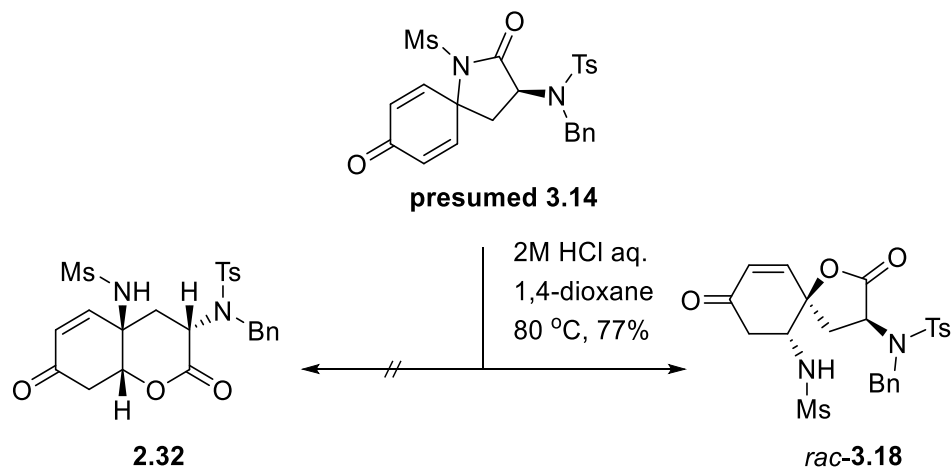
Scheme 3.8 Proposed diastereoselective rearrangement of presumed spirolactam **3.14**

Tyrosine derivative **2.29** was advanced to the desired *N*-acyl sulfonamide **2.30** substantially by the method outlined earlier, with only minor modifications regarding purifications. Saponification of compound **3.15** also partially removed the TBDMS group on the phenolic oxygen, and thus crude **3.16** was purified by column chromatography (3:2 pentane/acetone, $R_f=0.75$). The target compound **2.30** was obtained as indicated in Scheme 3.9, and its oxidative cyclization of **2.30** under the previously described conditions afforded presumed **3.14** in good yield.



Scheme 3.9 Synthesis of presumed tyrosine-derived spirolactam **3.14**

Initial attempts to induce the transposition of **3.14** to **2.32** (or its diastereomer) by treatment with aqueous LiOH in THF with minimum amount of water, PPTS in 6:1 THF/water or aqueous 2M HCl in dioxane, at room temperature, were uniformly unsuccessful, returning only intact starting material. However, heating a dioxane solution of presumed **3.14** and 3 equivalents of aqueous 2M HCl to 80°C overnight resulted in formation of a new compound, the spectra of which were consistent with the anticipated structure **2.32** (Scheme 3.10). Weaker acids such as PPTS were completely ineffective for this transformation. Surprisingly, substance **2.32** was racemic. This puzzling observation induced us to ascertain the structure of **2.32** by X-ray diffractometry (XRD), whereupon it transpired that presumed **2.32** was in fact racemic **3.18** (Figure 3.1).



Scheme 3.10 Attempts to induce the transposition of **3.14** to **2.32**

This unexpected result led us to question the structure of the products of oxidative cyclization of phenolic *N*-acyl sulfonamides, because it was difficult to envision a sensible mechanism for the formation of **3.18** from presumed **3.14**. This mandated an unequivocal structural determination of the product of oxidative cyclization.

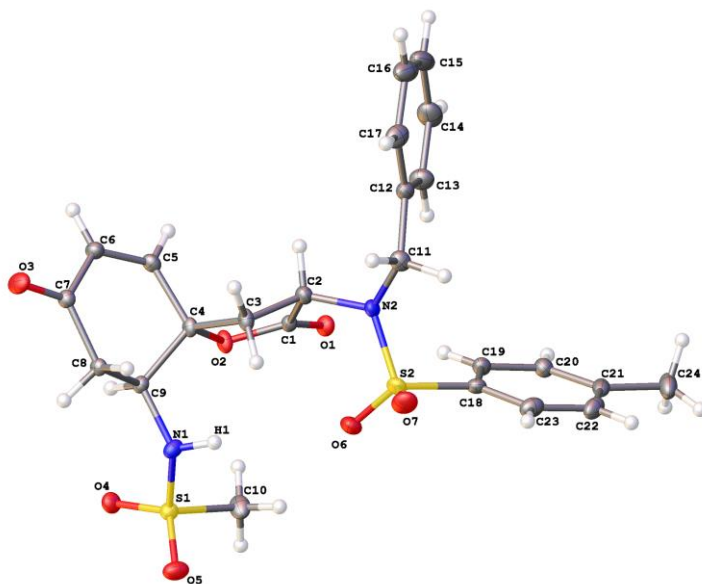
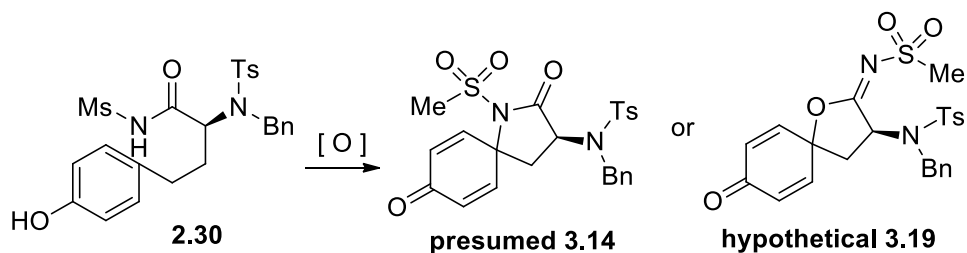


Figure 3.1. X-ray structure of compound **3.18**

3.5 Spectral properties of presumed **3.14** vs. those of other spirocyclic compounds

The work of Kita (Scheme 1.4, p. 3) and the lactonic nature of compound **3.18** suggested that the product of oxidative cyclization might have been structure **3.19** (Scheme 3.11). The NOESY-2D spectrum of such a product (Figure 3.2) shows a correlation between the signals at



Scheme 3.11 Possible Structures of the Product of Oxidative Cyclization of **2.30**

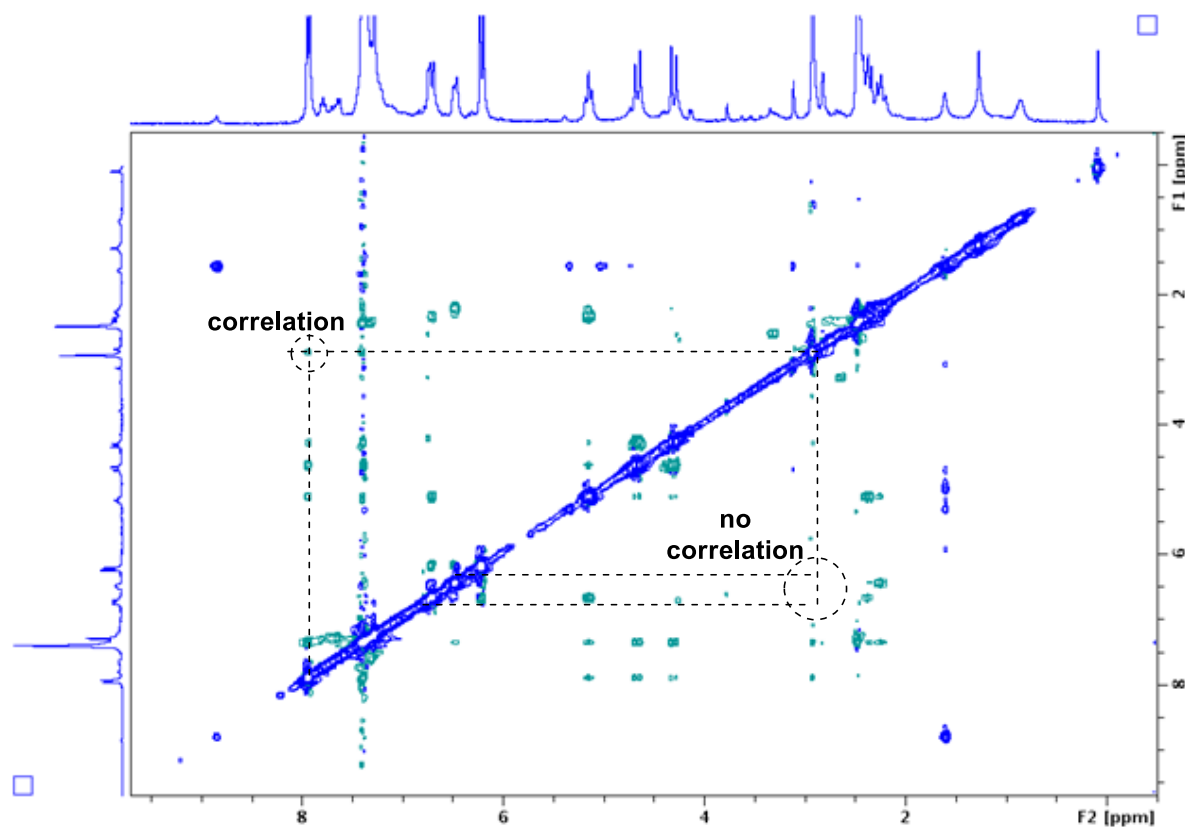


Figure 3.2 NOESY spectrum of the product of oxidative cyclization of **2.30**

2.92 ppm (the methyl group of the methanesulfonyl segment) and 7.94 ppm (the tosyl unit), signifying that those two groups are in close proximity. However, no correlation is apparent between the methanesulfonyl group and the hydrogens of the dienone, even though a correlation would be expected for structure **3.14**. The NOESY spectrum of the product is therefore more consistent with structure **3.19**. The absence of NOESY correlations, however, does not constitute structural proof. We thus turned to ^{13}C spectrometry as a possible means of distinguishing the two structures.

A member of our group, N. Jain, prepared and characterized a number of spirocyclic lactams structurally related to the ones produced in the course of this research.¹⁶ The consequent accumulation of ^{13}C NMR data enabled a comparison of the chemical shifts of carbons *a* and *b* in the product of oxidative cyclization of **2.30** and related substrates (Figure 3.3) with the corresponding atoms in compounds of secure structure.

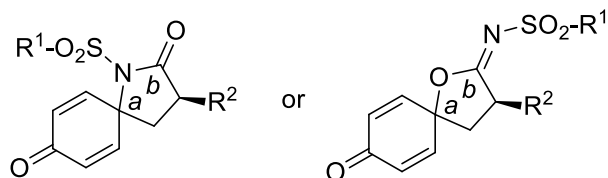


Figure 3.3 Definition of carbon atoms *a* and *b* in the products of oxidative cyclization

As apparent from Table 3.4, atoms *a* in the substances prepared in the course of this work resonate at a chemical shift that is about 5 ppm more downfield than that of lactone **1.16** and 10 ppm more downfield than that of Jain spirolactams. In contrast, the chemical shifts of atoms *b* are well within the range of those of the Jain products. In the absence of data for authentic compounds of the type **3.19** it seemed imprudent to draw conclusions from such a comparison. This mandated an unequivocal structural determination through X-ray crystallography.

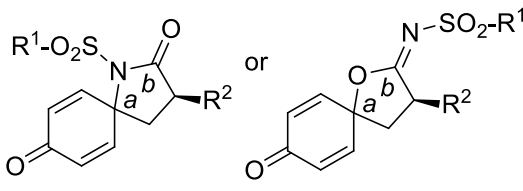
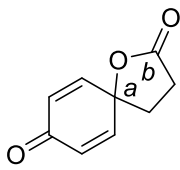
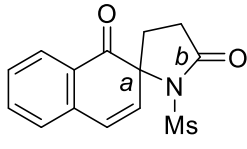
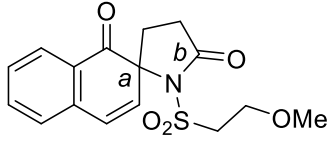
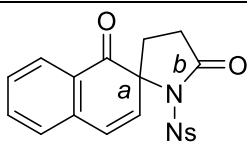
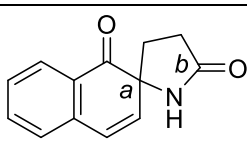
| Compounds | Chemical shift of C- <i>a</i> | Chemical shift of C- <i>b</i> |
|---|--|--|
|  | Range: 81.2 (R = 2,4,6-triisopropyl) to 84.8 ppm (R = Ns) R ¹ = Me, R ² = N(Ts)Bn: 83.1 ppm | Range: 171.1 (R = 2,4,6-triisopropyl) to 179.0 (R = tBu) R ¹ = Me, R ² = N(Ts)Bn: 167.3 ppm |
|  <p>1.16</p> | 78.6 | 175.4 |
|  <p>3.31</p> | 71.4 | 174.7 |
|  <p>3.32</p> | 70.9 | 174.7 |
|  <p>3.33</p> | 71.1 | 173.2 |
|  <p>3.34</p> | 65.0 | 178.8 |

Table 3.4 Comparison of ¹³C chemical shifts of the products of oxidative cyclization obtained in this study with those of authentic spirolactams

Attempts to crystallize presumed **3.14** in order to obtain an X-ray structure were unsuccessful. On the other hand, crystals suitable for X-ray diffractometry were obtained for presumed **3.11a**, which was revealed to be in fact **3.13a** (Figure 3.4).

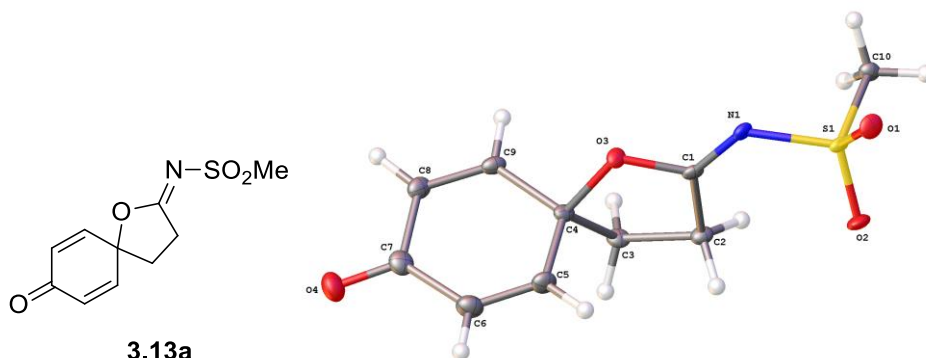
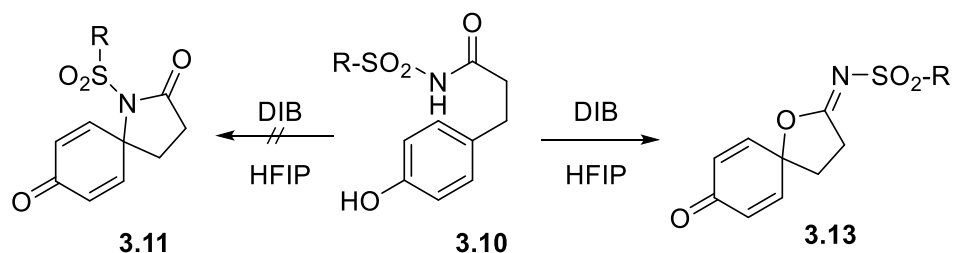


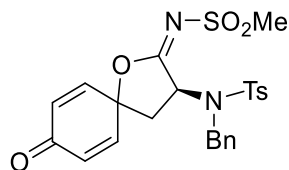
Figure 3.4 X-ray structure of compound **3.13a**

A comment is in order at this point. The room-temperature ^1H and ^{13}C spectra of **3.13a** and related products suggest the presence of a single compound, indicating that either the *N*-sulfonyl iminolactone exists as a single geometric isomer (*E*, as revealed by the above X-ray structure) or that the interconversion of the *E* and *Z* isomers is rapid on the NMR time scale. No attempt was made to address / clarify this matter.

Regardless, on the basis of the foregoing, one must infer that all products of oxidative cyclization of the *N*-acyl sulfonamides described herein are likely to be spiro-iminolactones of the type **3.13**, instead of spirolactams **3.11** (Scheme 3.12). In particular, the product obtained



Scheme 3.12 Interpretation of oxidative cyclization revisited

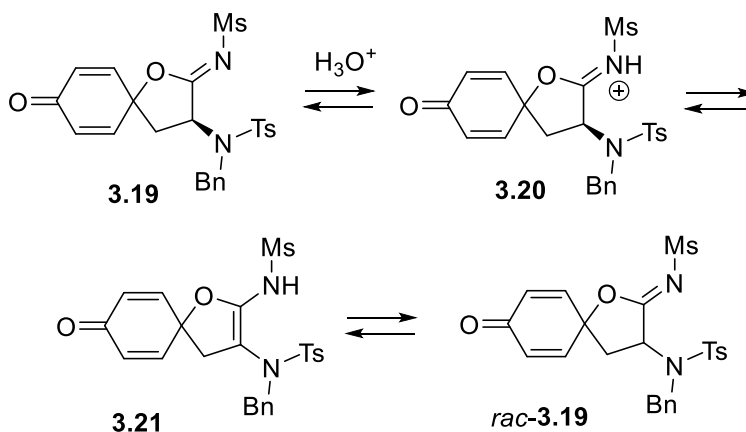


3.19

Figure 3.5 Probable structure of compound **3.19**

from **2.30** is likely to be **3.19** (Figure 3.5) instead of **3.14**. The resistance of these *N*-sulfonyl iminolactones toward hydrolysis was truly surprising. Recall that they survive intact upon column chromatography or exposure to 2M HCl in dioxane, at room temperature, for days.

A plausible mechanism for the formation of **3.18** from **3.19** must rationalize the fact that the rearranged product is obtained in racemic form, but in a highly diastereoselective manner. Racemization seemed likely to occur upon acid-catalyzed equilibration of **3.19** with its enamido tautomer, **3.21**, as per Scheme 3.13:

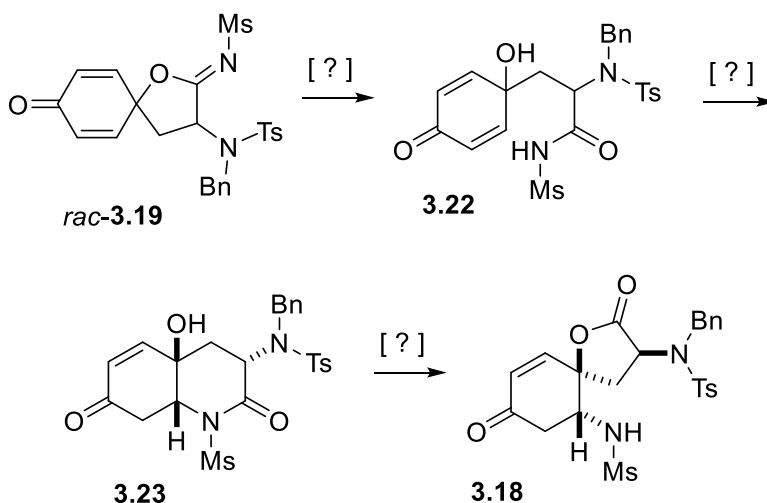


Scheme 3.13 Proposed mechanistic pathway for the formation of *rac*-**3.19**

In support of the above hypothesis, it was determined that compound **3.19**, recovered seemingly unchanged after treatment with 2M HCl in aqueous dioxane at room temperature for 24 hours, had in fact racemized; its optical rotation having changed from $[\alpha]_{\text{D}}^{23} +14$ (c 0.18, acetone) to near zero: $[\alpha]_{\text{D}}^{23} -0.5$ (c 0.18, acetone). This iminolactone-enamido equilibrium may

contribute to the surprising stability of these *N*-sulfonyl iminolactones toward hydrolysis at ambient temperature.

The fact that the mesylamido substituent in **3.18** is *cis* to the alkyl branch of the lactone, suggests the possible intervention of cyclic intermediate **3.23**, which could arise through cyclization of **3.22** (Scheme 3.14).



Scheme 3.14 Proposed mechanistic pathway for the formation of *rac*-**3.18**

A molecular mechanics (MM+) simulation provided support for the preferential formation of **3.24** upon cyclization of **3.22** under reversible conditions, the former containing ca. 3 kcal/mol less energy than its diastereomer **3.25** (Figure 3.6). This difference appears to be the consequence of an unfavorable 1,3-diaxial interaction between the nitrogen functionality and the OH group in the more energetic isomer **3.25**.

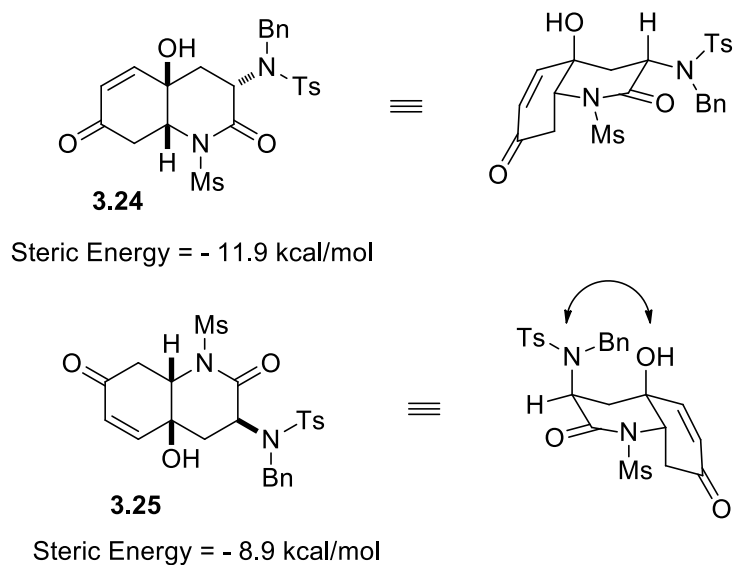
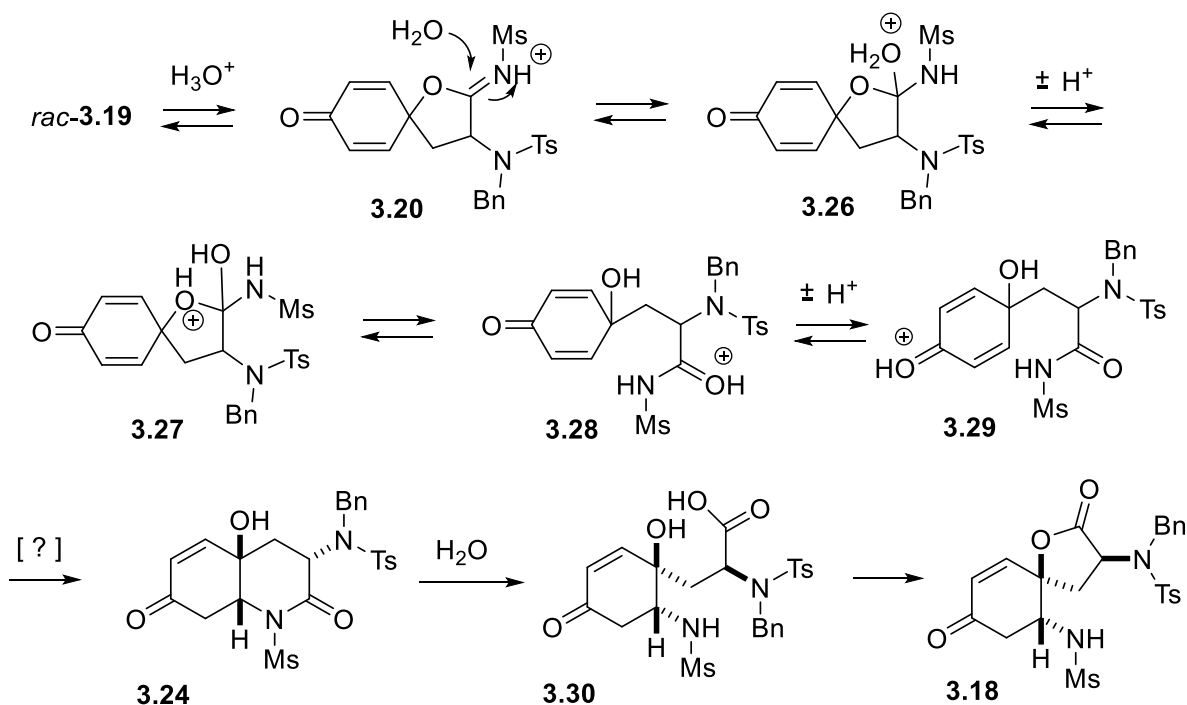


Figure 3.6 Calculated (MM+) steric energies of diastereomers **3.24** and **3.25**

A plausible overall mechanism for the rearrangement of *rac*-**3.19** may thus be as follows:



Scheme 3.15 A possible mechanism for the rearrangement of *rac*-**3.19**

Conclusion

The present work revealed that the oxidative cyclization of *para*-phenolic *N*-acyl-sulfonamides in the presence of (diacetoxyiodo)benzene produces spirocyclic *N*-sulfonyl iminolactones instead of *N*-sulfonyl lactams. This is in sharp contrast to the behavior of similar naphtholic substrates.

Substrate concentration had no effect on the efficiency of formation of *N*-sulfonyl iminolactones, enabling the conduct of such reactions at concentrations of up to 1M. Additionally, a surprising resistance to hydrolysis was observed for these heretofore undocumented *N*-sulfonyl iminolactones. Such a resistance may arise from a facile equilibrium between the iminolactone and its enamide-type tautomer.

Attempts to induce an acid-catalyzed rearrangement of a tyrosine-derived iminolactone revealed that substrate racemizes easily at room temperature, probably through the aforementioned equilibrium. However, a highly diastereoselective rearrangement to a structurally unusual spirolactone was still observed. A mechanistic rationale for this has been provided on the basis of experimental and computational evidence.

References

1. Reviews: (a) Ciufolini, M. A.; Braun, N. A.; Canesi, S.; Ousmer, M.; Chang, J.; Chai, D. *Synthesis*. **2007**, 24, 3759–3772. (b) Pouységu, L.; Deffieux, D.; Quideau, S. *Tetrahedron*. **2010**, 66, 2235.
2. Review: Tohma, H.; Kita, Y. *Adv. Synth. Catal.* **2004**, 346, 111-124.
3. Shuklov, I.A.; Dubrovina, N. V.; Börner, A. *Synthesis*. **2007**, 19, 2925-2943.
4. Kesavan, V.; Bonnet-Delpon, D.; Bégué, J-P. *Tetrahedron Lett.* **2000**, 41, 2895. 128.
5. Cf. Decken, A.; Eisnor, C. R.; Gossage, R. A.; Jackson, S. M. *Inorganica Chimica Acta*. **2006**, 359, 1743.
6. Ousmer, M.; Braun, N. A.; Bavoux, C.; Perrin, M.; Ciufolini, M. A. *J. Am. Chem. Soc.* **2001**, 123, 7534-7538.
7. (a) Knapp, S.; Gibson, F. S. *Org. Synth.* **1992**, 70, 101. (b) Knapp, S. In *Advances in Heterocyclic Natural Product Synthesis*, Vol. 3; Pearson, W. H., Ed.; JAP Press: Greenwich CT, **1996**, Chap. 2.
8. Braun, N. A.; Ousmer, M.; Bray, J. D.; Bouchu, D.; Peters, K.; Peters, E.; Ciufolini, M. A. *J. Org. Chem.* **2000**, 65, 4397-4408.
9. Paladino, M.; Zaifman, J.; Ciufolini, M. A. *Org. Lett.* **2015**, 17, 3422–3425.
10. Canesi, S.; Bouchu, D.; Ciufolini, M. A. *Angew. Chem. Int. Ed.* **2004**, 43, 4336-4338.
11. Scheffler, G.; Seike, H.; Sorensen, E. J.; *Angew. Chem. Int. Ed.* **2000**, 39, 4593-4596.
12. Mizutani, H.; Jun Takayama, J.; Honda, T. *Synlett*. **2005**, 2, 328–330.
13. Liang, H.; Ciufolini, M. A. *Chem. Eur. J.* **2010**, 16, 13262.

14. Kan, T.; Fukuyama, T. *Chem. Commun.* **2004**, 4, 353-539. (b) Canesi, S. *Ph.D. Dissertation*, Université Claude Bernard Lyon 1, **2004**.
15. Liang, H.; Ciufolini, M. A. *Tetrahedron*. **2010**, 66, 5884.
16. Jain, N.; Ciufolini, M. A. *Synlett*. **2015**, 26, 631.
17. Xu, S.; Ciufolini, M. A. *Org. Lett.* **2015**, 17, 2424–2427
18. (a) Ritter, J. J.; Minieri, P. P. *J. Am. Chem. Soc.* **1948**, 70, 4045. (b) Ritter, J. J.; Kalish, J. *J. Am. Chem. Soc.* **1948**, 70, 4048. (c) Krimen, L. I.; Cota, D. J. *Org. React.* **1969**, 17, 213.
19. (a) Canesi, S.; Bouchu, D.; Ciufolini, M. A. *Org. Lett.* **2005**, 7, 175. (b) Liang, H.; Ciufolini, M. A. *J. Org. Chem.* **2008**, 73, 4299. (c) Chau, J.; Ciufolini, M. A. *Org. Synth.* **2013**, 90, 190.
20. Chau, J.; Ciufolini, M. A. *Mar. Drugs*. **2011**, 9, 2046.
21. (a) Cecchi, L.; De Sarlo, F.; Machetti, F. *Chem. Eur. J.* **2008**, 14, 7903. (b) Guideri, L.; De Sarlo, F.; Machetti, F. *Chem. Eur. J.* **2013**, 19, 665.
22. Xu, S.; unpublished results from this laboratory.
23. Hinman, A.; Du Bois, J. *J. Am. Chem. Soc.* **2003**, 125, 11510.
24. (a) Wipf, P.; Jung, J-K. *Chem. Rev.* **1999**, 99, 1469. (b) Canesi, S.; Belmont, P.; Bouchu, D.; Rousset, L.; Ciufolini, M. A. *Tetrahedron Lett.* **2002**, 43, 5193. (c) Rodríguez, S.; Wipf, P. *Synthesis* **2004**, 2767.
25. Boger, D. L.; Ledebor, M. W.; Kume, M. *J. Am. Chem. Soc.* **1999**, 121, 1098-1099.
26. (a) Mendelsohn, B. A.; Lee, S.; Kim, S.; Teyssier, F.; Aulakh, V. S.; Ciufolini, M. A. *Org. Lett.* **2009**, 11, 1539. (b) Xu, S.; unpublished results from this laboratory.
27. We thank Dr. S. Xu for providing quantities of this material for the present study.

28. This study was carried out by M. Ciufolini using the MM+ program provided with the HyperChem® software.
29. Tang, D.; unpublished results from this laboratory.
30. Jain, N.; unpublished results from this laboratory.
31. Ciufolini, M. A.; Sylvain Canesi, S.; Ousmer, M.; Braun, N. A. *Tetrahedron*. **2006**, *62*, 5318-5337.
32. Liang, H. *Ph.D. Dissertation*, University of British Columbia, **2010**.

Appendices

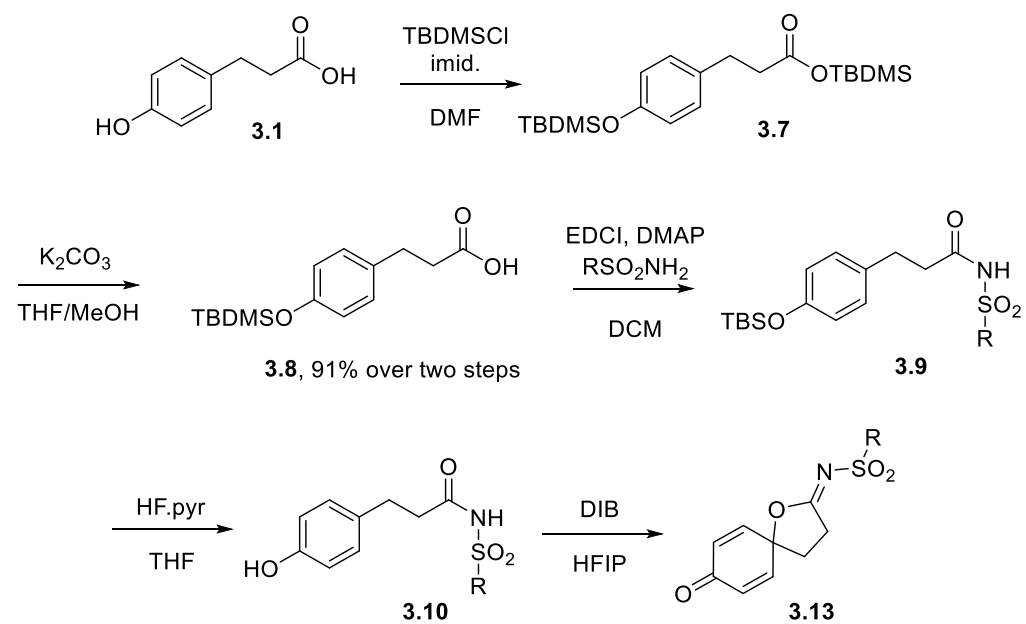
Appendix A: Experimental Section

General. Unless specified otherwise, reactions were performed under dry argon in oven-dried glassware equipped with Teflon™ stirbars. Flasks were fitted with rubber septa for the introduction of substrates, reagents and solvents via syringe in a single portion. Flash chromatography was performed with SiliCycle SiliaFlash® F60 230-400 mesh silica gel. Thin layer chromatography was performed on EMD Silica gel 60 F254 plates and visualized under UV light (254 nm) or by treatment with alkaline KMnO₄ stain. Tetrahydrofuran was distilled from Na/benzophenone, while dichloromethane was distilled over CaH₂ prior to use. All other commercially available chemicals were used without further purification.

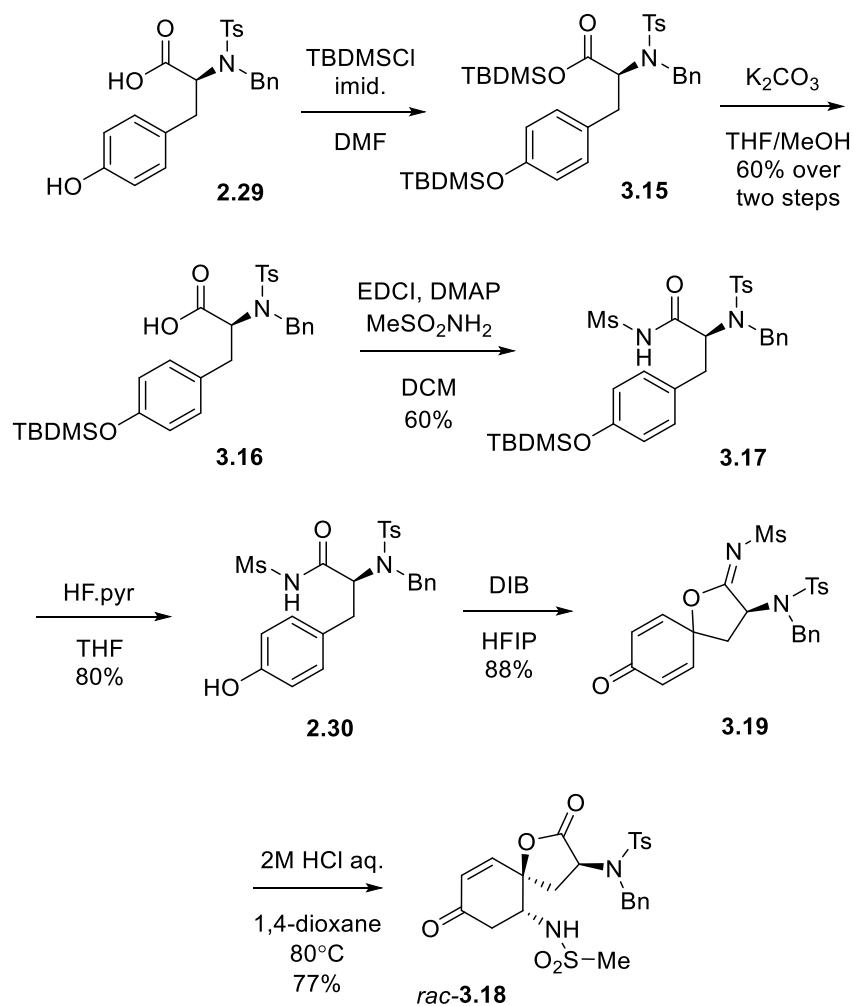
Instrumentation. ¹H and ¹³C NMR spectra were recorded on Bruker model AVANCE II+ 300 (300 MHz for ¹H, 75.5 MHz for ¹³C) spectrometer using deuterioacetone (acetone-*d*₆), deuterated dimethyl sulfoxide (DMSO-*d*₆) or deuterated chloroform (CDCl₃) as the solvent. Some frequencies in the ¹H NMR spectra were left unassigned due to the ambiguity of their assignment or overlap of signals from either multiple non-equivalent protons or protons from presumably rotamers. Chemical shifts are reported in parts per million (ppm) on the scale 88 and coupling constants, J, are in hertz (Hz). Multiplicities are reported as “s” (singlet), “d” (doublet), “dd” (doublet of doublets), “ddd” (doublet of doublets of doublets), “t” (triplet), “q” (quartet), “quin” (quintuplet), “sex” (sextet), “m” (multiplet), and further qualified as “app” (apparent) and “br” (broad). Infrared (IR) spectra (cm⁻¹) were recorded from solution in CHCl₃. Optical rotations were measured at the sodium D line (589 nm). High-resolution mass spectra (m/z) were

recorded in the electrospray (ESI) mode on a Micromass LCT mass spectrometer by the UBC Mass Spectrometry laboratory. Melting points (uncorrected) were measured on a Mel-Temp apparatus. X-ray crystal measurements were made on a Bruker APEX DUO diffractometer by Dr. Brian Pratick of UBC.

A.1. Sequence to various sulfonyl-iminolactones from **3.1**



A.2. Sequence to various sulfonyl-iminolactones from **2.29**



A.3. Preparation of compound **3.7**

Imidazole (0.56 g, 8.23 mmol, 6.0 equiv) was added to a solution of 3-(4-Hydroxyphenyl)propionic acid **3.1** (0.31 g, 1.83 mmol, 1.0 equiv) in DMF (9.15 mL), followed by addition of TBDMSCl (0.83 g, 5.49 mmol, 3.0 equiv). The mixture was stirred at r.t. overnight. Then DMF was evaporated under vacuum. The residue was redissolved in EtOAc (10 mL) to reach a clear solution, washed with water (5 x 5 mL). The organic layer was further washed with brine (3 mL), dried over Na₂SO₄(s) and evaporated. The residue was dried under high vacuum, affording (0.29g, 65% yield) as crude oil and used for the next step without purification.

A.4. Preparation of compound **3.8**

Compound **3.7** (1.00 g, 2.53 mmol, 1.0 equiv) was dissolved in a mixture of 4:3 THF/MeOH (5 mL). K₂CO₃ (0.53 g, 3.80 mmol, 1.5 equiv) was added and the mixture was stirred vigorously at r.t. overnight. The resulting mixture was filtered through Celite®, successively rinse with 1:1 EtOAc/MeOH and concentrated under vacuum. The crude was partitioned between 3:2 water and EtOAc (10 mL) and the pH of aqueous layer was adjusted to pH = 2 (1M HCl). The organic layer was washed once with brine (which was previously acidified to pH = 2 using 1M HCl before combining with the organic layer), dried over Na₂SO₄(s) and evaporated. The crude was dried thoroughly under high vacuum until all the volatile TBDMS-byproduct is removed, yielding a white solid (0.64 g, 91% yield) which is used for the next step without further purification.

A.5. Preparation of compound **3.9a – 3.9f**

To a solution of **3.8** (1.07 mmol, 1.0 equiv) in DCM (5.4 mL) was added EDCI (0.27g, 1.39 mmol, 1.3 equiv), DMAP (0.33 g, 2.89 mmol, 2.7 equiv) and appropriate sulfonamide (1.61 mmol, 1.5 equiv) with good stirring. The reaction mixture was stirred at r.t. overnight, after which time TLC showed that the reaction was complete. The reaction was quenched with 1M HCl to pH = 1 and extracted with dichloromethane (3×10 mL). The combined extracts were washed with brine (10 mL), dried (Na_2SO_4) and evaporated. The residue was dried under high vacuum and purified by flash column chromatography on silica gel depending on the substrate.

A.6. Preparation of compound **3.10a – 3.10f**

To a solution of corresponding **3.9a – 3.9f** (0.33 mmol, 1.0 equiv) in THF (1.65 mL) was added HF.pyridine (1.98 mmol, 6.0 equiv). The reaction mixture was stirred at r.t., monitored by TLC. When the starting material appeared to be fully consumed (from 5 hours to overnight for different sulfonamides), the reaction was quenched with solid Na_2CO_3 , filtered through ca. 2 cm of silica pad, rinsed with corresponding solvent system used for chromatography depending on the substrate. The residue was dried under high vacuum and purified by flash column chromatography (29%EtOAc: 70%Hexanes:1%AcOH) on silica gel. The resulting powder was further purified by recrystallization in DCM/hexanes.

A.7. Preparation of compound **3.13a – 3.13f**

The corresponding precursor among **3.10a – 3.10f** (0.15 mmol, 1.0 equiv) was dissolved in HFIP (2.9 mL), and was then syringed into a flask containing solid (diacetoxyiodo)benzene (52 mg, 0.16 mmol, 1.1 equiv). The mixture was immediately subject to an ultrasonic bath, sonicated for 20 min. The resulting mixture was filtered through 2 cm of silica pad, washed with 50% EtOAc:50% Hexanes. Remove the solvent under vacuum.

A.8. Preparation of compound **3.15**

Imidazole (1.91 g, 28.10 mmol, 6.0 equiv) was added to a solution of tyrosine-derived acid **2.29** (1.99 g, 4.68 mmol, 1.0 equiv) in DMF (23.4 mL), followed by addition of TBDMSCl (2.12 g, 14.05 mmol, 3.0 equiv). The mixture was stirred at r.t. overnight. Then DMF was evaporated under vacuum. The residue was redissolved in EtOAc (30 mL) to reach a clear solution, washed with water (5 x 15 mL). The organic layer was further washed with brine (10 mL), dried over Na₂SO₄(s) and evaporated. The residue was dried under high vacuum, affording (2.61g, 85% crude yield) as crude oil and used for the next step without purification.

A.9. Preparation of compound **3.16**

Compound **3.15** (2.61 g, 3.99 mmol, 1.0 equiv) was dissolved in a mixture of 4:3 THF/MeOH (40 mL). K₂CO₃ (0.53 g, 5.98 mmol, 1.5 equiv) was added and the mixture was stirred vigorously at r.t. for 7 hrs. The resulting mixture was filtered through Celite® and concentrated under vacuum. The crude was redissolved in EtOAc and acidified to pH = 2 (1M HCl). The

aqueous layer was extract thoroughly with EtOAc. The organic layers were combined and dried over $\text{Na}_2\text{SO}_4(\text{s})$ and evaporated. The crude was purified by flash column chromatography on silica gel (3:2 pentane/acetone, $R_f = 0.6$), yielding a yellow oil (1.52 g, 60% yield).

A.10. Preparation of compound **3.17**

To a solution of **3.16** (0.84g, 1.56 mmol, 1.0 equiv) in DCM (7.8 mL) was added EDCI (0.39g, 2.03 mmol, 1.3 equiv), DMAP (0.52 g, 4.22 mmol, 2.7 equiv) and mesyl sulfonamide (0.22 g, 2.33 mmol, 1.5 equiv) with good stirring. The reaction mixture was stirred at r.t. overnight, after which time TLC showed that the reaction was complete. The reaction was quenched with 1M HCl to pH = 1 and extracted with DCM (3×15 mL). The combined extracts were washed with brine (15 mL), dried (Na_2SO_4) and evaporated. The residue was dried under high vacuum and purified by flash column chromatography on silica gel (3:2 pentane/acetone, $R_f = 0.75$), yielding a light yellow solid (1.52 g, 60% yield).

A.11. Preparation of compound **2.30**

To a solution of corresponding **3.17** (0.11 g, 0.18 mmol, 1.0 equiv) in THF (0.92 mL) was added HFpyridine (0.03 mL, 1.10 mmol, 6.0 equiv). The reaction mixture was stirred at r.t overnight, after which time TLC showed that the reaction was complete. The reaction was quenched with solid Na_2CO_3 after being stirred overnight. The mixture was diluted with EtOAc, filtered through ca. 2 cm of silica pad, rinsed thoroughly with excess EtOAc. The residue was dried

under high vacuum and could be gradually recrystallized from 3:2 pentane/acetone, yielding a white solid (74 mg, 80% yield).

A.12. Preparation of compound **3.19**

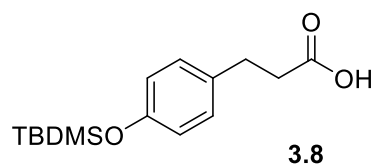
The corresponding precursor among **2.30** (9.3 mg, 0.02 mmol, 1.0 equiv) was dissolved in HFIP (0.37 mL), and was then syringed into a flask containing solid (diacetoxyiodo)benzene (6.56 mg, 0.02 mmol, 1.1 equiv). The mixture was immediately subject to an ultrasonic bath, sonicated for 20 min. The resulting mixture was filtered through 2 cm of silica pad, washed with 50% EtOAc:50% Hexanes. Remove the solvent under vacuum, yielding a white solid (8.2 mg, 88% yield).

A.13. Preparation of compound *rac*-**3.18**

Compound **3.19** (0.10 g, 0.20 mmol, 1.0 equiv) was dissolved in 1,4-dioxane (4.0 mL), followed by addition of 2M HCl (0.3 mL, 3 equiv). The mixture was vigorously stirred at 80°C overnight. The resulting mixture was quenched with saturated NaHCO₃(aq.) to pH = 8, extracted with EtOAc (3 x 5 mL). The organic layers were combined and dried over Na₂SO₄(s). Remove the solvent under vacuum. Recrystallize from DCM/hexanes. (0.08 g, 77% yield).

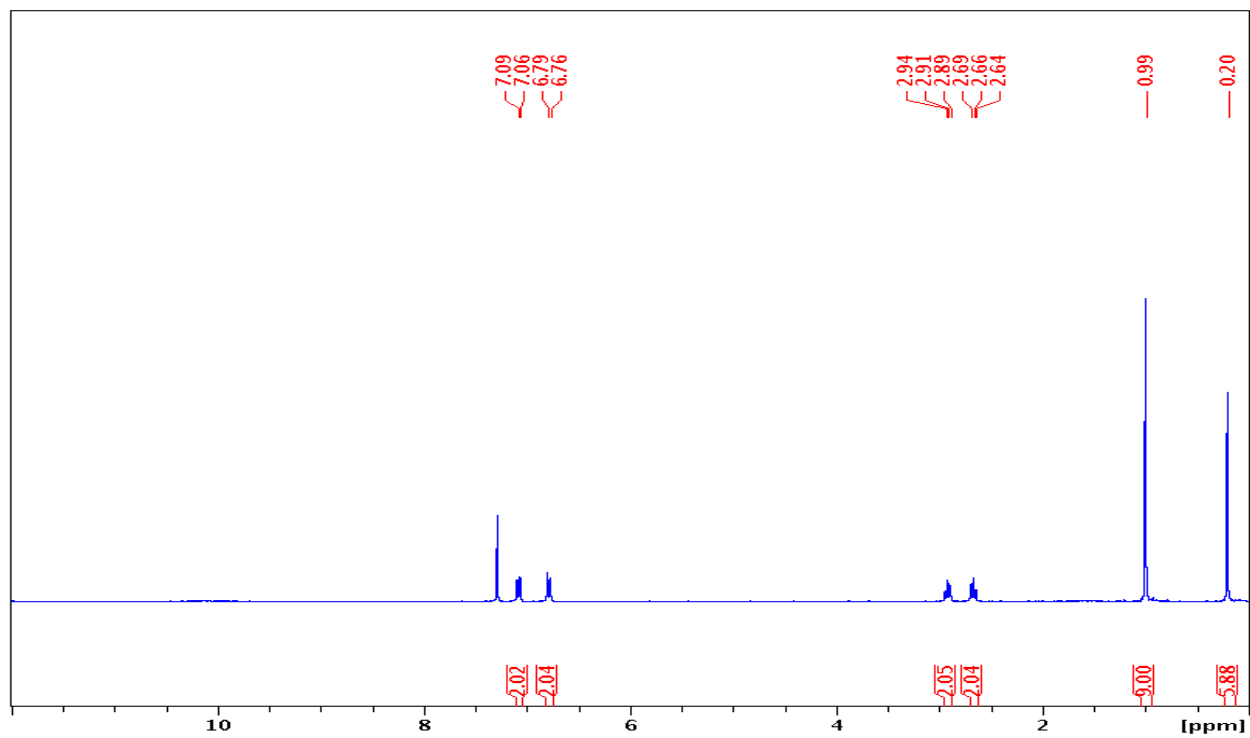
Appendix B: Experimental Data and Spectra

B.1. Experimental data of various intermediates to sulfonyl-iminolactones **3.13**

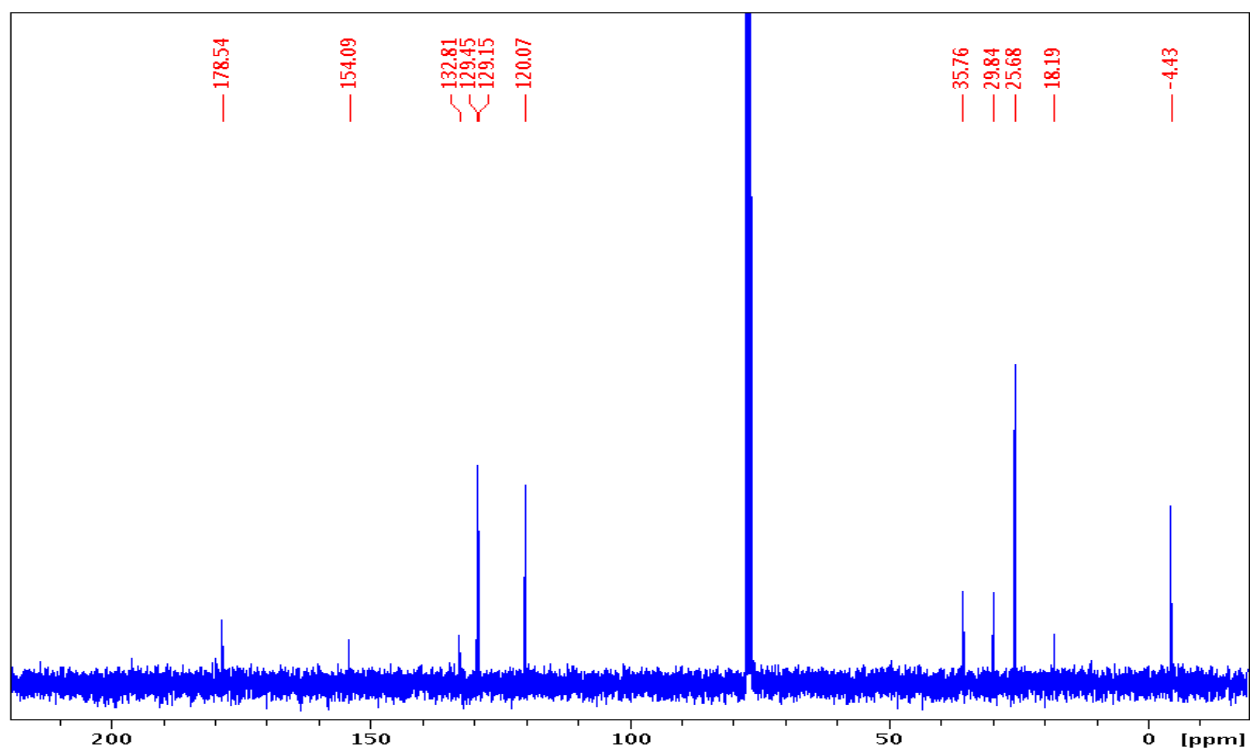


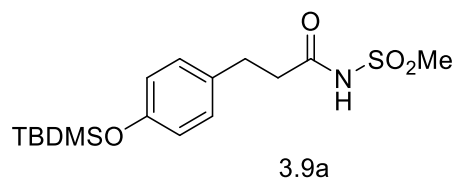
Compound 3.8: 0.64 g (91% yield) from 1.00 g of **3.1**, white solid, m.p.: 72-73°C. **IR:** 2928 (broad), 1701. **¹H:** 7.08 (d, 2H, $J = 8.4$), 6.78 (d, 2H, $J = 8.4$), 2.91 (t, 2H, $J = 8.0$), 2.66 (t, 2H, $J = 8.0$), 0.99 (s, 9H), 0.20 (s, 6H). **¹³C:** 178.5, 154.1, 132.8, 129.2, 120.1, 35.8, 29.8, 25.7, 18.2, -4.4. **HRMS:** calcd for C₁₅H₂₄O₃SSiNa [M+Na]⁺: 303.1392; found: 303.1381.

^1H NMR spectrum of **3.8** (300 MHz, CDCl_3)



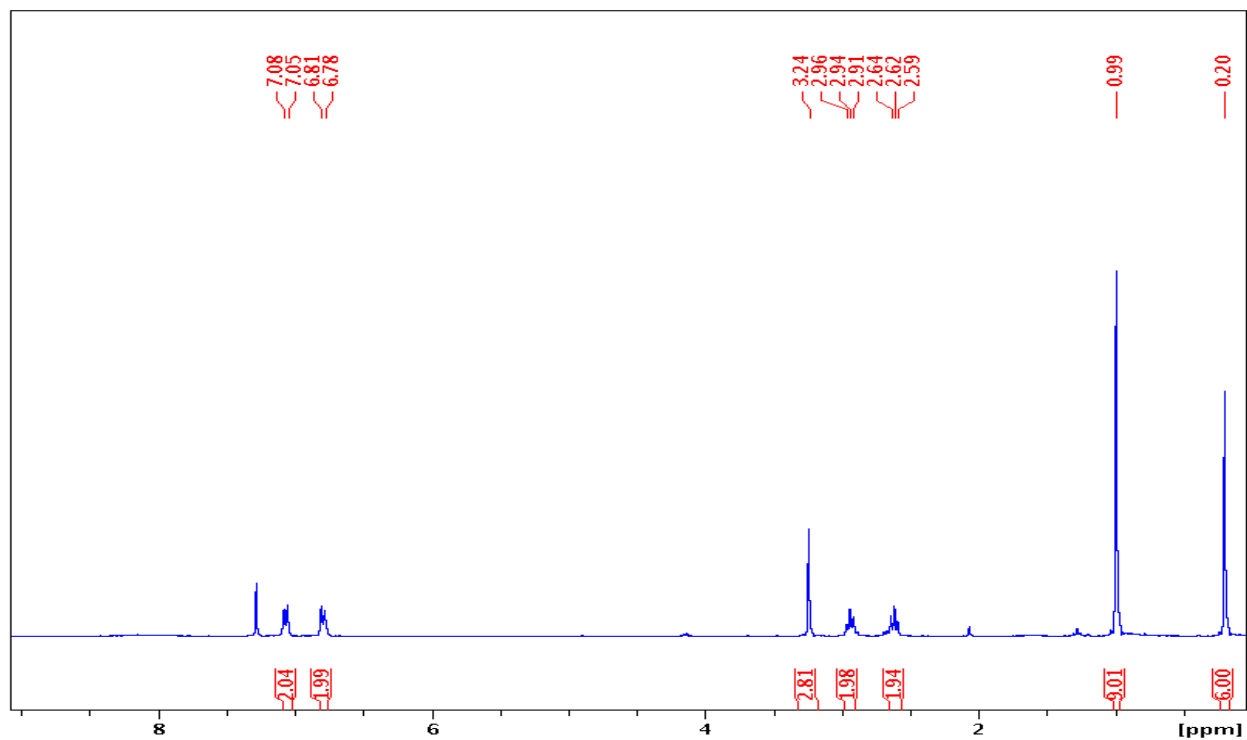
^{13}C NMR spectrum of **3.8** (75 MHz, CDCl_3)



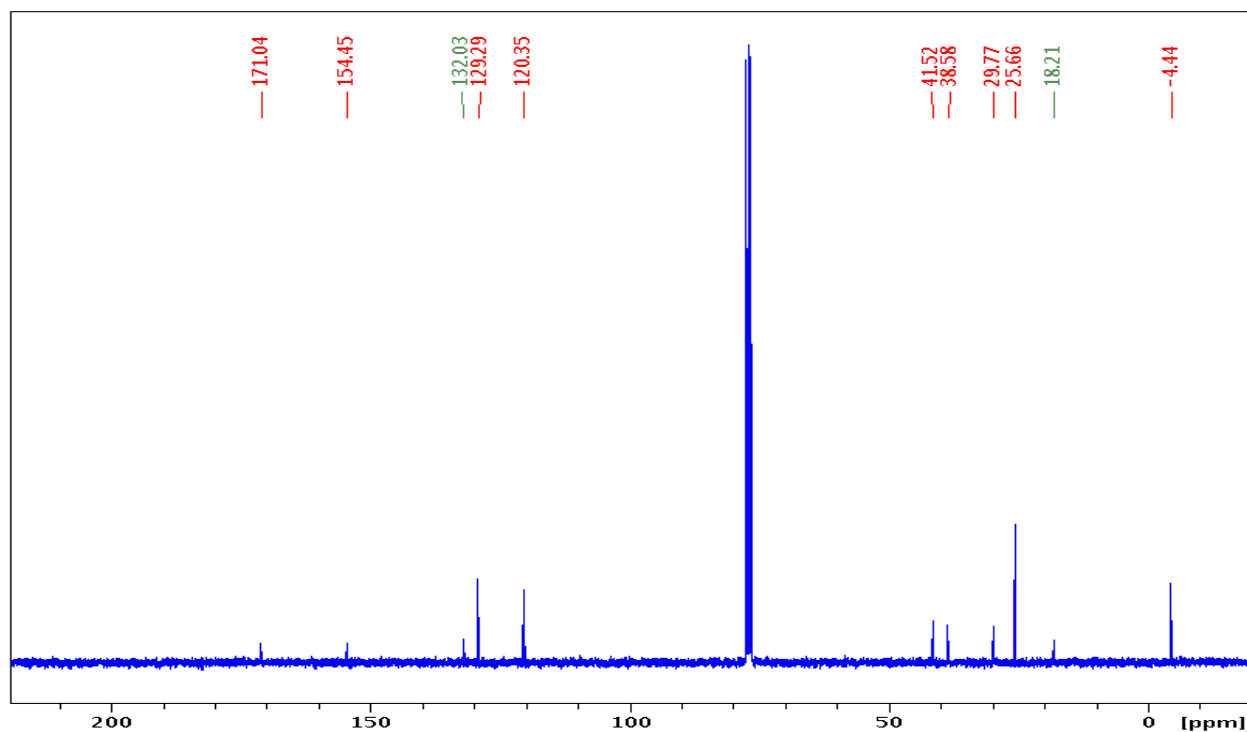


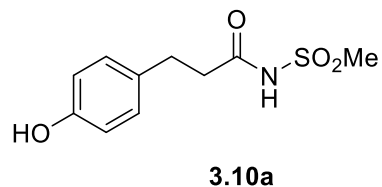
Compound 3.9a: 0.54 g (85% yield) from 0.51 g of **3.8**, off-white solid, m.p.: 84-85°C. **IR:** 3227 (broad), 1710. **¹H:** 7.06 (d, 2H, *J* = 8.3), 6.79 (d, 2H, *J* = 8.2), 3.24 (s, 3H), 2.94 (t, 3H, *J* = 7.5), 2.61 (t, 3H, *J* = 7.5), 0.99 (s, 9H), 0.20 (s, 6H). **¹³C:** 171.0, 154.5, 132.0, 129.3, 120.4, 41.5, 38.6, 29.8, 25.7, 18.2, -4.4. **HRMS:** calcd for C₁₆H₂₈NO₄SSi [M+H]⁺: 358.1508; found: 358.1510.

^1H NMR spectrum of **3.9a** (300 MHz, CDCl_3)



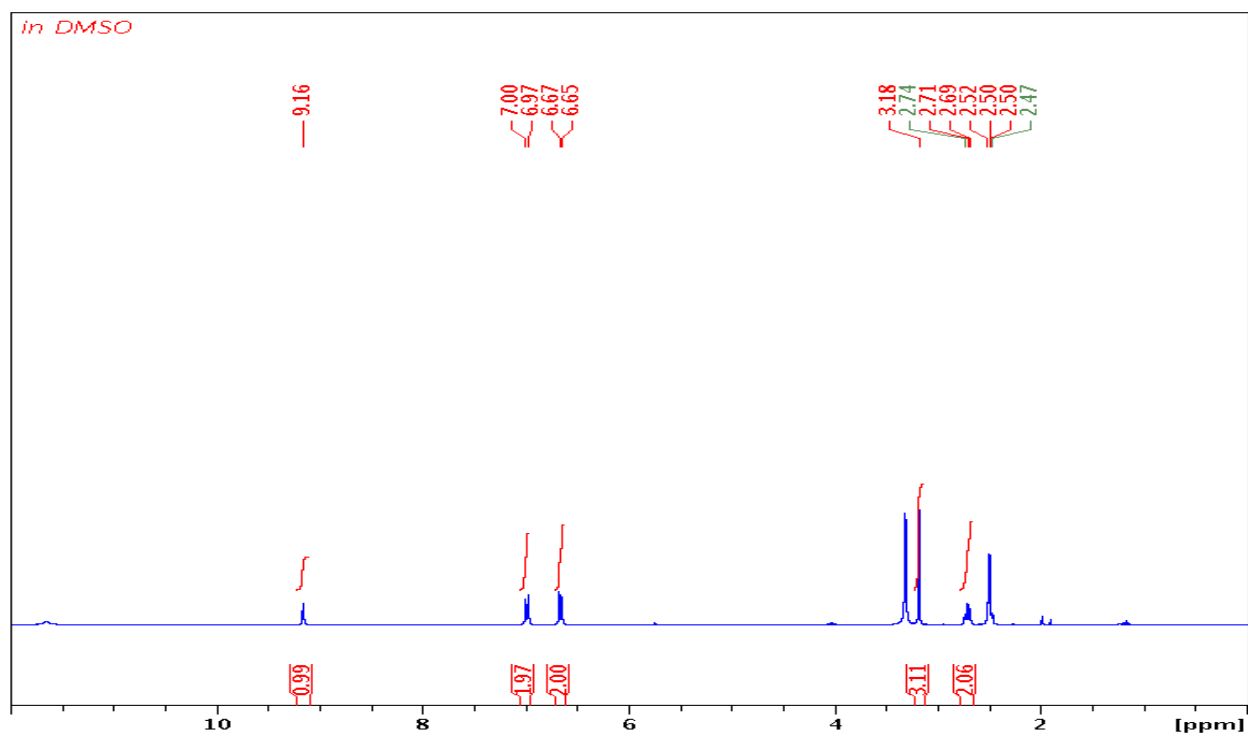
^{13}C NMR spectrum of **3.9a** (300 MHz, CDCl_3)



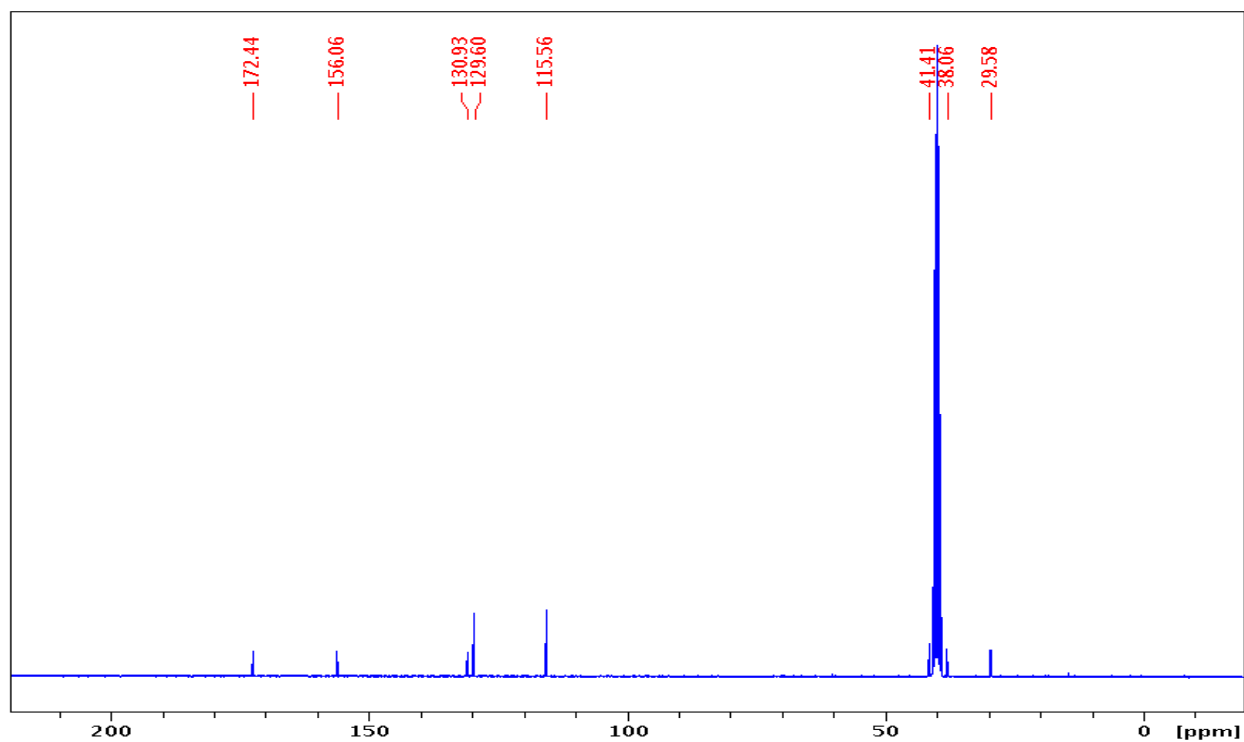


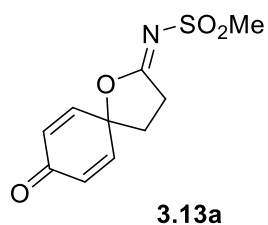
Compound 3.10a: 0.28 g (77% yield) from 0.54 g of **3.9a**, white solid, m.p.: 129°C. **IR:** 3248 (broad), 1724. **¹H (DMSO-*d*₆):** 9.16 (br, s, 1H), 6.99 (d, 2H, *J* = 8.4), 6.66 (d, 2H, *J* = 8.4), 3.18 (s, 3H), 2.71 (t, 2H, *J* = 7.5), 2.50 (t, 2H, *J* = 7.5). **¹³C (DMSO-*d*₆):** 172.4, 156.1, 130.9, 129.6, 115.6, 41.4, 38.1, 29.6. **HRMS:** found for C₁₀H₁₂NO₄S [M-H]⁻: 242.0486.

^1H NMR spectrum of **3.10a** (300 MHz, DMSO- d_6)



^{13}C NMR spectrum of **3.10a** (75 MHz, DMSO- d_6)

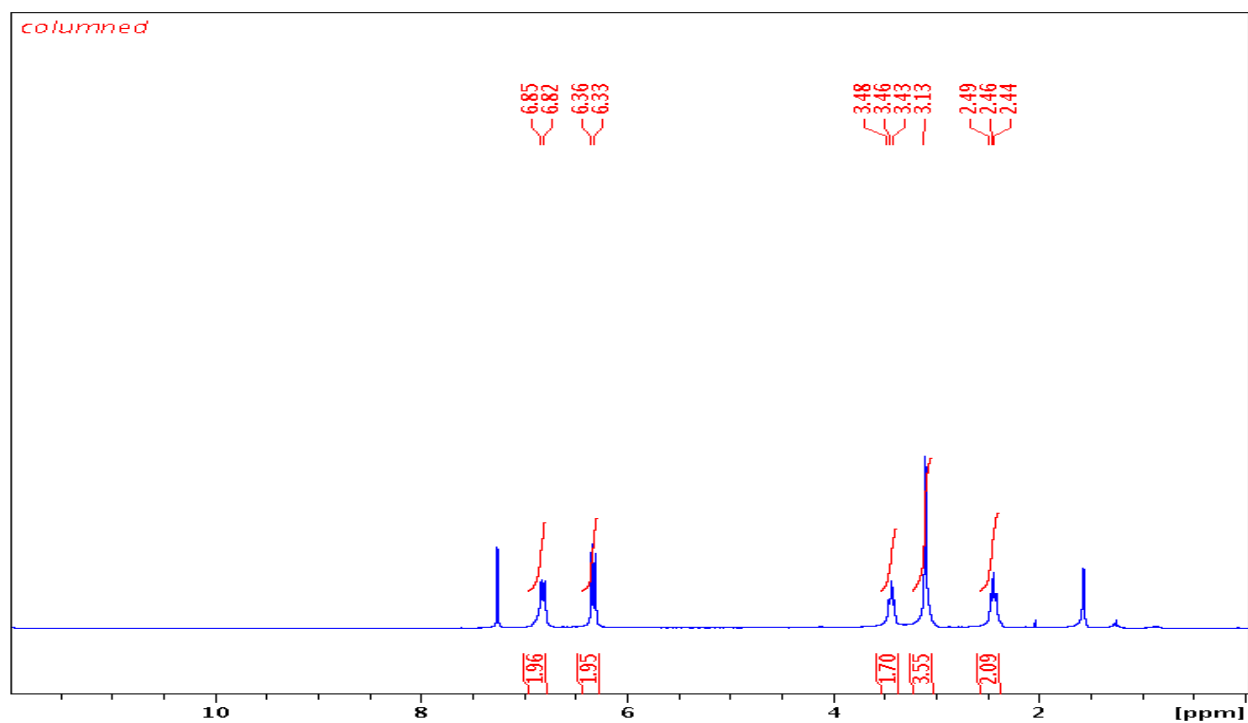




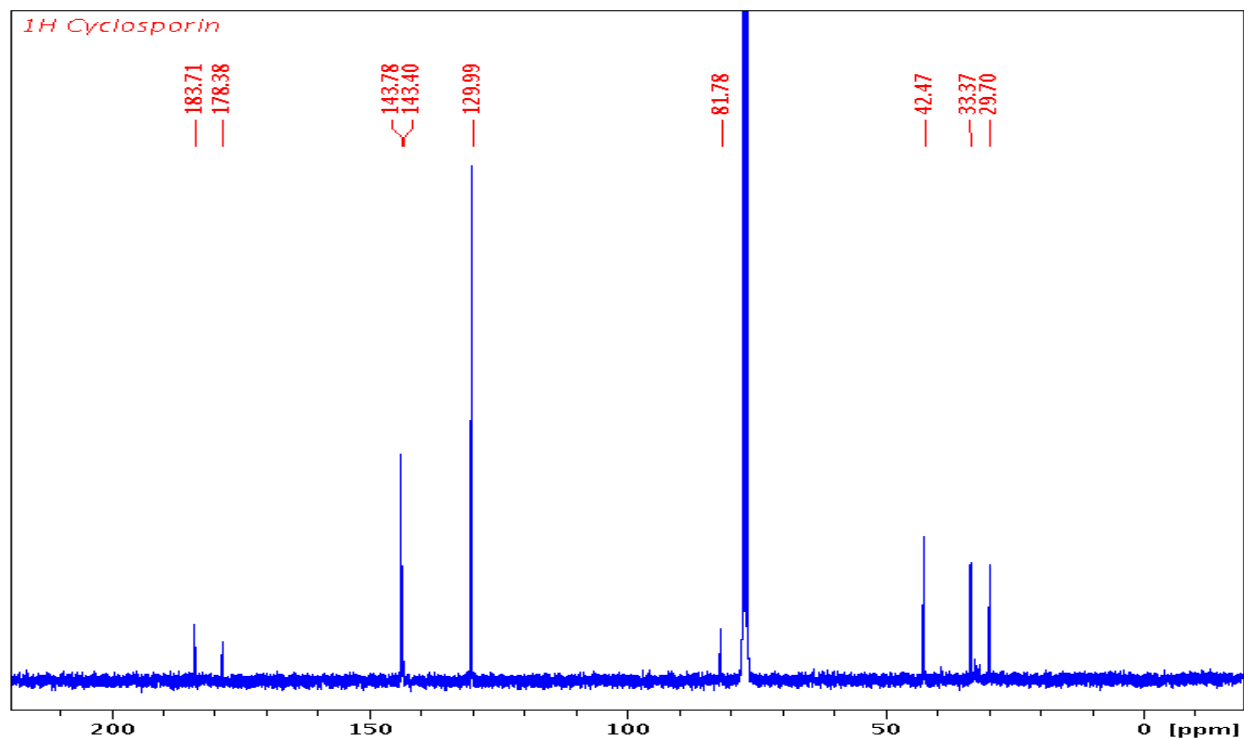
Compound 3.13a: 18.1 mg (93% yield) from 19.6 mg of **3.10a**, white solid, m.p.: 166-168°C.

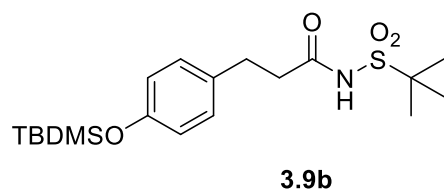
IR: 3024, 1674, 1630. **¹H:** 6.84 (d, 2H, *J* = 9.9), 6.35 (d, 2H, *J* = 10.0), 3.46 (t, 2H, *J* = 8.1), 3.13 (s, 3H), 2.71 (t, 2H, *J* = 8.1). **¹³C:** 183.7, 178.4, 143.8, 130.0, 81.8, 42.5, 33.4, 29.7. **HRMS:** calcd for C₁₀H₁₀NO₄S [M-H]⁻: 240.0331; found: 240.0337.

^1H NMR spectrum of **3.13a** (300 MHz, CDCl_3)



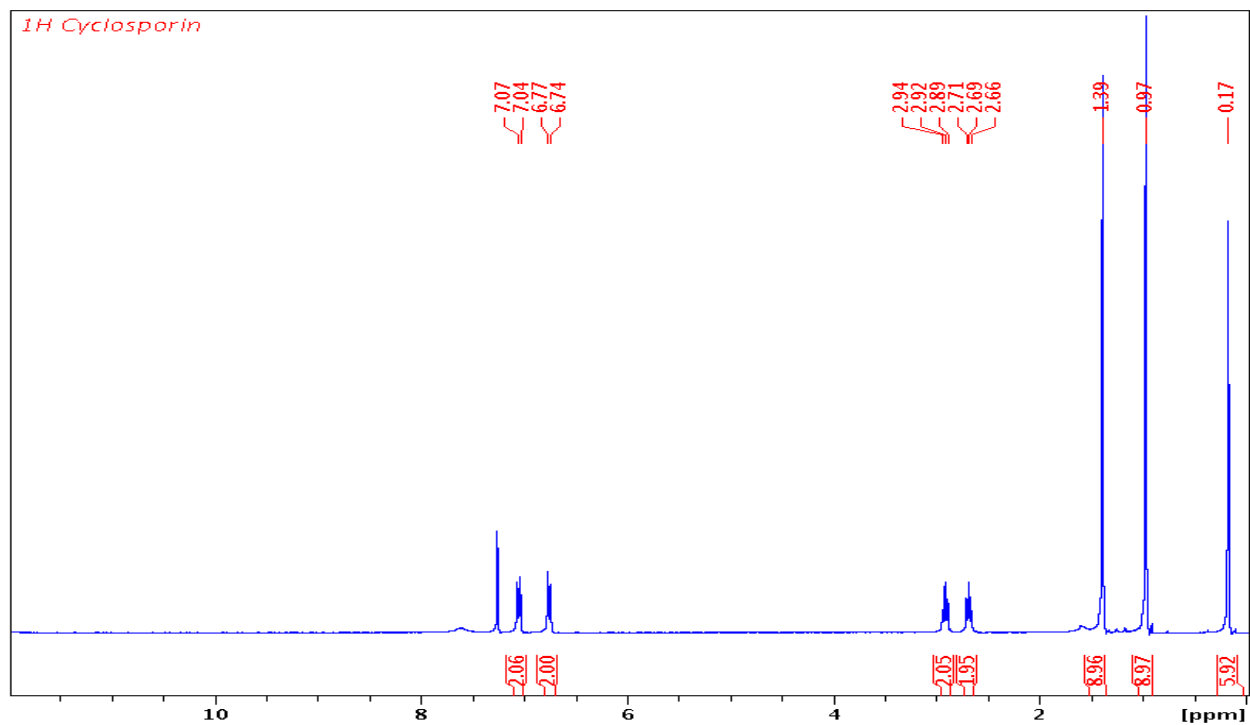
^{13}C NMR spectrum of **3.13a** (75 MHz, CDCl_3)



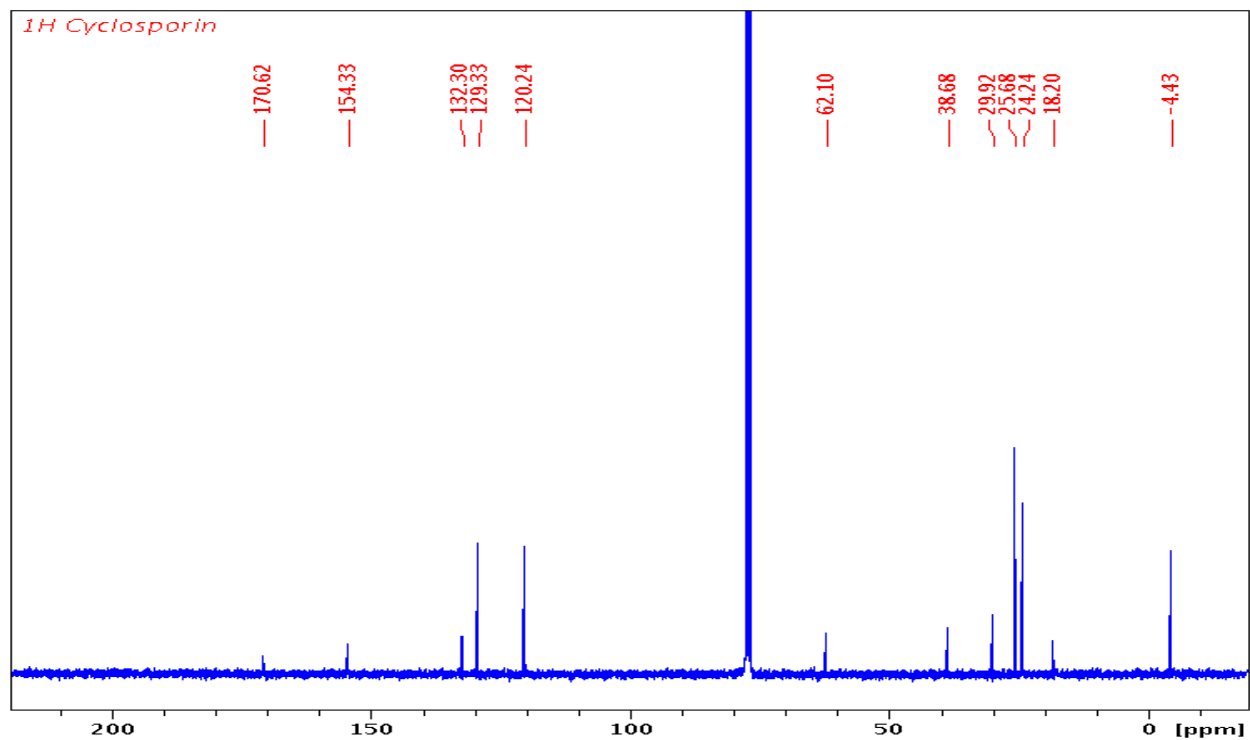


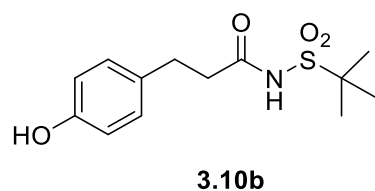
Compound 3.9b: 0.20 g (51% yield) from 0.30 g of **3.8**, colorless oil. **IR:** 3241 (broad), 1706. **¹H:** 7.06 (d, 2H, *J* = 8.3), 6.76 (d, 2H, *J* = 8.3), 2.92 (t, 2H, *J* = 7.4), 2.691 (t, 2H, *J* = 7.3), 1.39 (s, 9H), 0.97 (s, 9H), 0.17 (s, 6H). **¹³C:** 170.6, 154.3, 132.3, 129.3, 120.2, 62.1, 38.7, 29.9, 25.7, 24.2, 18.2, -4.4. **HRMS:** calcd for C₁₉H₃₃NO₄SSiNa [M+Na]⁺: 422.1797; found: 422.1792.

^1H NMR spectrum of **3.9b** (300 MHz, CDCl_3)



^{13}C NMR spectrum of **3.9b** (75 MHz, CDCl_3)

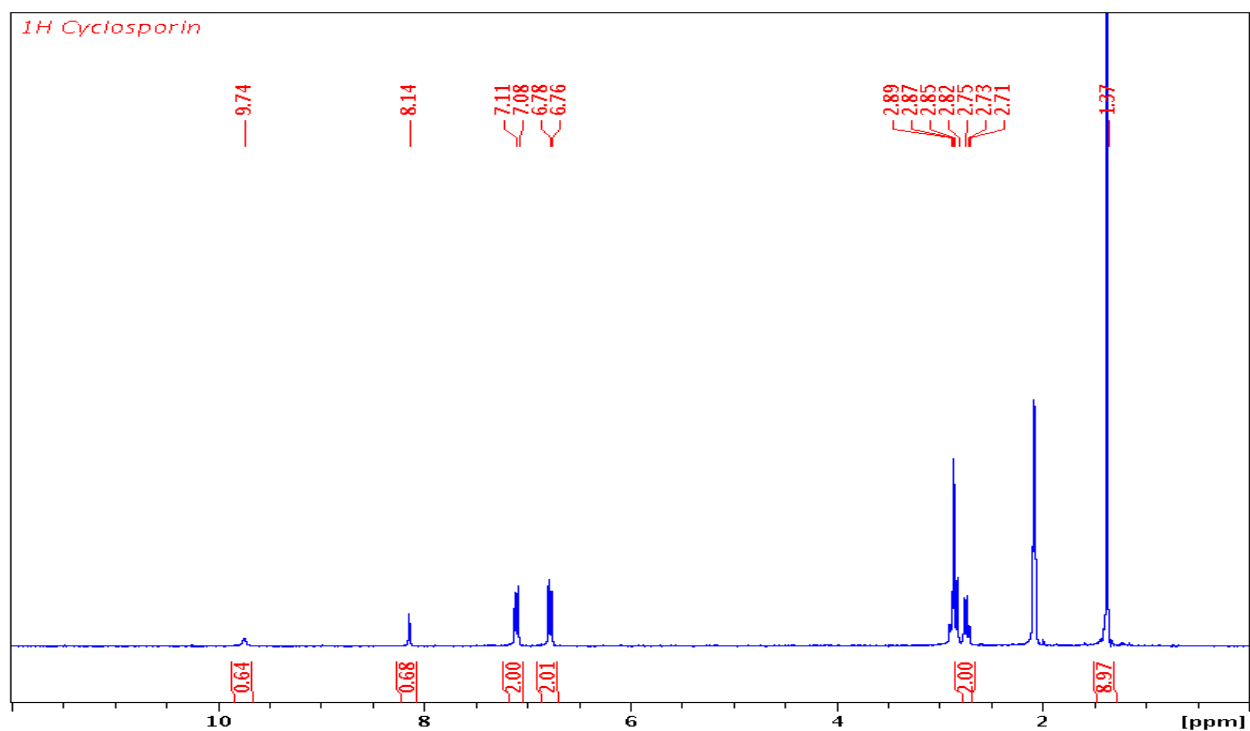




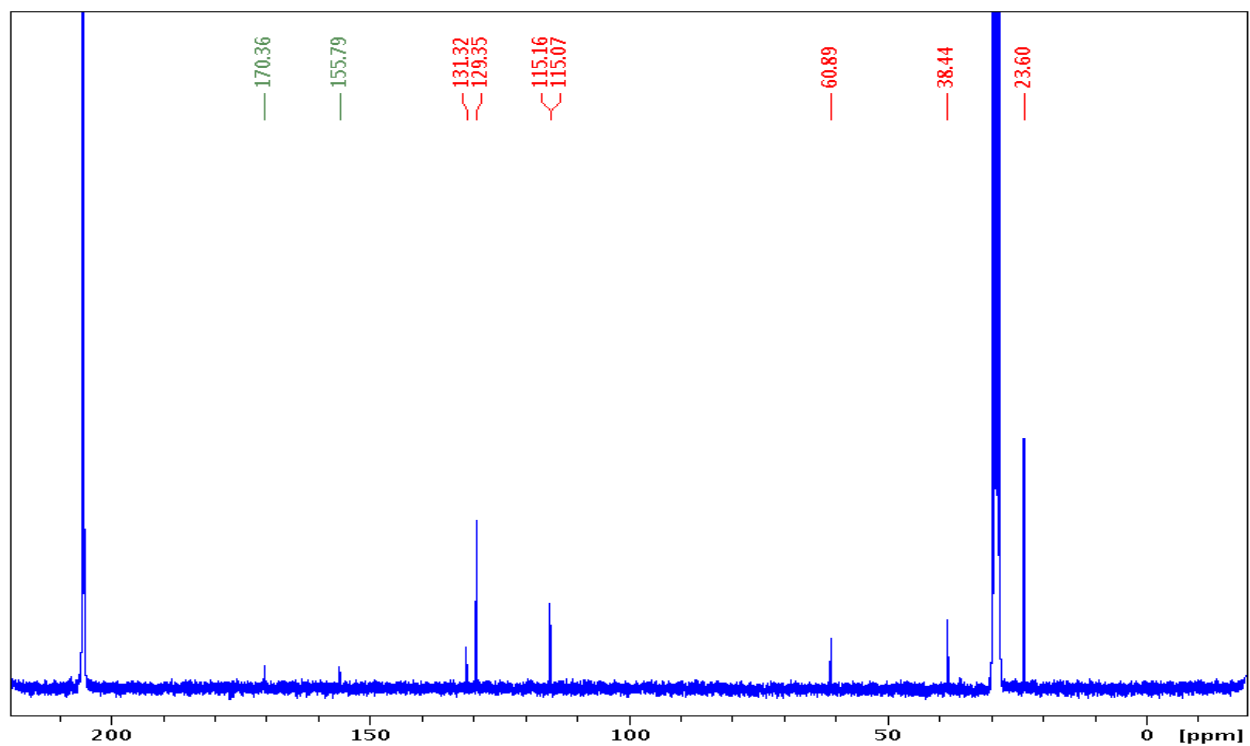
Compound 3.10b: 0.14 g (99% crude yield) from 0.19 g of **3.9b**, white solid, m.p.: 137-138°C.

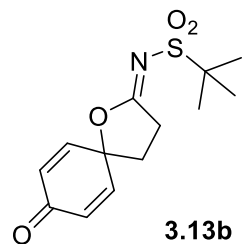
IR: 3447 (broad), 3239 (broad), 1709. **¹H (acetone-*d*₆):** 9.74 (br, s, 1H), 8.14 (br, s, 1H), 7.10 (d, 2H, *J* = 8.4), 6.77 (d, 2H, *J* = 8.4), 2.87 (t, 3H, *J* = 7.3), 2.73 (t, 3H, *J* = 7.3), 1.37 (s, 9H). **¹³C (acetone-*d*₆):** 170.4, 155.8, 131.3, 129.35, 115.2, 115.1, 60.9, 38.4, 23.6. **HRMS:** calcd for C₁₃H₁₈NO₄S [M-H]⁻: 284.0957; found: 284.0956.

^1H NMR spectrum of **3.10b** (300 MHz, acetone- d_6)



^{13}C NMR spectrum of **3.10b** (75 MHz, acetone- d_6)



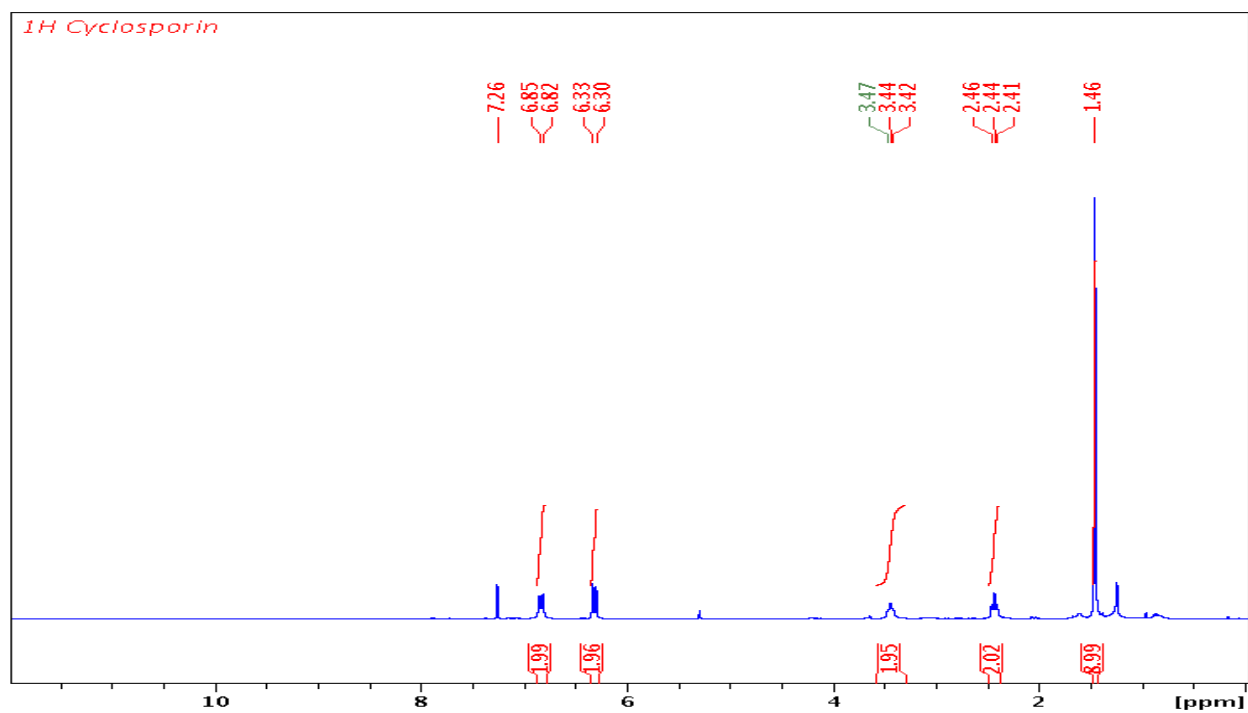


Compound 3.13b: 11.8 mg (86% yield) from 13.4 mg of **3.10b**, white solid, m.p.: 186-187°C.

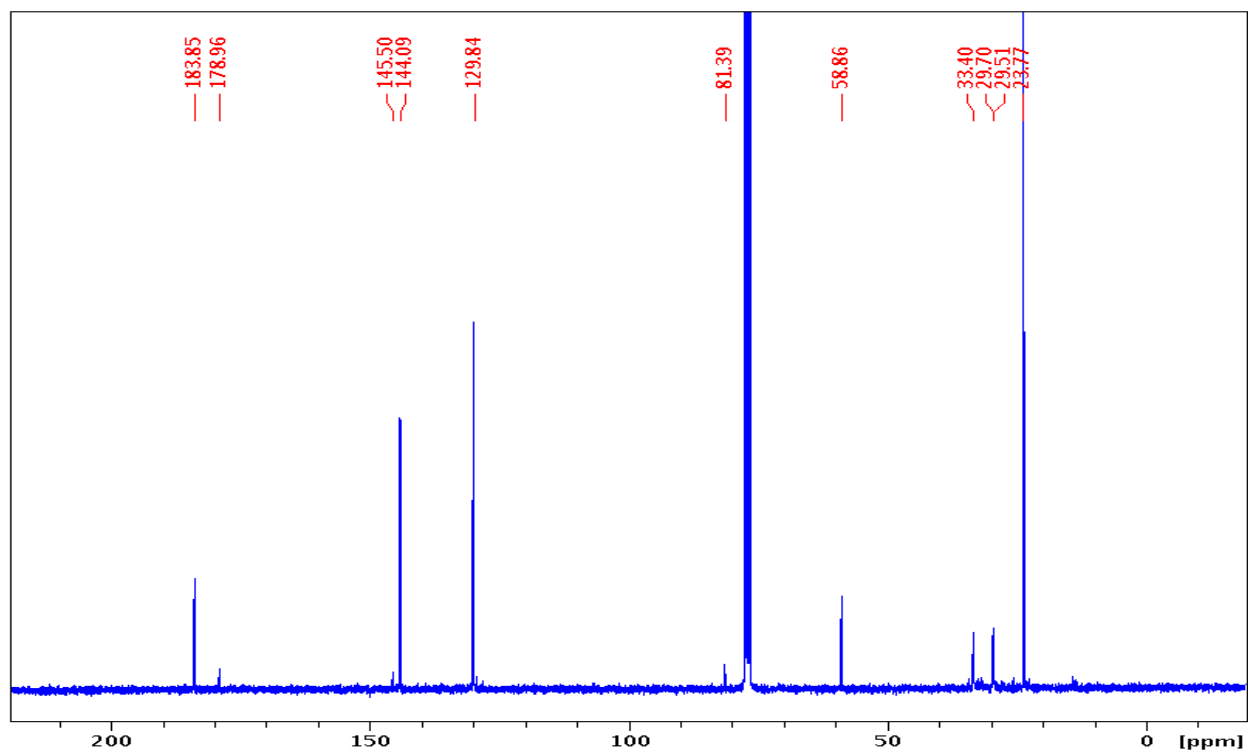
IR: 2984, 1674, 1634. **¹H:** 6.84 (d, 2H, *J* = 9.8), 6.31 (d, 2H, *J* = 9.8), 3.44 (t, 2H, *J* = 7.4), 2.44 (t, 2H, *J* = 7.9), 1.46 (s, 9H). **¹³C:** 183.9, 179.0, 145.5, 144.1, 130.0, 81.4, 58.9, 33.4, 29.5, 23.8.

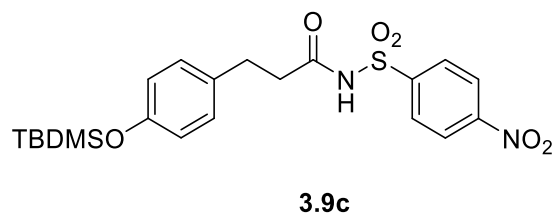
HRMS: calcd for C₁₃H₁₆NO₄S [M-H]⁻: 282.0800; found: 282.0804.

^1H NMR spectrum of **3.13b** (300 MHz, CDCl_3)



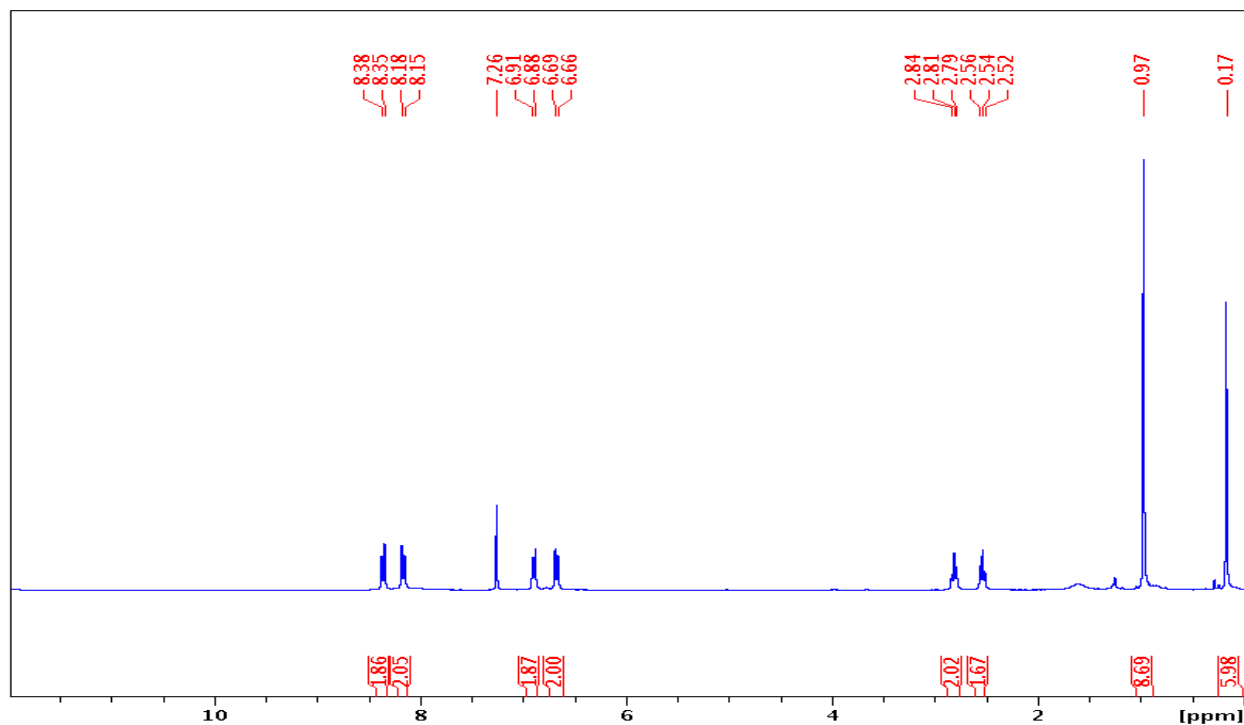
^{13}C NMR spectrum of **3.13b** (75 MHz, CDCl_3)



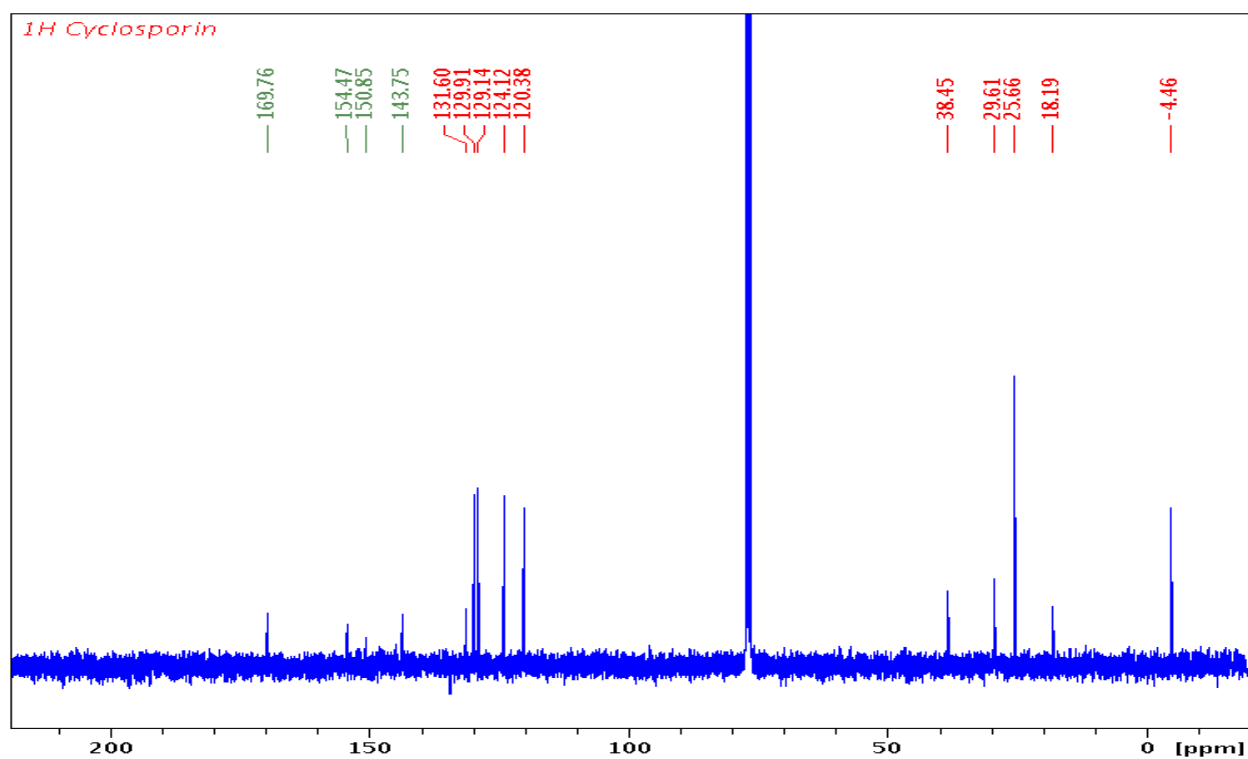


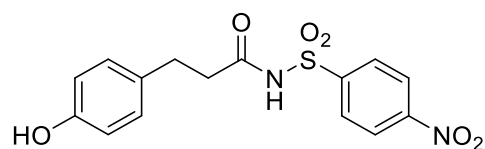
Compound 3.9c: 0.37 g (75% yield) from 0.3 g of **3.8**, yellow solid, m.p.: 52-53°C. **IR:** 3236, 1700, 1511, 1349. **¹H:** 8.37 (d, 2H, *J* = 8.7), 8.17 (d, 2H, *J* = 8.7), 6.90 (d, 2H, *J* = 8.2), 6.68 (d, 2H, *J* = 8.2), 2.81 (t, 2H, *J* = 7.3), 2.54 (t, 2H, *J* = 7.3), 0.97 (s, 9H), 0.17 (s, 6H). **¹³C:** 169.8, 154.5, 150.9, 143.8, 131.6, 130.0, 129.1, 124.1, 120.4, 38.5, 29.6, 25.7, 18.2, -4.5. **HRMS:** calcd for C₂₁H₂₇N₂O₆SSi [M-H]⁻: 463.1359; found: 463.1353.

^1H NMR spectrum of **3.9c** (300 MHz, CDCl_3)



^{13}C NMR spectrum of **3.9c** (75 MHz, CDCl_3)

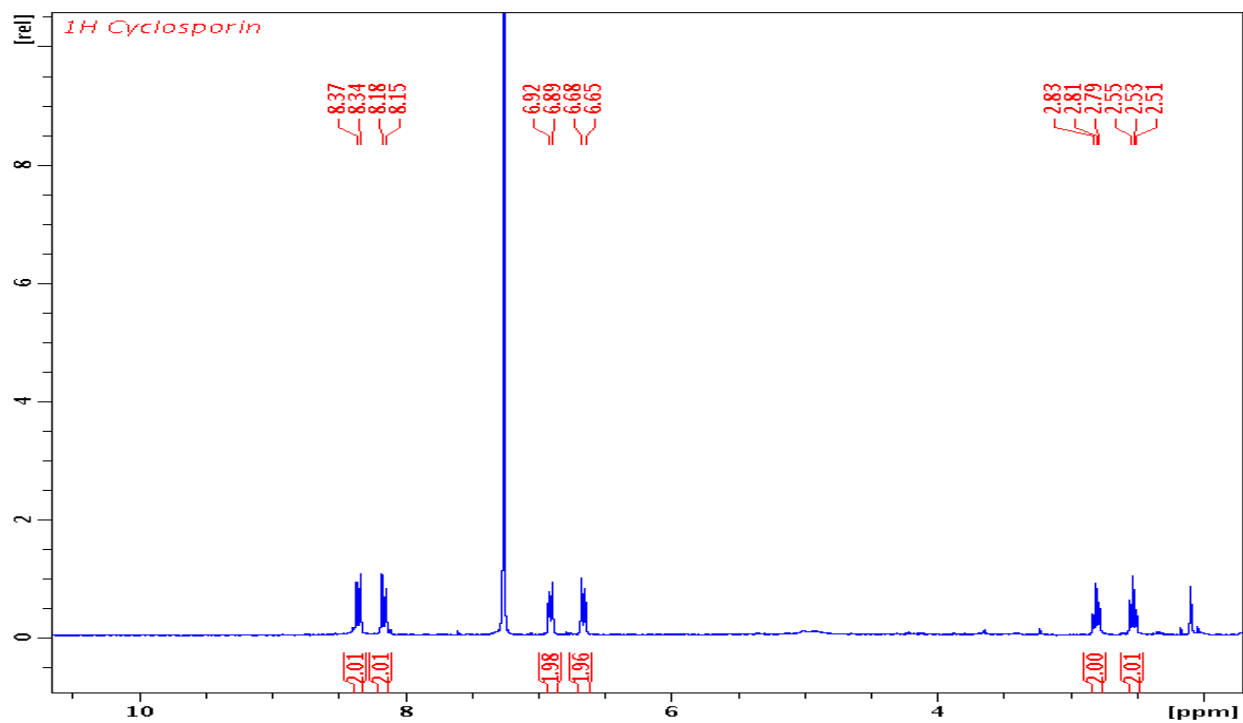




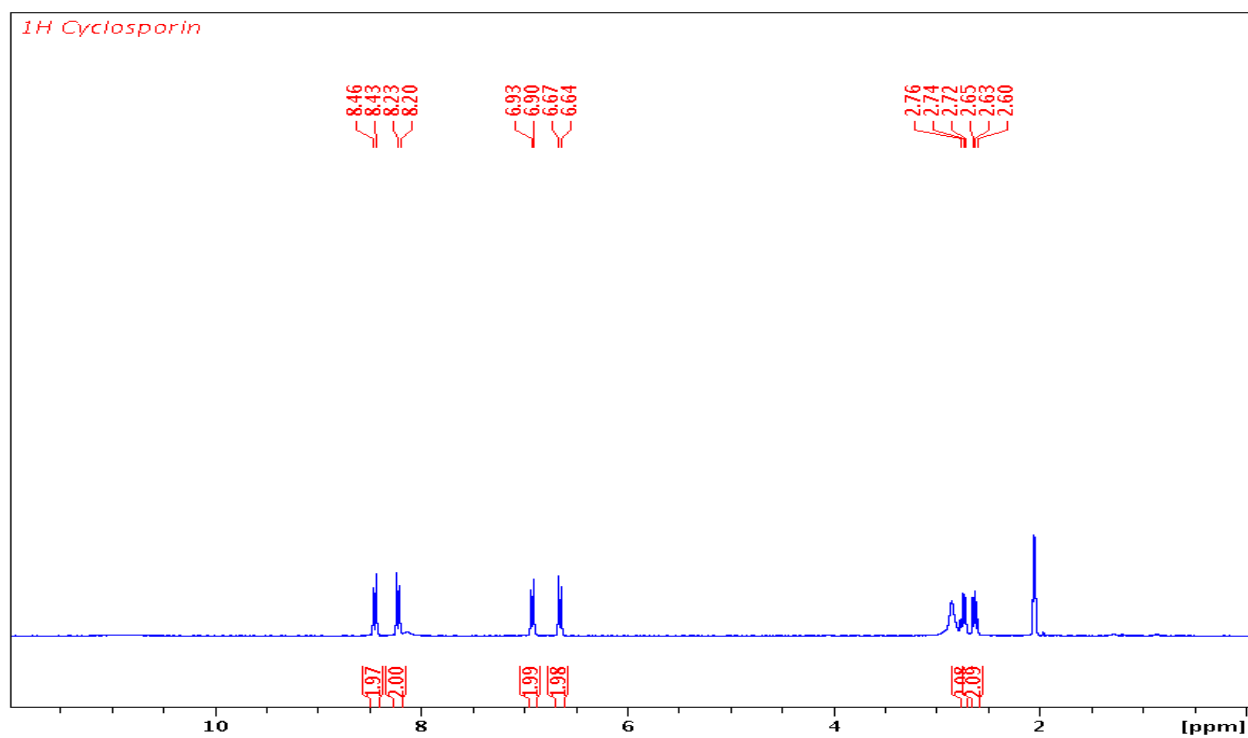
3.10c

Compound 3.10c: 25 mg (80% yield) from 41 mg of **3.9c**, white needle-shaped crystals (flash column chromatography 50%EtOAc:50%Hexanes; recrystallized from DCM/ hexanes), m.p.: 131°C. **IR:** 3473 (broad), 3250 (broad), 1706, 1531, 1350. **¹H:** 8.36 (d, 2H, $J = 8.8$), 8.17 (d, 2H, $J = 8.8$), 6.91 (d, 2H, $J = 8.4$), 6.67 (d, 2H, $J = 8.4$), 2.81 (t, 2H, $J = 7.4$), 2.53 (t, 2H, $J = 7.4$). **¹H (acetone-*d*₆):** 8.45 (d, 2H, $J = 8.8$), 8.22 (d, 2H, $J = 8.8$), 6.92 (d, 2H, $J = 8.5$), 6.66 (d, 2H, $J = 8.4$), 2.74 (t, 2H, $J = 7.4$), 2.63 (t, 2H, $J = 7.4$). **¹³C (acetone-*d*₆):** 171.6, 156.8, 151.8, 146.0, 131.8, 130.6, 130.2, 125.1, 116.1, 38.8, 30.3. **HRMS:** calcd for C₁₅H₁₄N₂O₆SNa [M+Na]⁺: 373.0470; found: 373.0472.

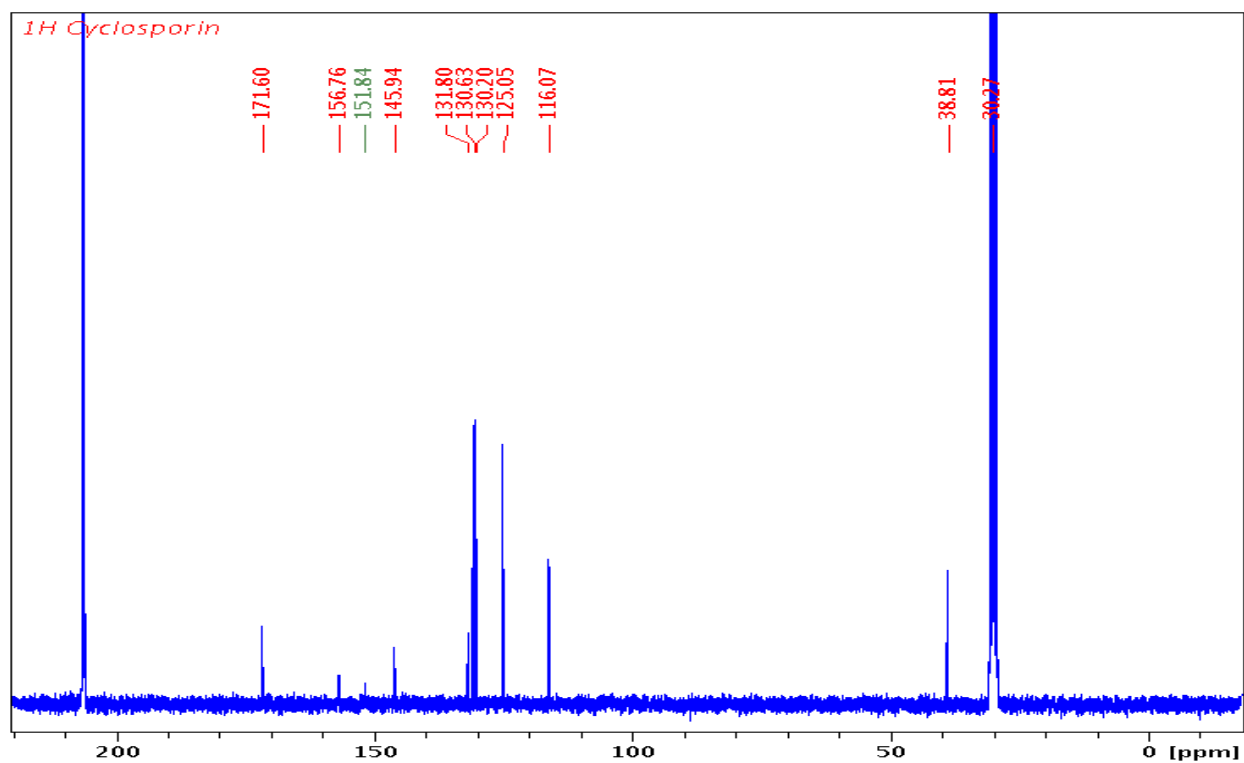
^1H NMR spectrum of **3.10c** (300 MHz, CDCl_3)

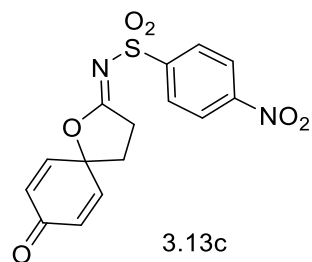


^1H NMR spectrum of **3.10c** (300 MHz, acetone- d_6)



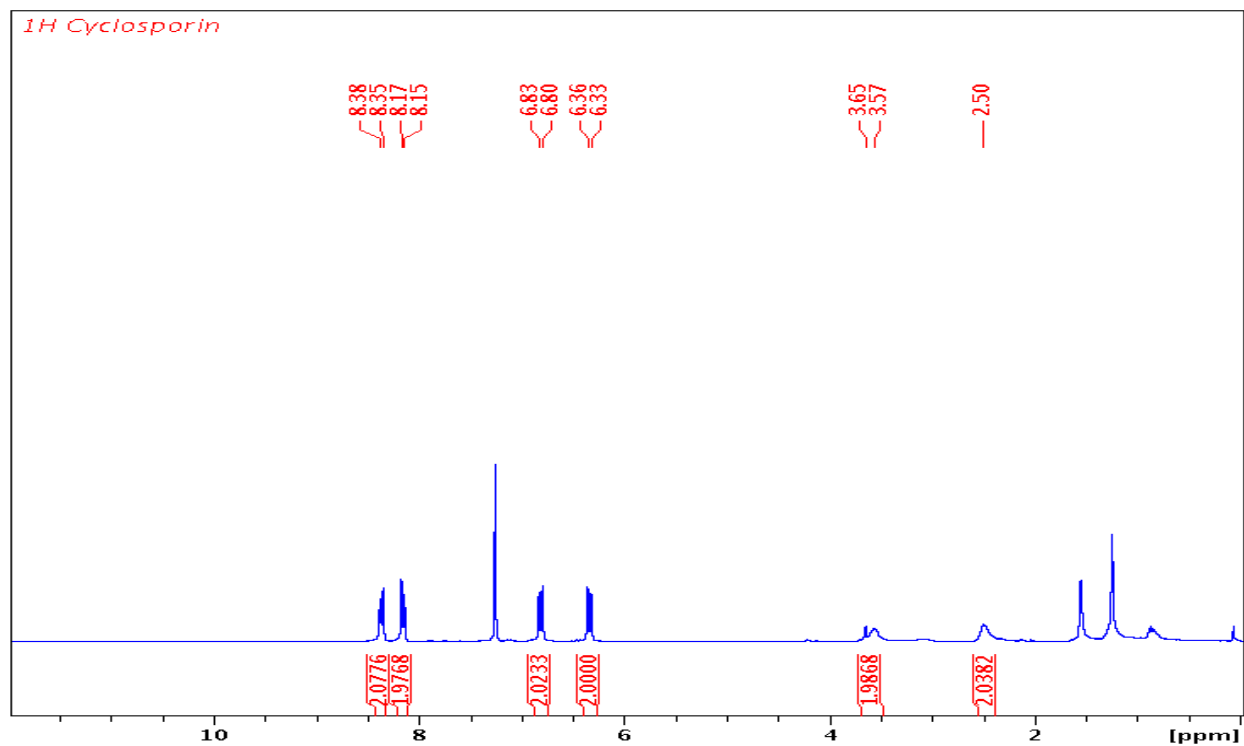
^{13}C NMR spectrum of **3.10c** (75 MHz, acetone- d_6)



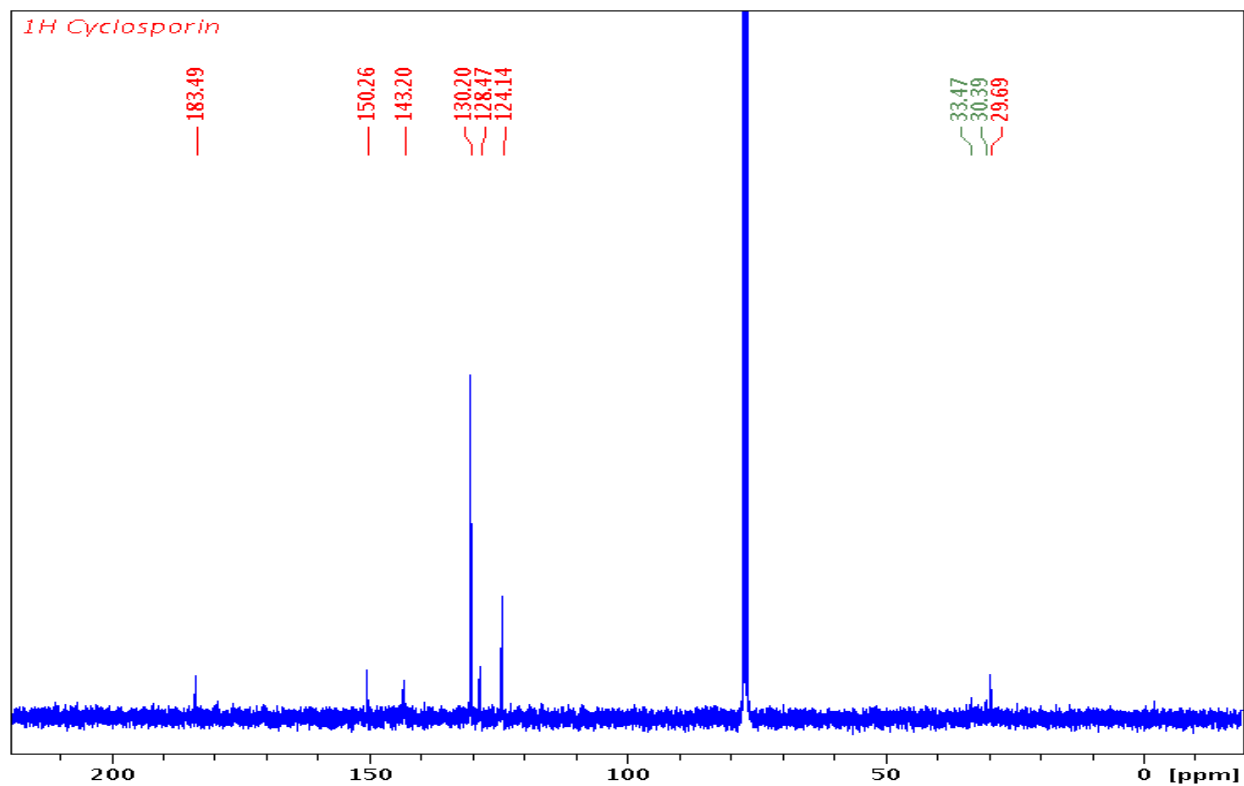


Compound 3.13c: 8.5 mg (57% yield) from 15 mg of **3.10c**, yellow solid, m.p.: 180-182°C. **IR:** 3106, 2923, 1675, 1628. **¹H:** 8.37 (d, 2H, *J* = 8.2), 8.16 (d, 2H, *J* = 8.1), 6.82 (d, 2H, *J* = 8.3), 6.35 (d, 2H, *J* = 8.3), 3.57 (broad, 2H), 2.50 (broad, 2H). **¹³C:** 183.5, 150.3, 146.2, 143.2, 130.2, 128.5, 124.1, 82.7, 33.5, 29.7. **¹³C (DMSO-*d*₆, 70°C):** 184.5, 150.3, 146.9, 145.4, 142.2, 129.1, 128.5, 124.6, 84.8, 32.2, 31.7. **HRMS:** calcd for C₁₅H₁₂N₂O₆SNa [M+Na]⁺: 371.0314; found: 371.0316.

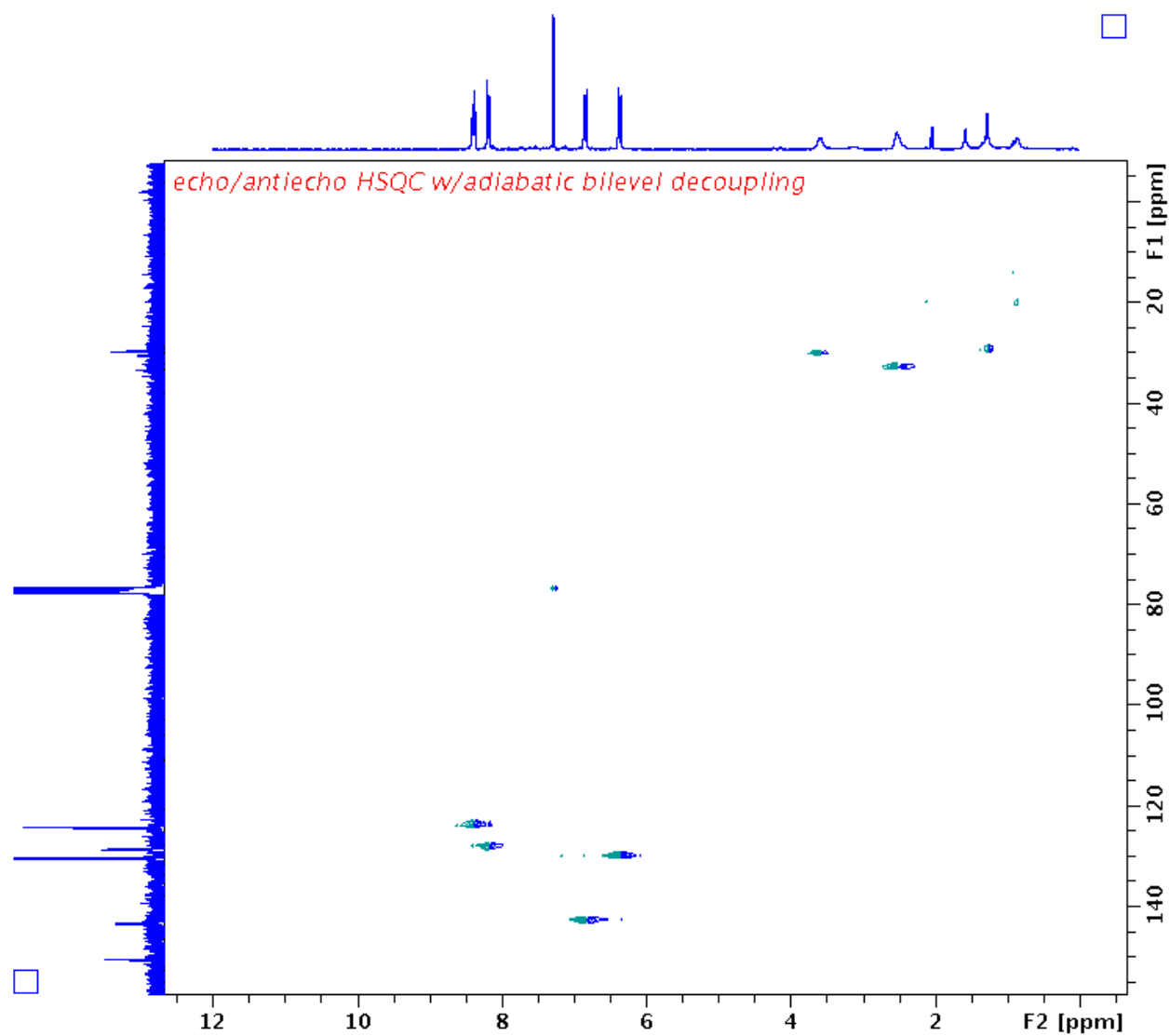
^1H NMR spectrum of **3.13c** (300 MHz, CDCl_3)



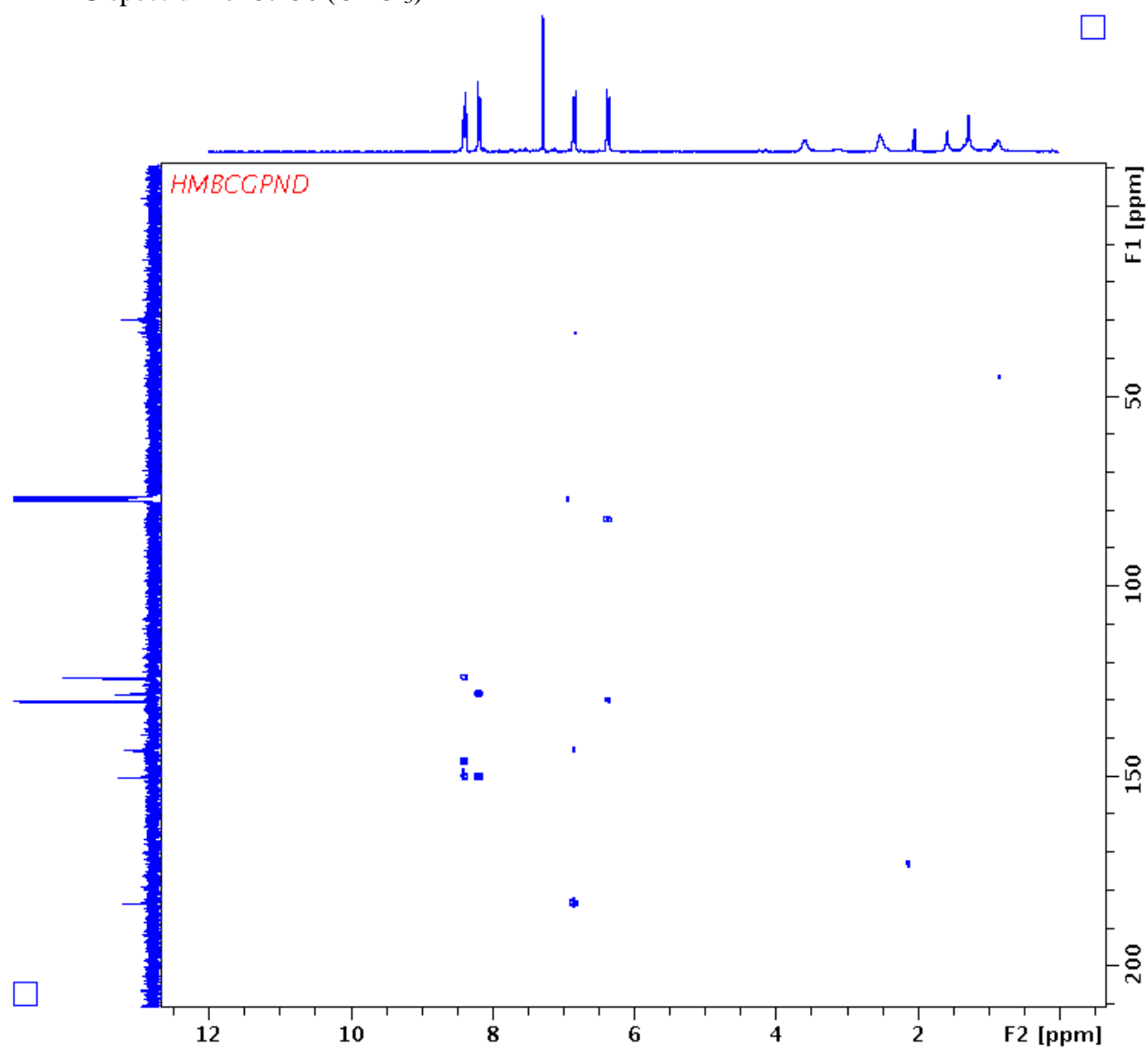
^{13}C NMR spectrum of **3.13c** (75 MHz, CDCl_3)



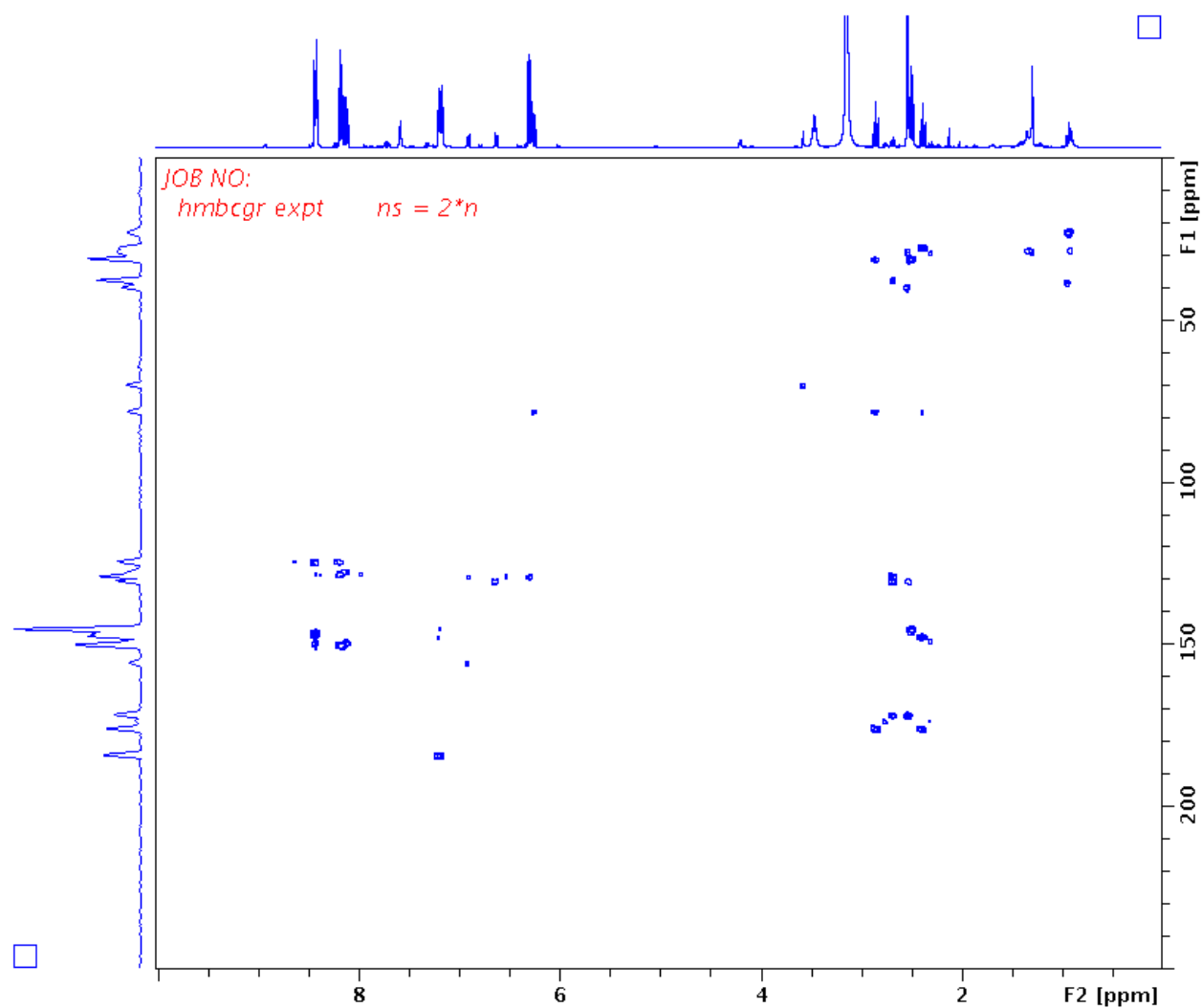
HSQC spectrum of **3.13c** (CDCl₃)



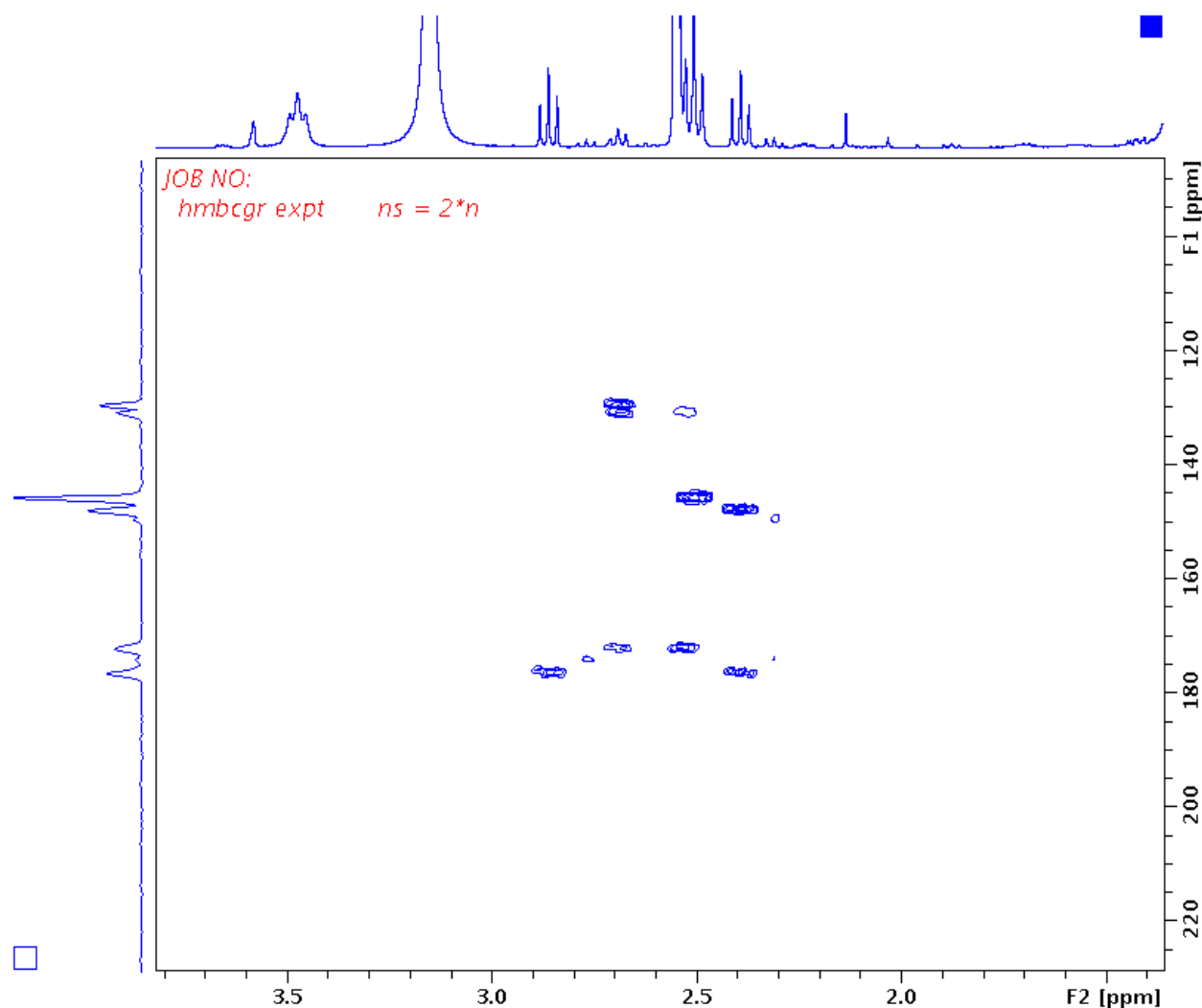
HMBC spectrum of **3.13c** (CDCl₃)



HMBC spectrum of **3.13c** (DMSO-*d*₆, 70°C)

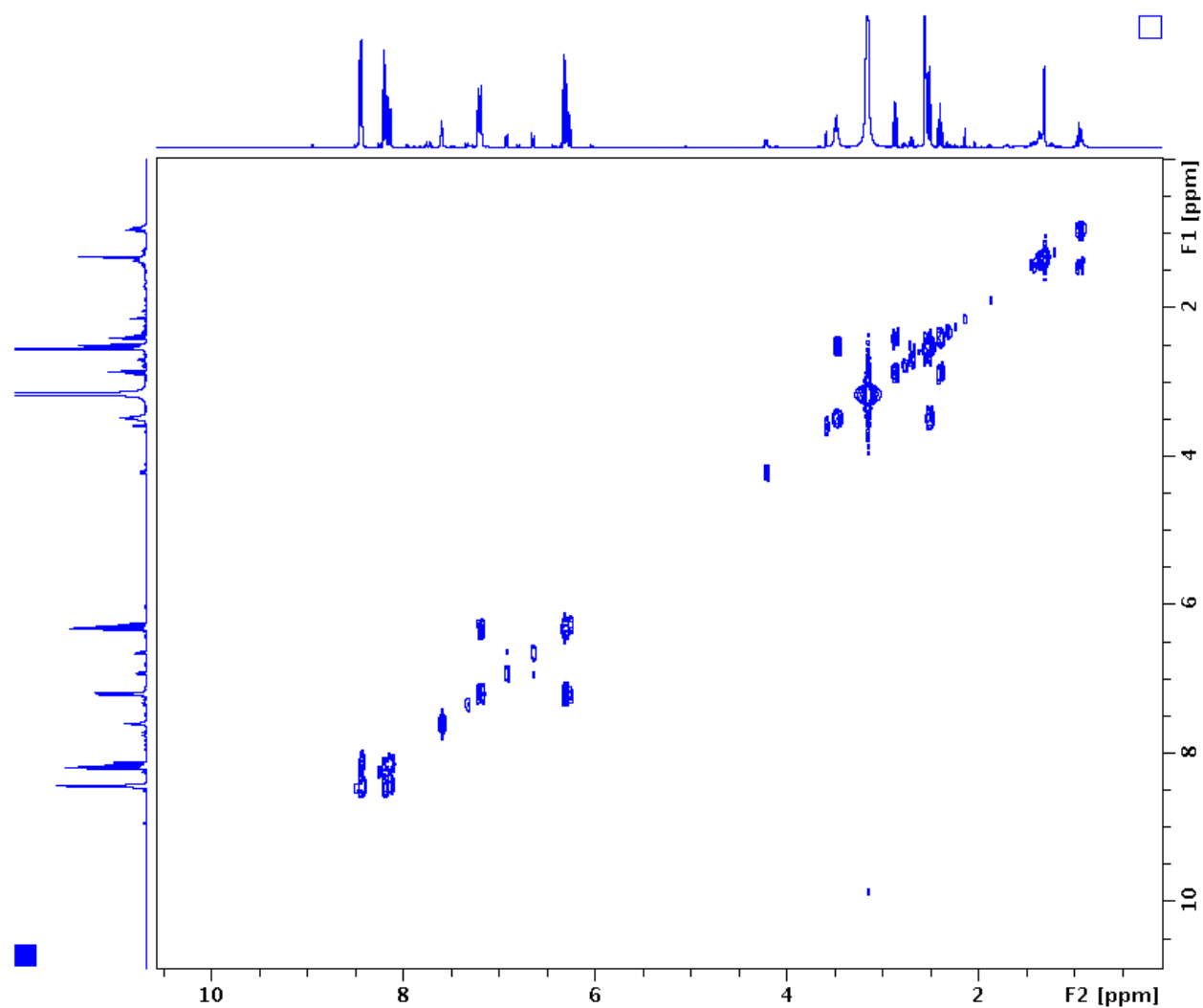


Expanded **HMBC** spectrum of **3.13c** (DMSO-*d*₆, 70°C)

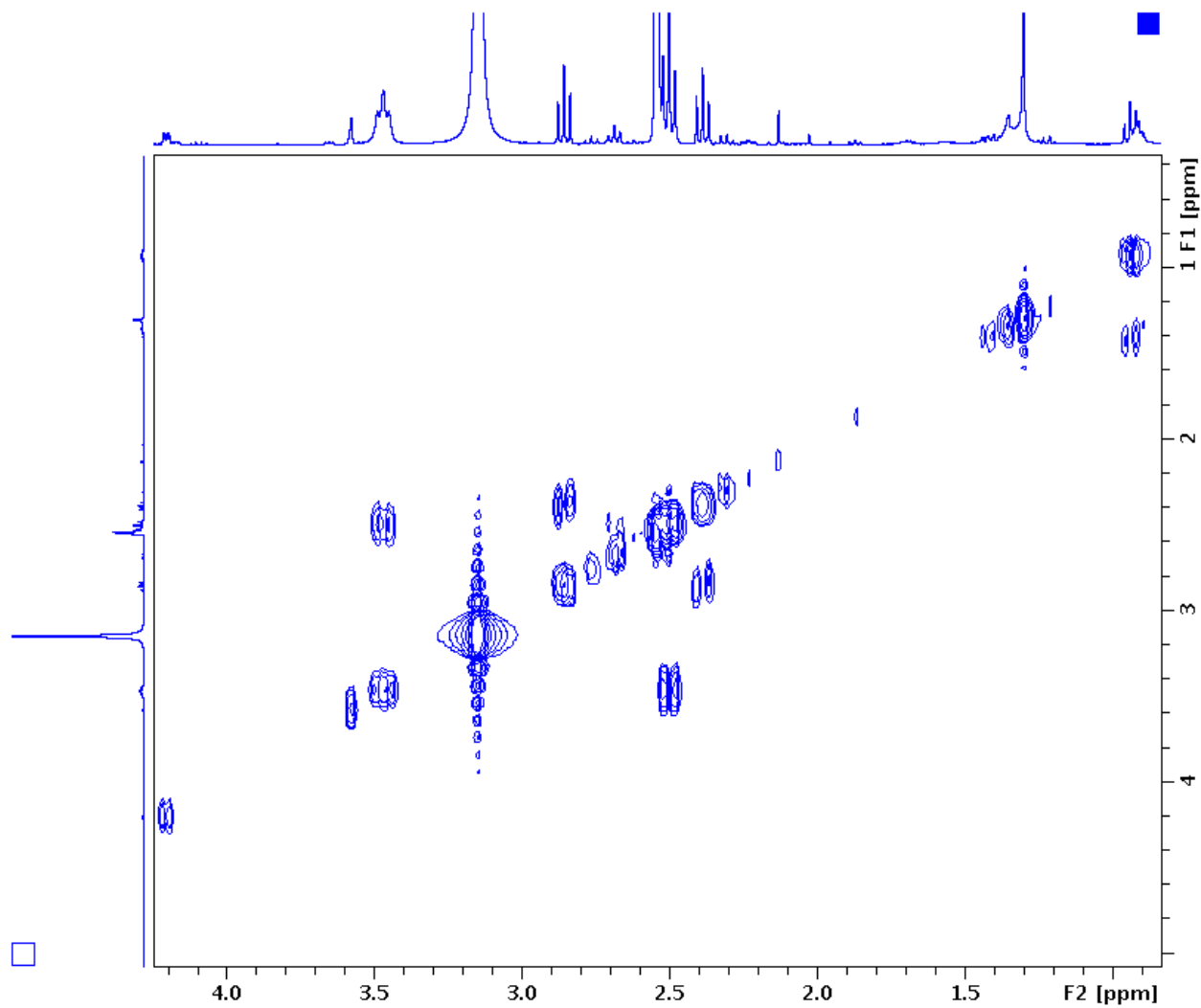


The HMBC correlation between C=N carbon and adjacent CH₂ protons was not observed at r.t. in CDCl₃ nor in ¹³C(¹H decoupled) experiment. However, despite the compound seems to undergo hydrolysis in DMSO at 70°C, target peaks are significantly sharpened and new correlation was observed. Thus, we are able to determine the chemical shift of the by far missing C=N carbon via the correlation between C=N carbon and adjacent CH₂ protons at 145.9 ppm and 2.94 ppm.

COSY spectrum of **3.13c** (DMSO-*d*₆, 70°C)

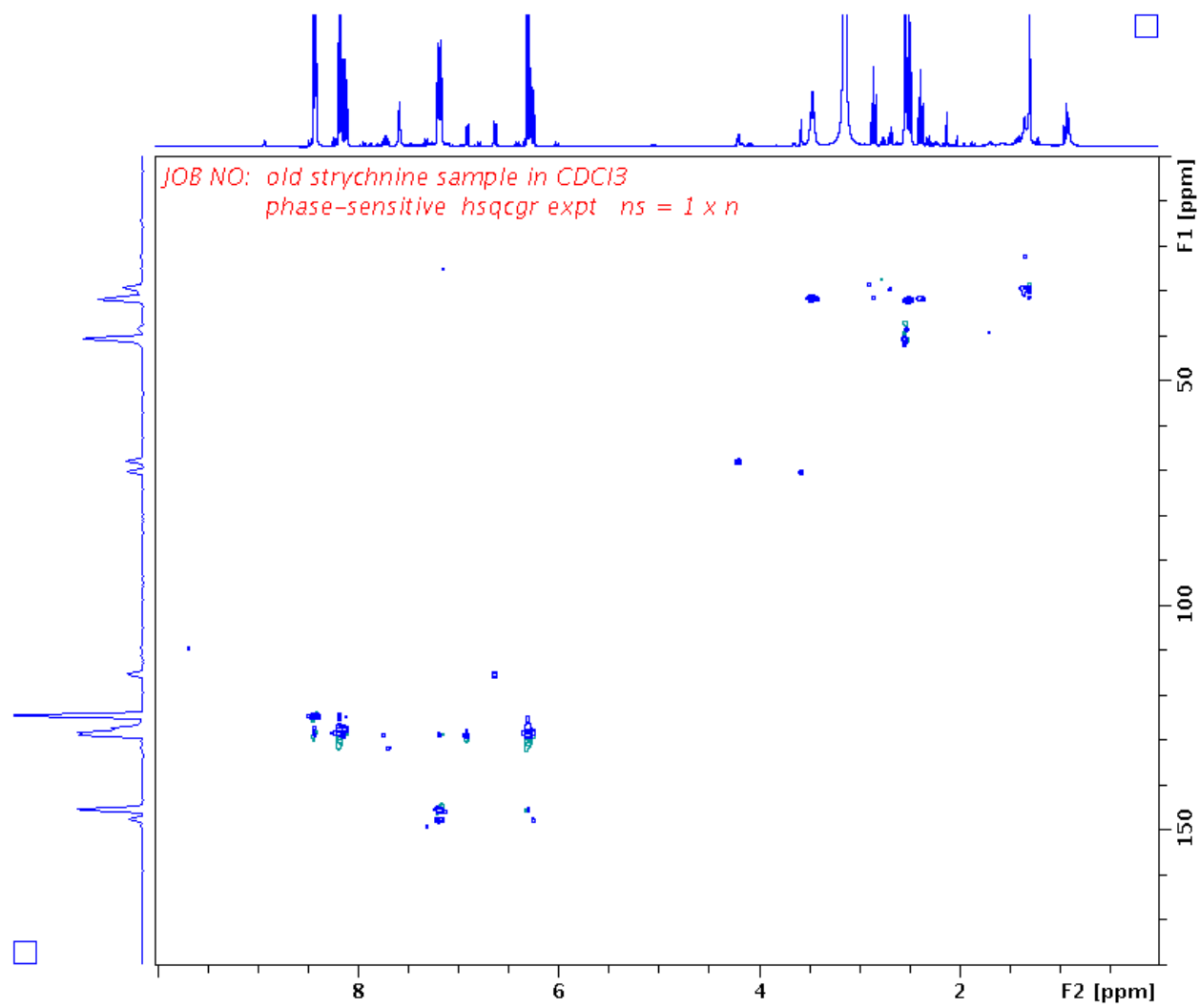


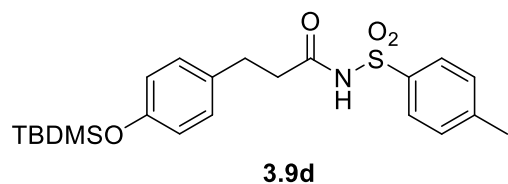
Expanded COSY spectrum of **3.13c** (DMSO-*d*₆, 70°C)



Correlation between triplets at 2.48 ppm and 3.45 ppm verifies the chemical shifts of the CH₂'s in compound **3.13c** in DMSO-*d*₆.

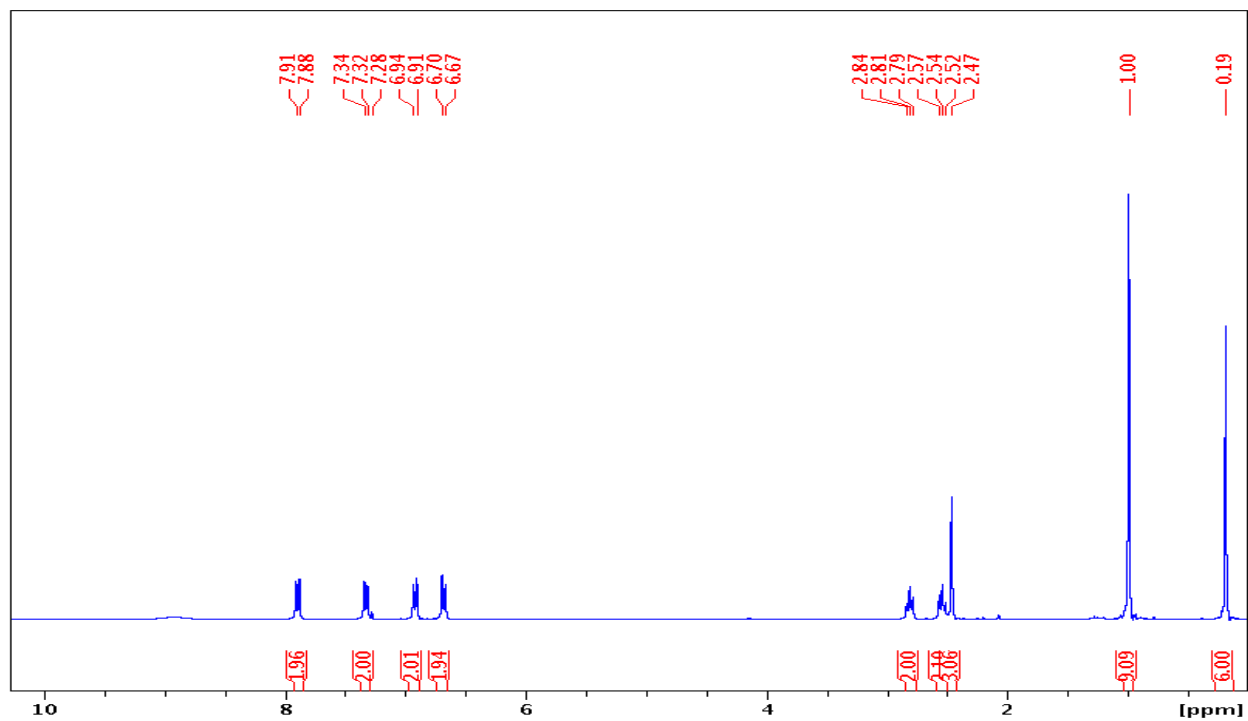
HSQC spectrum of **3.13c** (DMSO-*d*₆, 70°C)



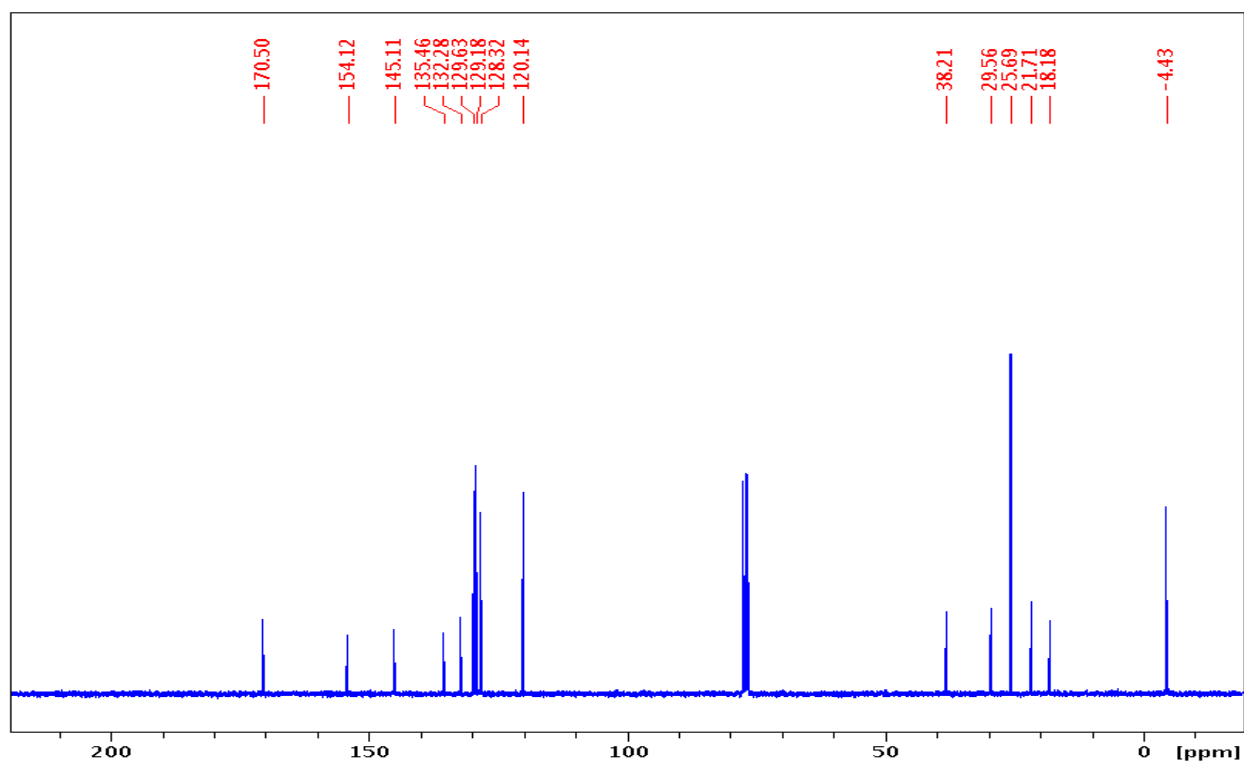


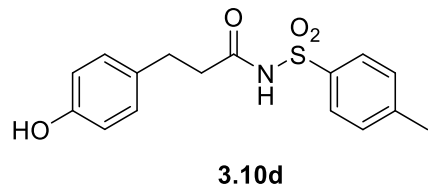
Compound 3.9d: 0.26 g (83% yield) from 0.20 g of **3.8**, thick colorless oil. **IR:** 3237, 2929, 1700, 1510. **¹H:** 7.90 (d, 2H, $J = 8.2$), 7.33 (d, 2H, $J = 8.1$), 6.92 (d, 2H, $J = 8.3$), 6.68 (d, 2H, $J = 8.3$), 2.81 (t, 2H, $J = 7.6$), 2.54 (t, 2H, $J = 7.6$), 2.47 (s, 3H), 0.99 (s, 9H), 0.19 (s, 6H). **¹³C:** 170.5, 154.1, 145.1, 135.5, 132.3, 129.6, 129.2, 128.3, 120.1, 38.2, 29.6, 25.7, 21.7, 18.2, -4.4. **HRMS:** calcd for C₂₂H₃₂NO₄SSi [M+H]⁺: 434.1821; found: 434.1818.

^1H NMR spectrum of **3.9d** (300 MHz, CDCl_3)



^{13}C NMR spectrum of **3.9d** (75 MHz, CDCl_3)

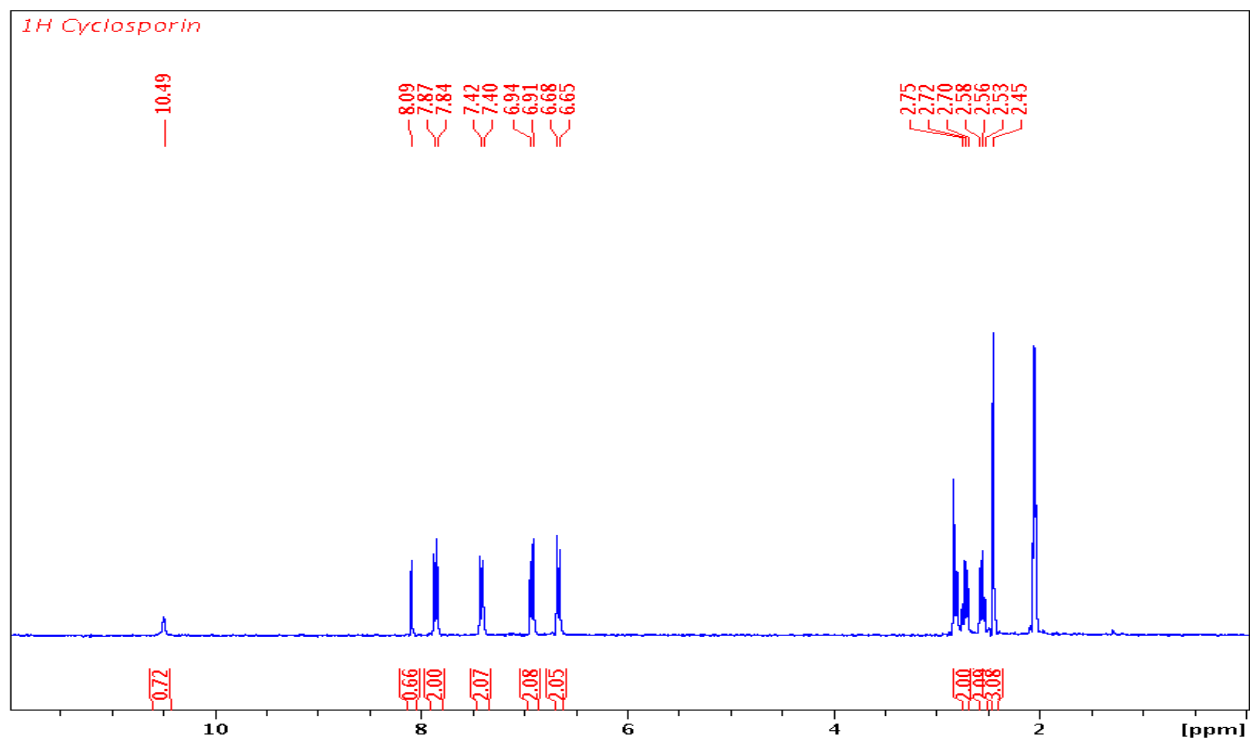




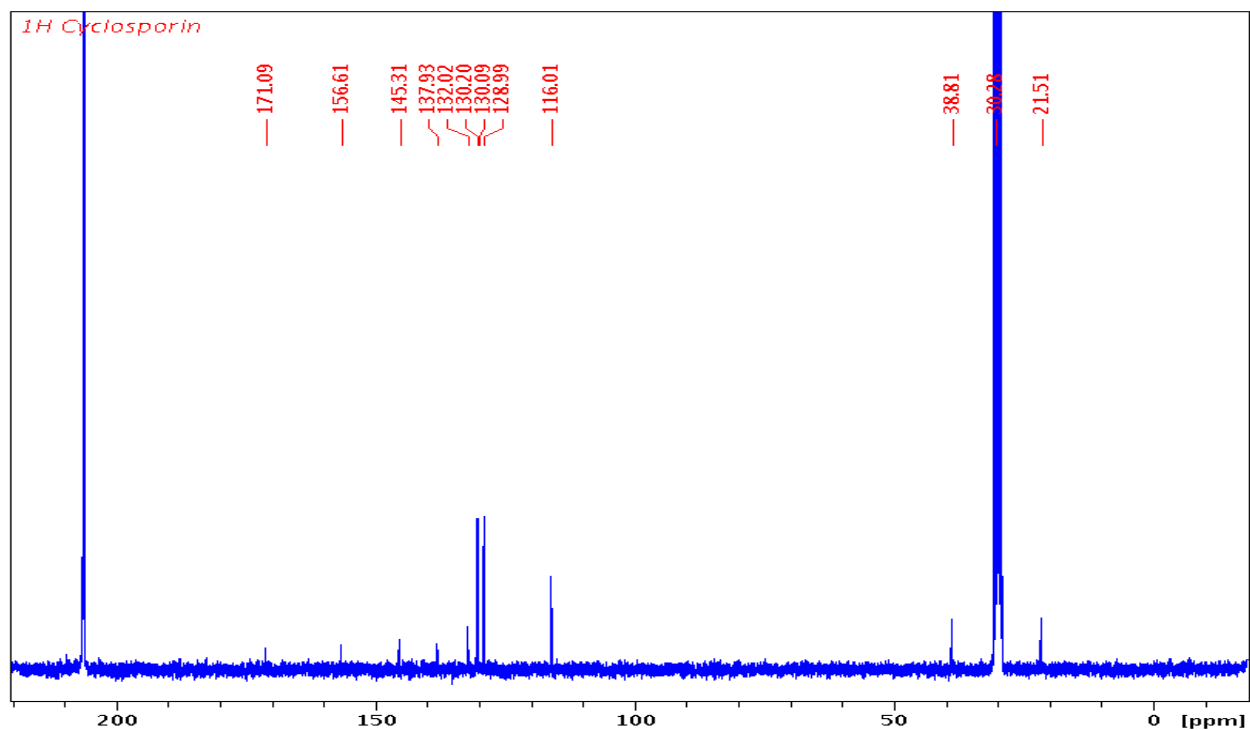
Compound 3.10d: 81.9 mg (87% crude yield) from 127.6 mg of **3.9d**, white solid, m.p.: 136°C.

IR: 3438 (broad), 3241 (broad), 1697. **¹H:** 8.28 (br, s, 1H), 7.88 (d, 2H, $J = 8.3$), 7.33 (d, 2H, $J = 8.3$), 6.91 (d, 2H, $J = 8.4$), 6.68 (d, 2H, $J = 8.4$), 4.98 (br, s, 1H), 2.79 (t, 2H, $J = 7.6$), 2.49 (t, 2H, $J = 7.6$), 2.45 (s, 3H). **¹³C:** 169.9, 154.3, 145.3, 135.7, 131.8, 129.6, 129.4, 128.4, 115.5, 38.4, 29.5, 21.7. **¹H (acetone-*d*₆):** 10.49 (br, s, 1H), 8.09 (br, s, 1H), 7.86 (d, 2H, $J = 8.3$), 7.41 (d, 2H, $J = 8.3$), 6.93 (d, 2H, $J = 8.4$), 6.67 (d, 2H, $J = 8.4$), 2.72 (t, 2H, $J = 7.6$), 2.53 (t, 2H, $J = 7.6$), 2.45 (s, 3H). **¹³C (acetone-*d*₆):** 171.1, 156.6, 145.3, 137.9, 133.0, 130.2, 130.1, 129.0, 116.0, 38.8, 30.3, 21.5. **HRMS:** calcd for C₁₆H₁₈NO₄S [M+H]⁺: 320.0957; found: 320.0959.

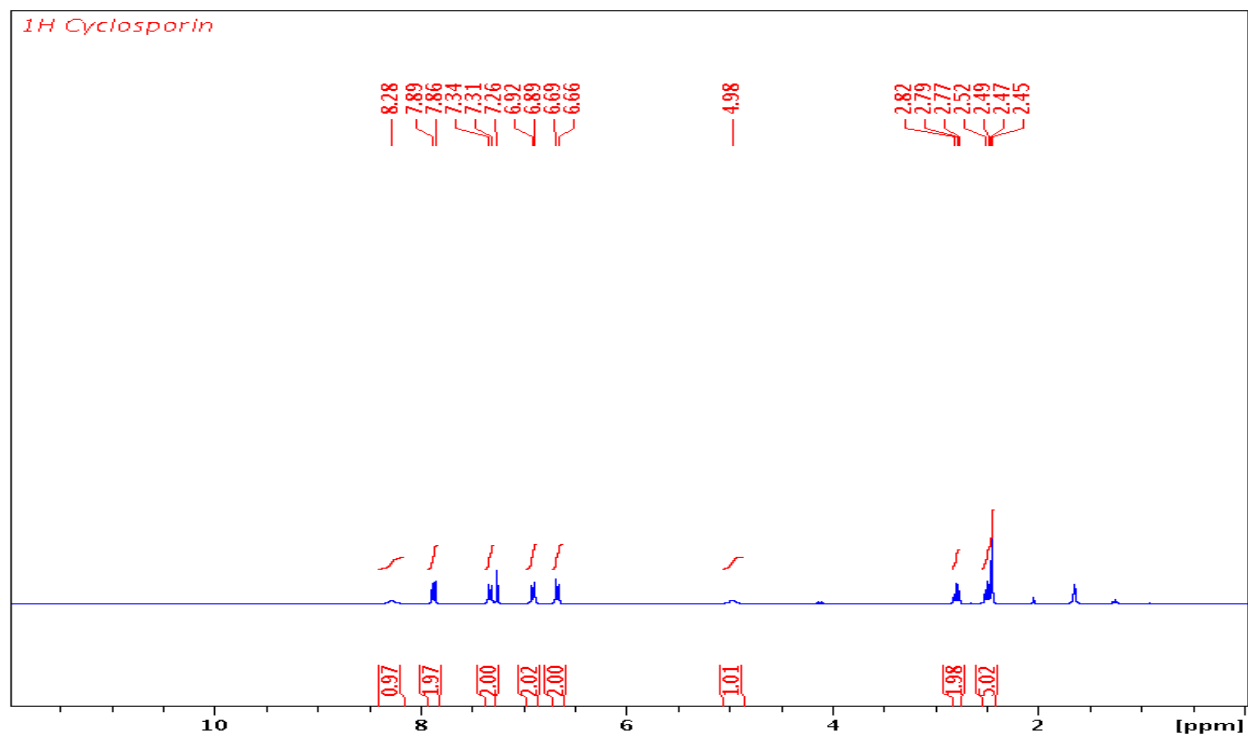
^1H NMR spectrum of **3.10d** (300 MHz, acetone- d_6)



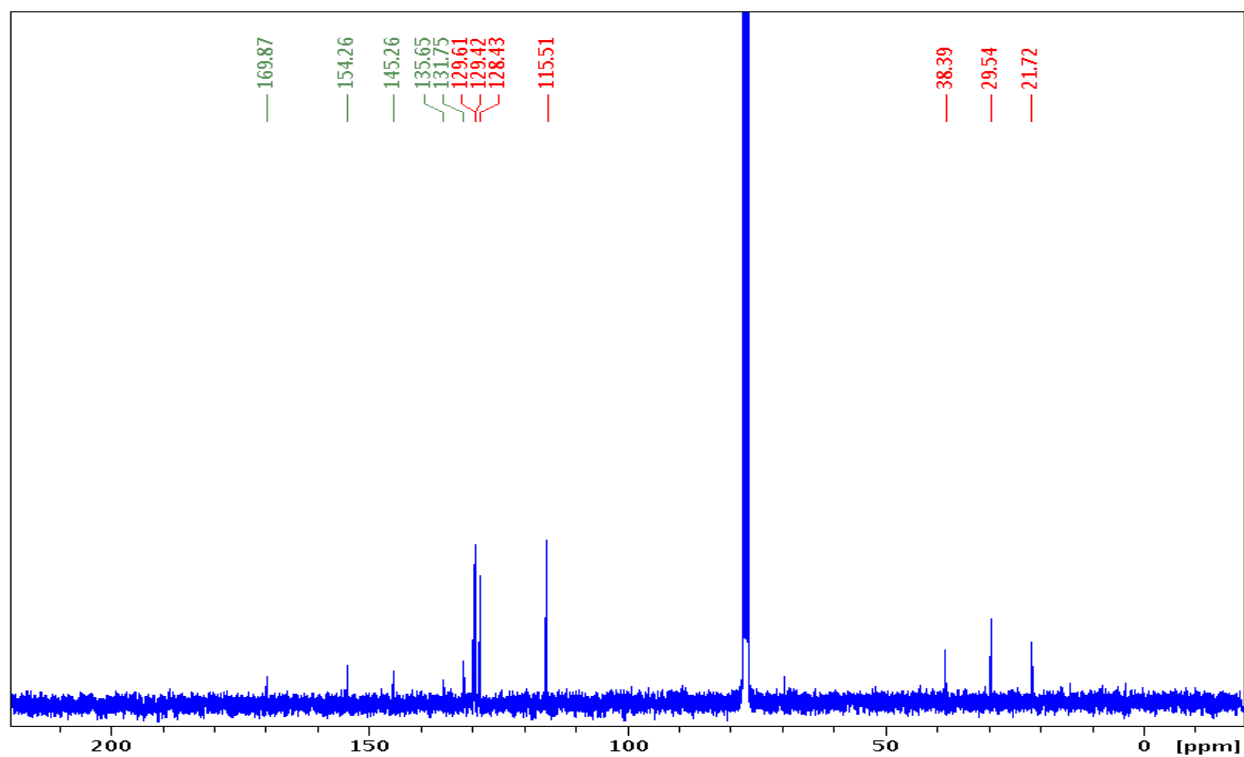
^{13}C NMR spectrum of **3.10d** (75 MHz, acetone- d_6)

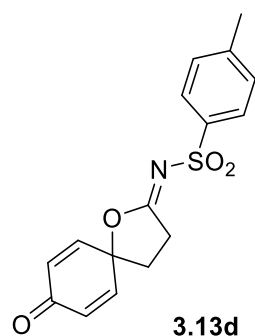


^1H NMR spectrum of **3.10d** (300 MHz, CDCl_3)



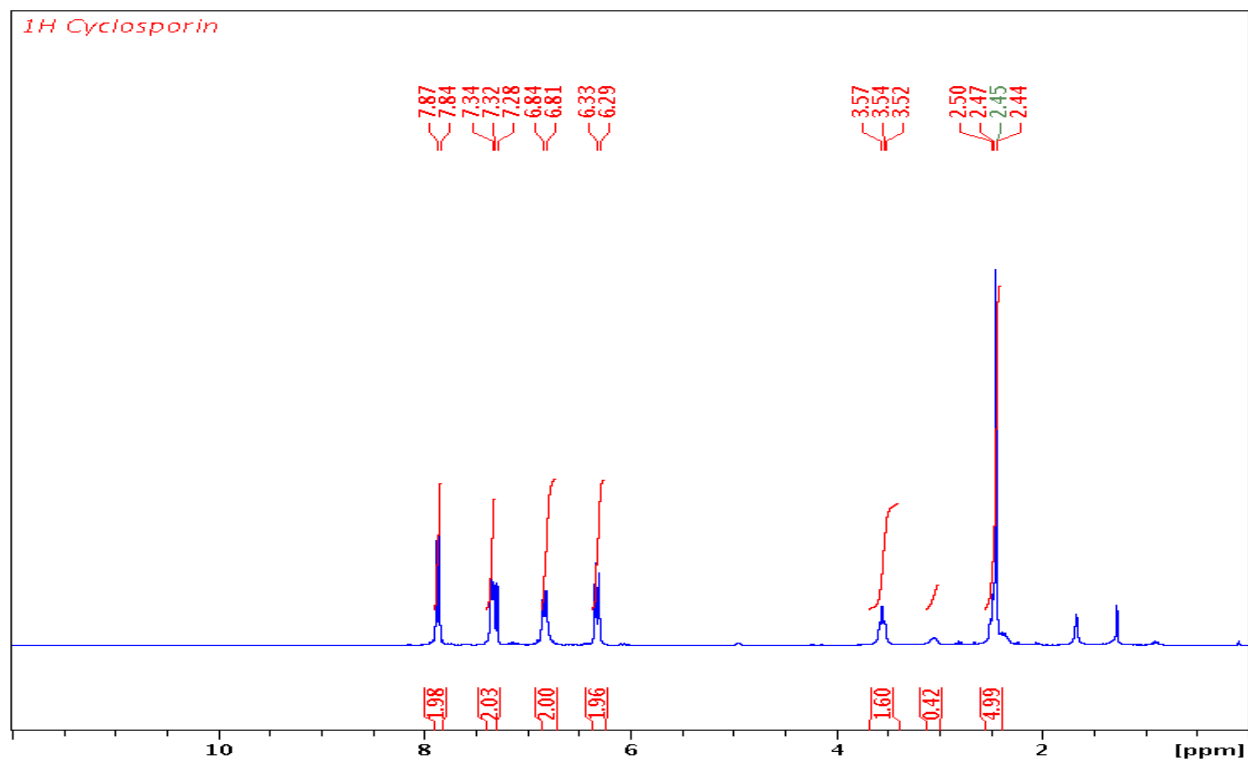
^{13}C NMR spectrum of **3.10d** (75 MHz, CDCl_3)



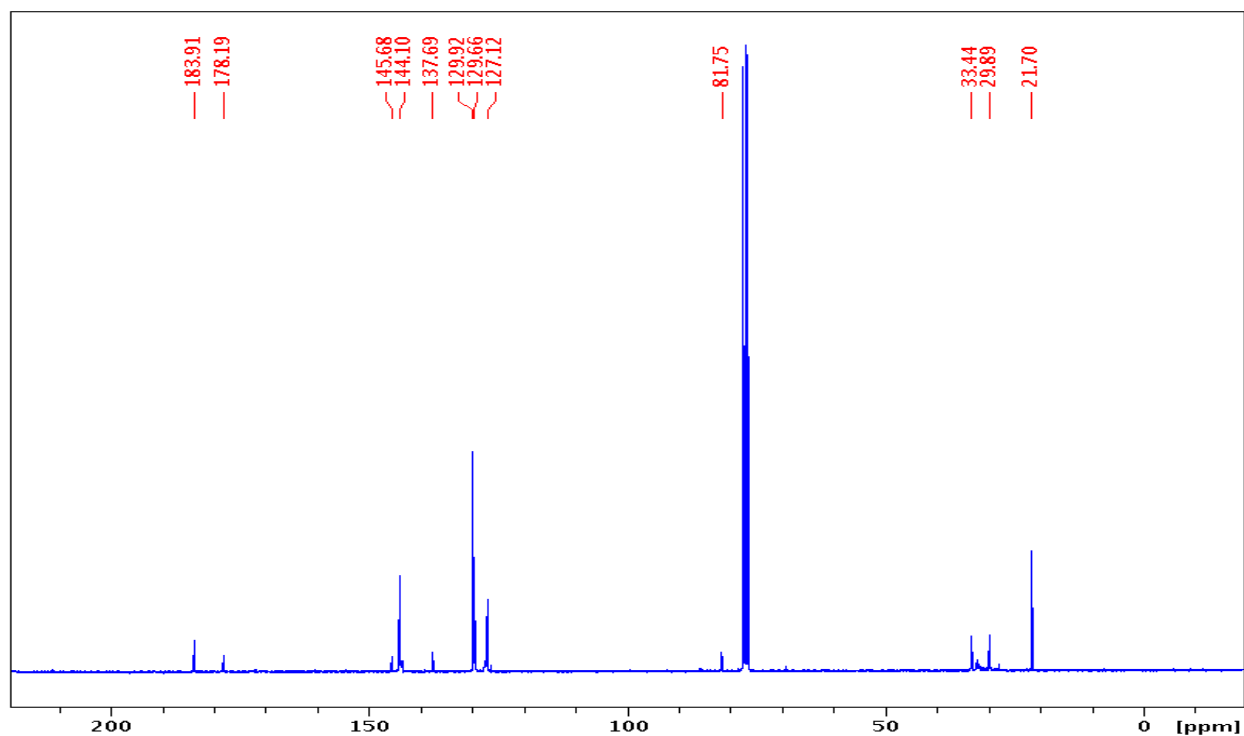


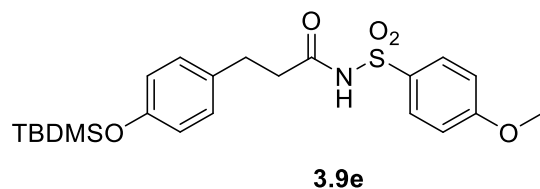
Compound 3.13d: 11 mg (91% yield) from 12 mg of **3.10d**, tint pale yellow oil. **IR:** 3055, 2923, 1674, 1626. **¹H:** 7.87 (d, 2H, $J = 8.2$), 7.34 (d, 2H, $J = 9.2$), 6.83 (d, 2H, $J = 9.2$), 6.34 (d, 2H, $J = 8.2$), 3.56 (t, 2H, $J = 7.4$), 2.48 (t, 2H, $J = 7.4$), 2.45 (s, 3H). **¹³C:** 183.9, 178.2, 145.7, 144.1, 137.7, 129.9, 129.7, 127.1, 81.8, 33.4, 29.9, 21.7. **HRMS:** calcd for C₁₆H₁₄NO₄S [M-H]⁻: 316.0644; found: 316.0645.

^1H NMR spectrum of **3.13d** (300 MHz, CDCl_3)



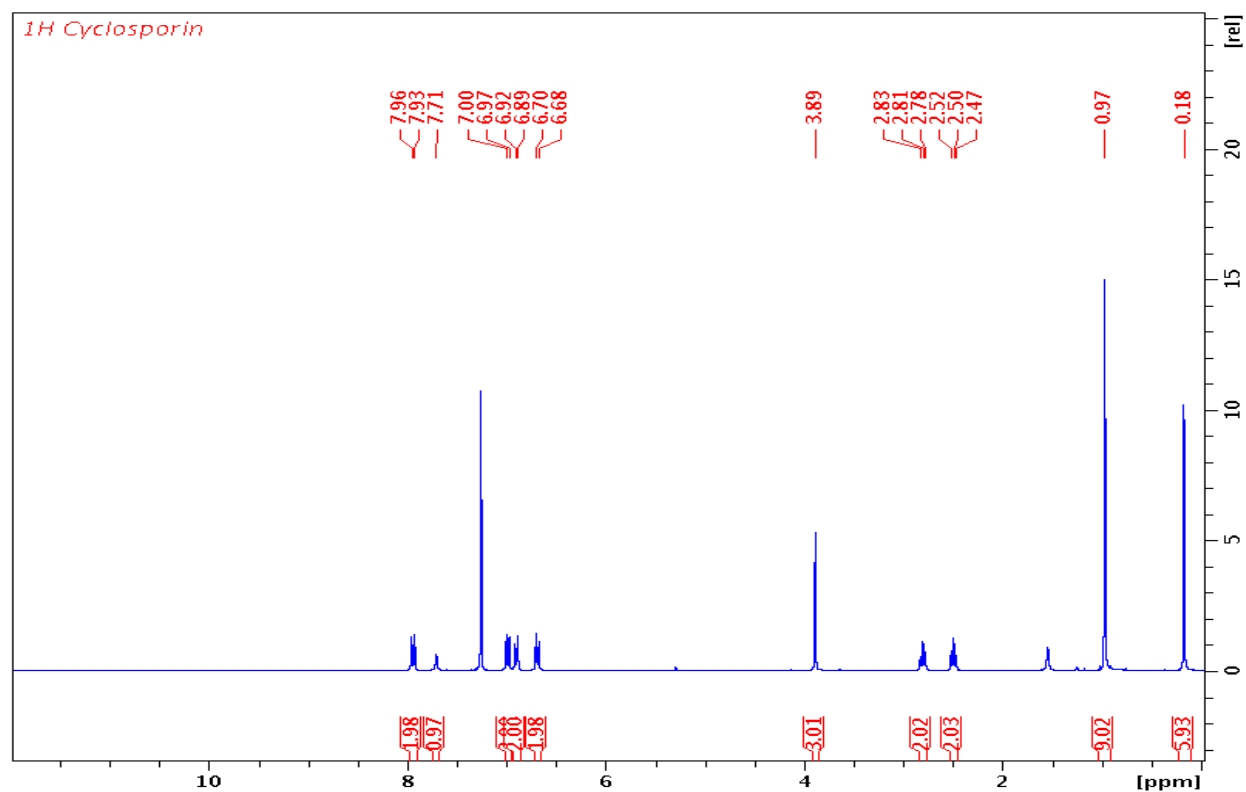
^{13}C NMR spectrum of **3.13d** (75 MHz, CDCl_3)



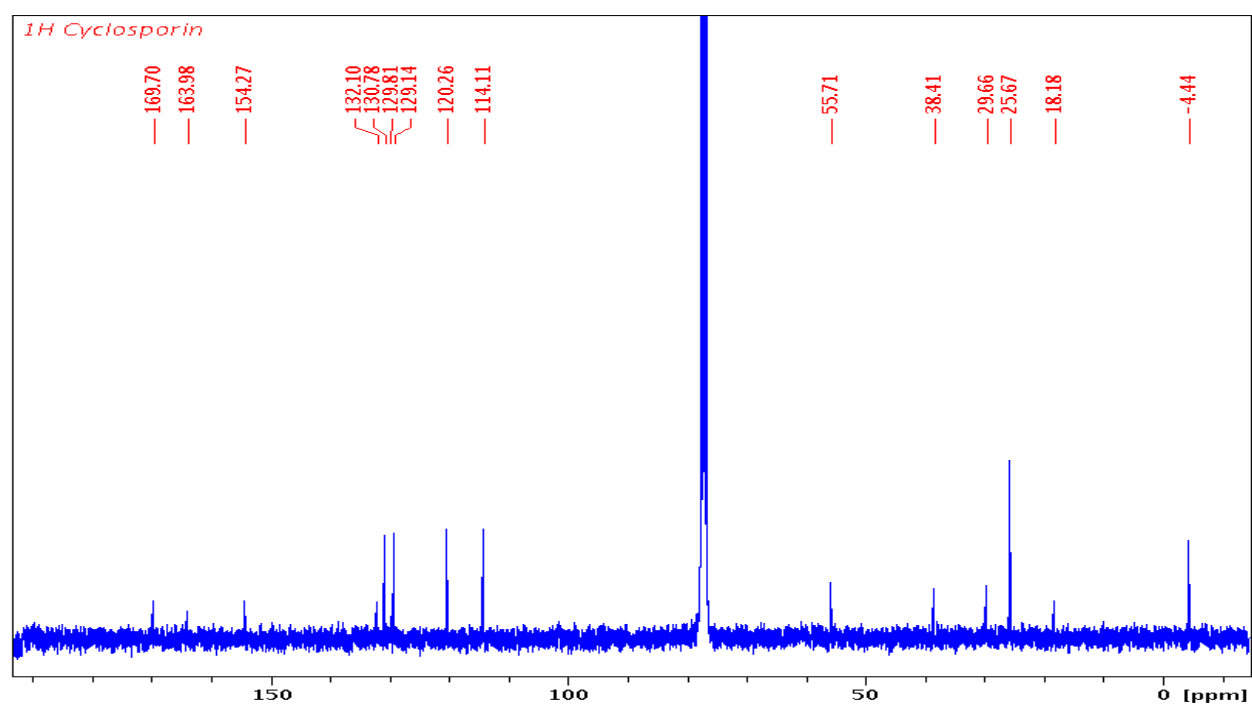


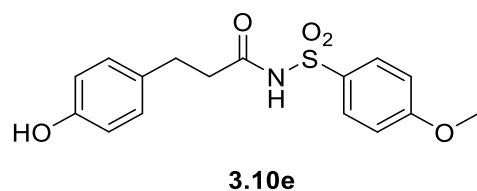
Compound 3.9e: 0.1 g (92% yield) from 0.15 g of **3.8**, colorless oil. **IR:** 3242 (broad), 1720, 1695. **¹H:** 7.96 (d, 2H, $J = 9.0$), 7.01 (d, 2H, $J = 8.9$), 6.92 (d, 2H, $J = 8.4$), 6.71 (d, 2H, $J = 8.4$), 3.91 (s, 3H), 2.83 (t, 2H, $J = 7.5$), 2.52 (t, 2H, $J = 7.5$), 0.99 (s, 9H), 0.19 (s, 6H). **¹³C:** 169.8, 164.0, 154.3, 132.1, 130.8, 129.8, 129.1, 120.3, 114.1, 55.7, 38.4, 29.7, 25.7, 18.2, -4.4. **HRMS:** calcd for C₂₂H₃₂NO₅SSi [M+H]⁺: 450.1770; found: 450.1769.

^1H NMR spectrum of **3.9e** (300 MHz, CDCl_3)



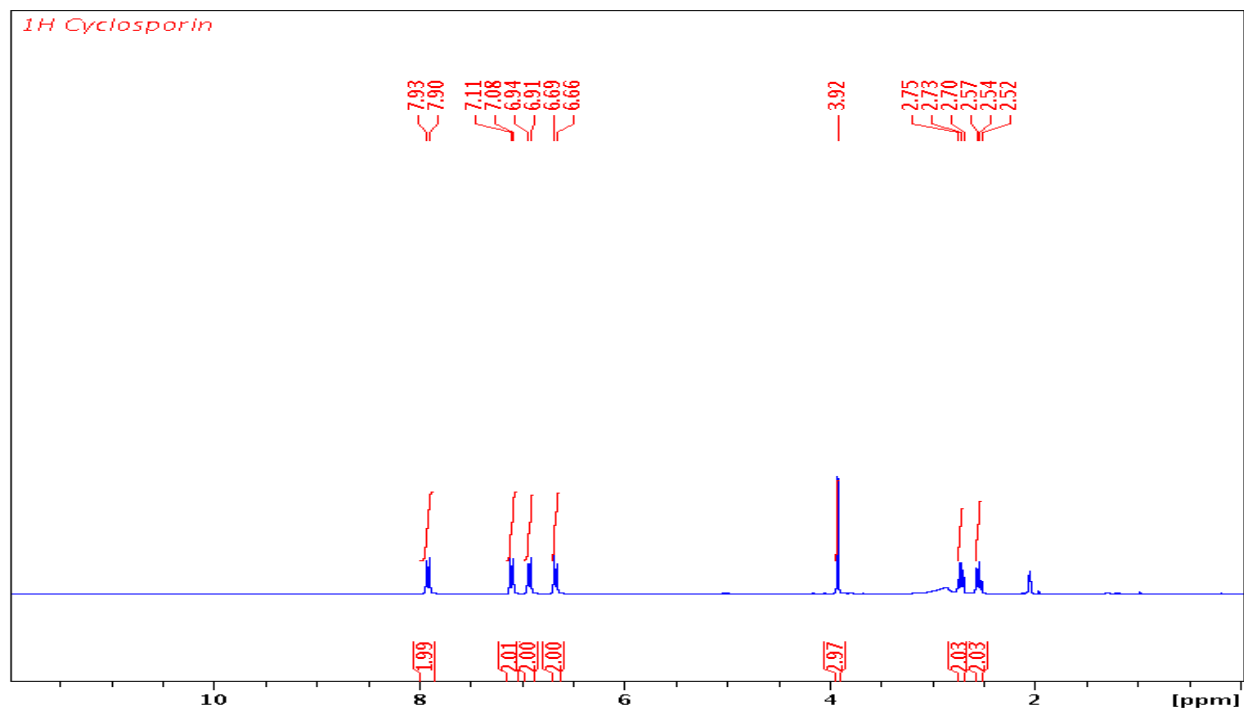
^{13}C NMR spectrum of **3.9e** (75 MHz, CDCl_3)



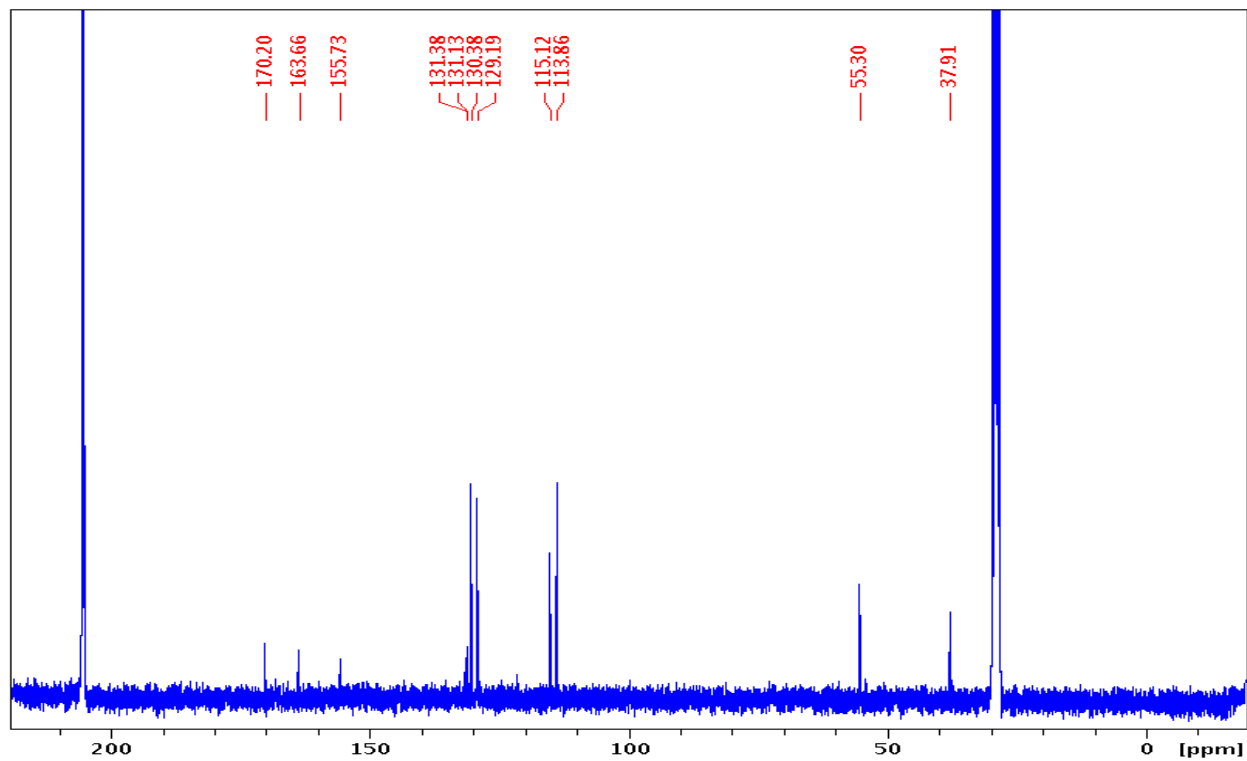


Compound 3.10e: 93 mg (84% yield) from 150 mg of **3.9e**, white solid, m.p.: 152°C. **IR:** 3459 (broad), 3243 (broad), 1698. **¹H (acetone-*d*₆):** 7.92 (d, 2H, *J* = 8.9), 7.10 (d, 2H, *J* = 8.9), 6.93 (d, 2H, *J* = 8.4), 6.68 (d, 2H, *J* = 8.4), 3.92 (s, 3H), 2.73 (t, 2H, *J* = 7.5), 2.54 (t, 2H, *J* = 7.5). **¹³C (acetone-*d*₆):** 170.2, 163.7, 155.7, 131.4, 131.1, 130.4, 129.2, 115.1, 113.9, 55.3, 37.9, 29.5. **HRMS:** calcd for C₁₆H₁₈NO₅S [M+H]⁺: 336.0906; found: 336.0902.

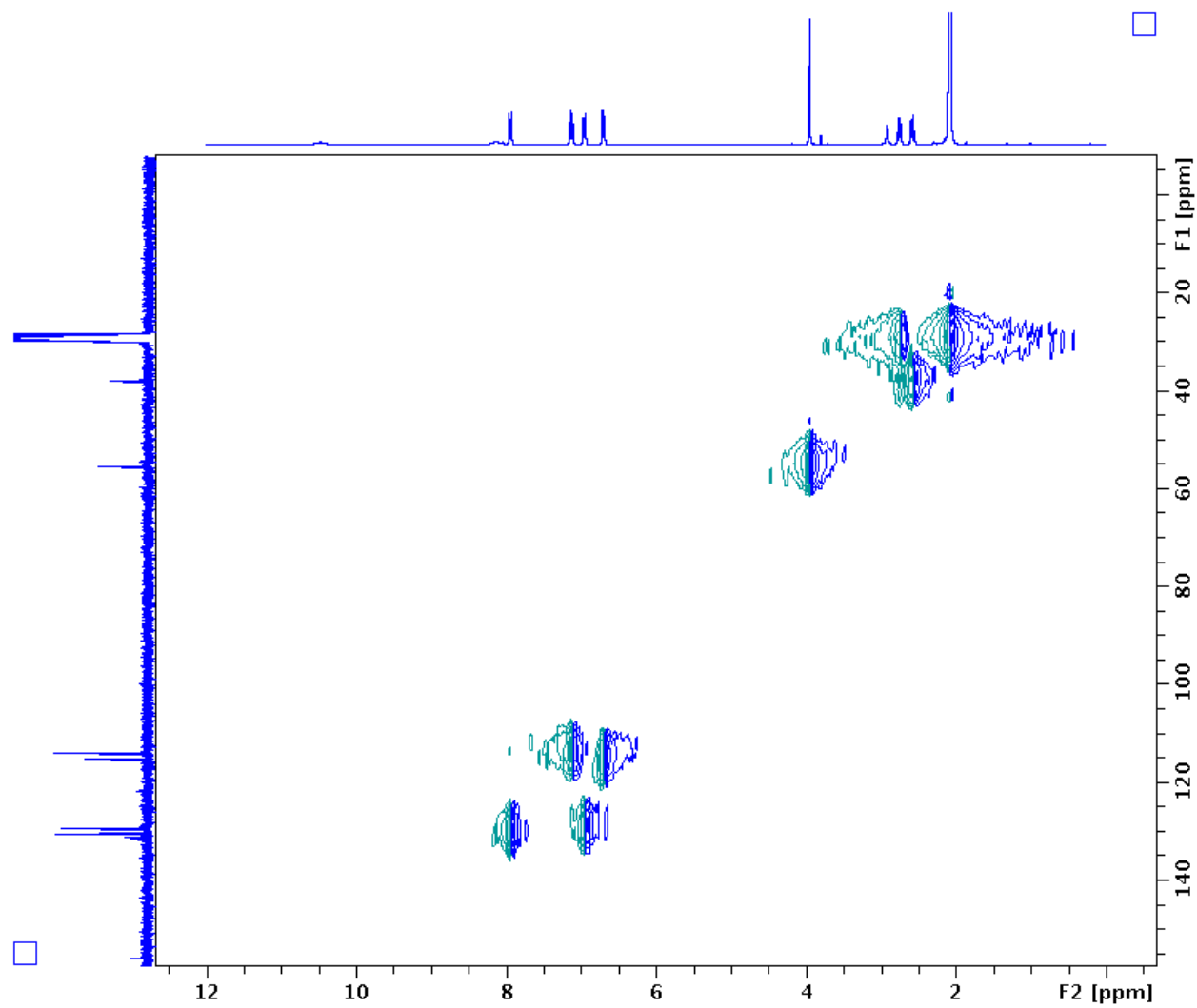
^1H NMR spectrum of **3.10e** (300 MHz, acetone- d_6)

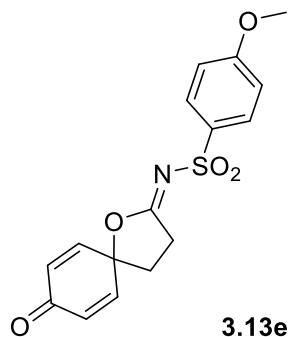


^{13}C NMR spectrum of **3.10e** (75 MHz, acetone- d_6)



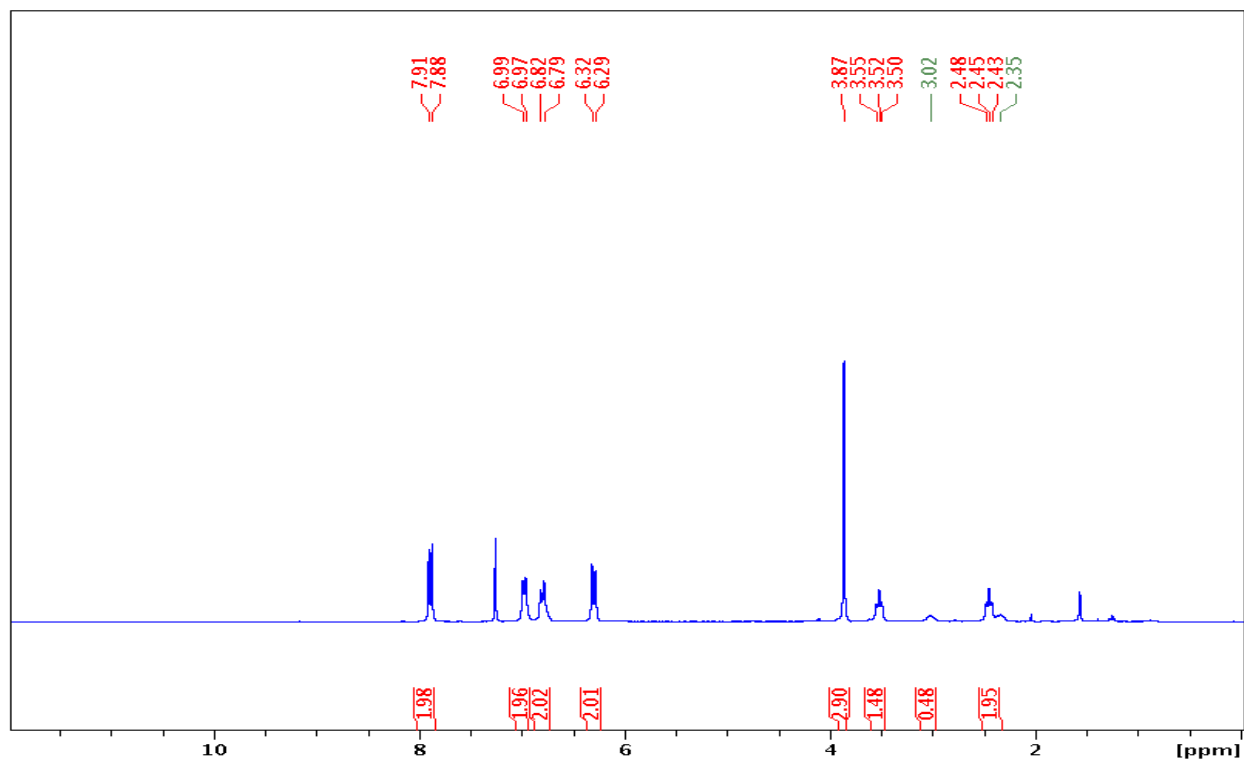
HSQC spectrum of **3.10e** (acetone- d_6)



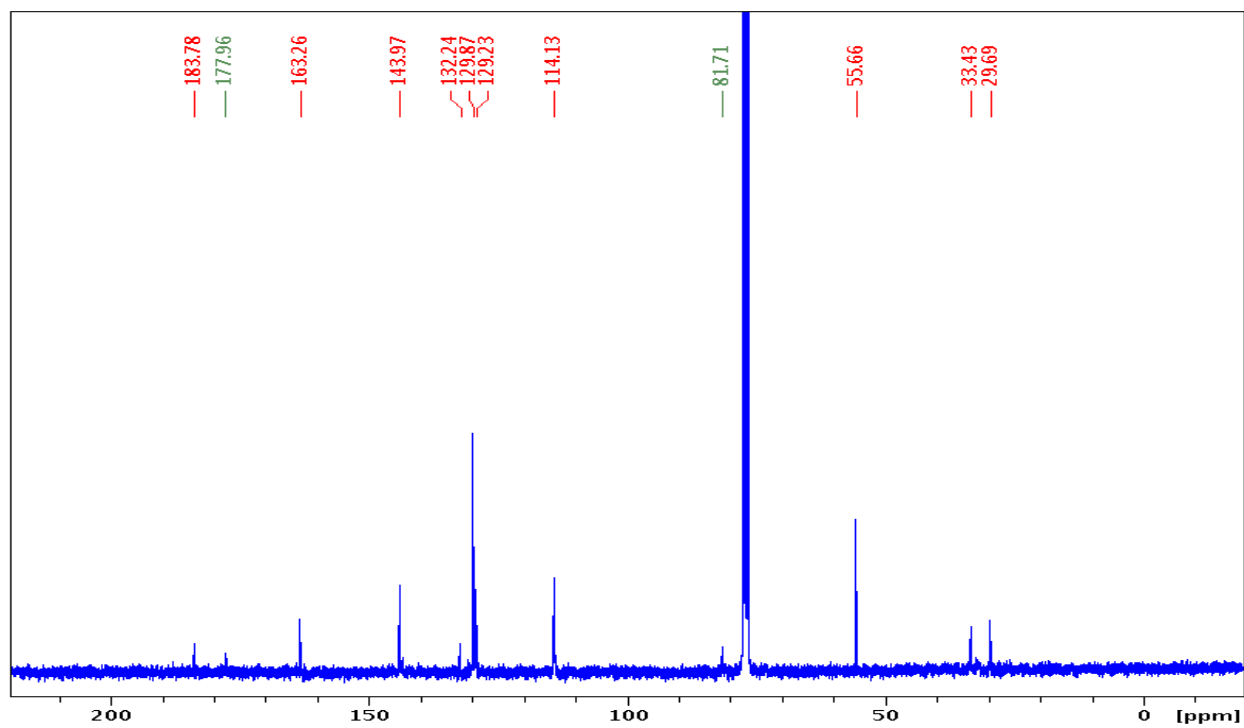


Compound 3.13e: 13 mg (81% yield) from 16.2 mg of **3.10e**, off-white solid, m.p.: 75-78°C. **¹H** (3:1 rotamer ratio, asterisks denote minor rotamer peaks, CDCl₃): 7.90 (d, 2H, *J* = 8.8), 6.98 (d, 2H, *J* = 8.2), 6.81 (d, 2H, *J* = 9.8), 6.31 (d, 2H, *J* = 9.8), 3.87 (s, 3H), 3.52 (t, 2H, *J* = 8.0), 3.02* (m, 2H), 2.45 (t, 2H, *J* = 8.0), 2.35* (m, 2H). **¹H** (DMSO-*d*₆, 105°C): 7.80 (d, 2H, *J* = 9.0), 7.10 (d, 4H, *J* = 9.3), 6.24 (d, 2H, *J* = 10.0), 3.87 (s, 3H), 3.36 (t, 2H, *J* = 7.9), 2.43 (t, 2H, *J* = 7.9). **¹³C**: 183.8, 178.0, 163.3, 144.0, 132.2, 129.9, 129.2, 114.1, 81.7, 55.7, 33.4, 29.7. **IR**: 2936, 1673, 1629. **HRMS**: calcd for C₁₆H₁₆NO₅S [M+H]⁺: 334.0749; found: 334.0742.

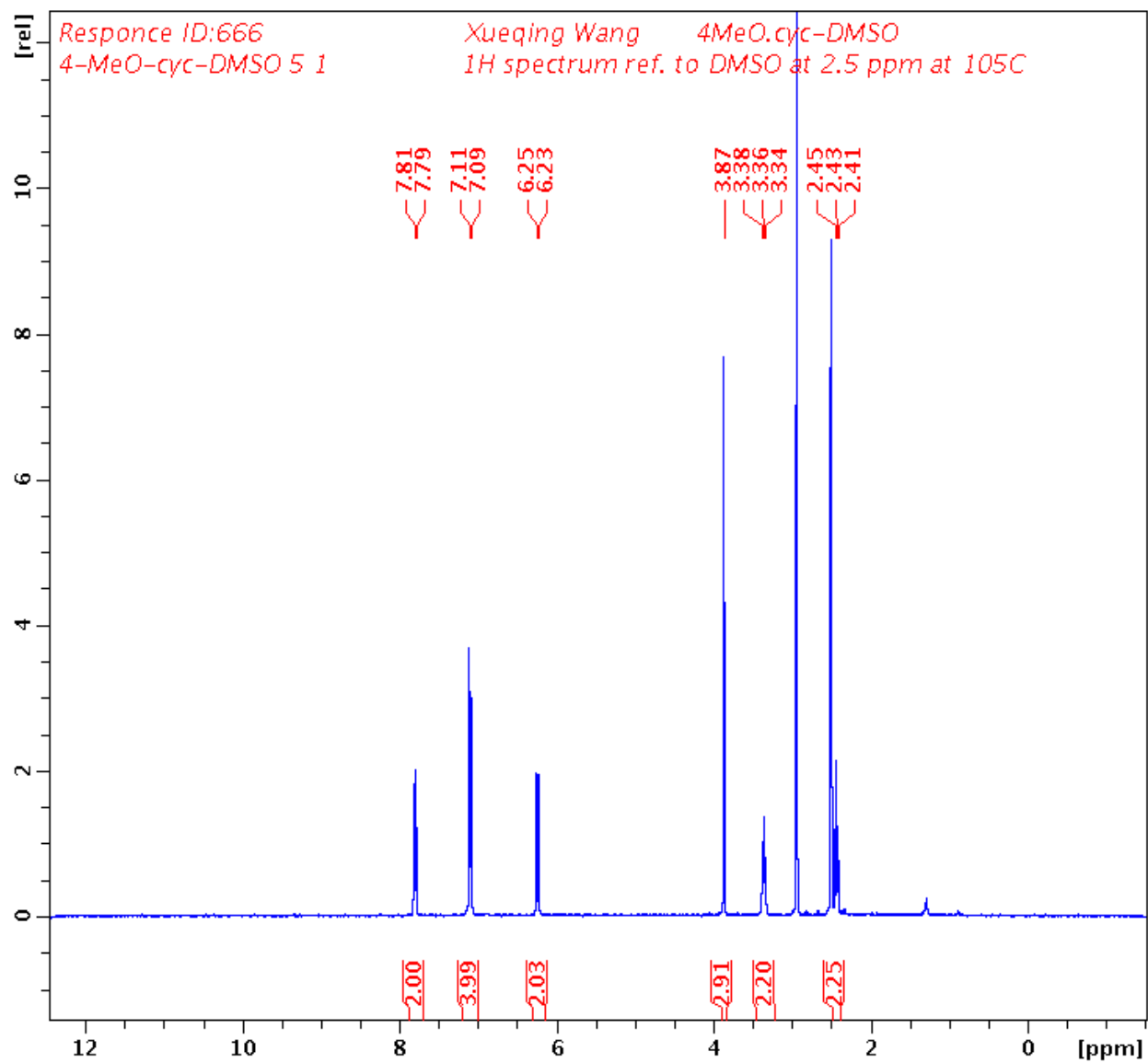
^1H NMR spectrum of **3.13e** (300 MHz, CDCl_3)

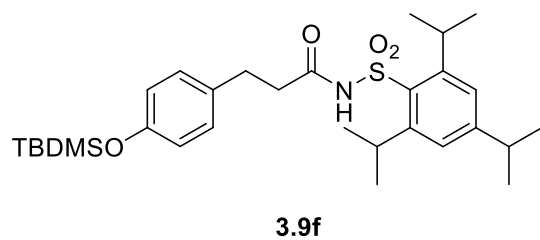


^{13}C NMR spectrum of **3.10e** (75 MHz, CDCl_3)



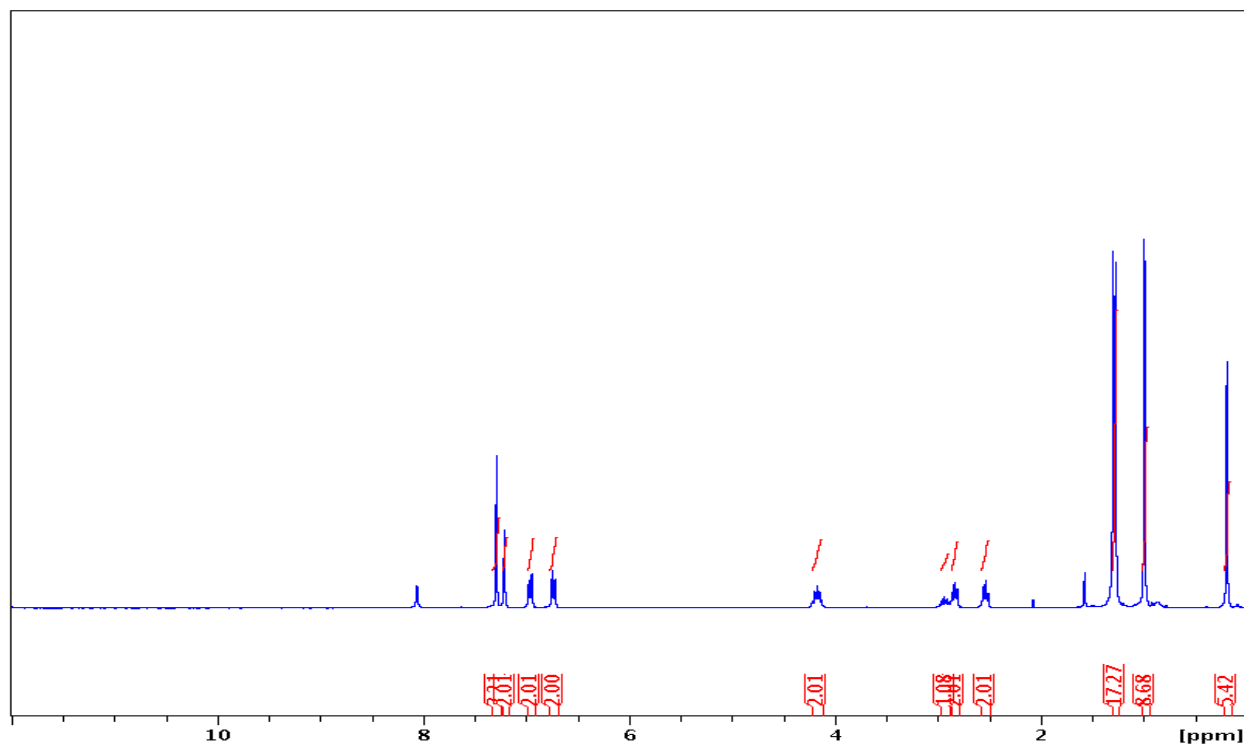
^1H NMR spectrum of **3.13e** (400 MHz, $\text{DMSO-}d_6$, 105°C)



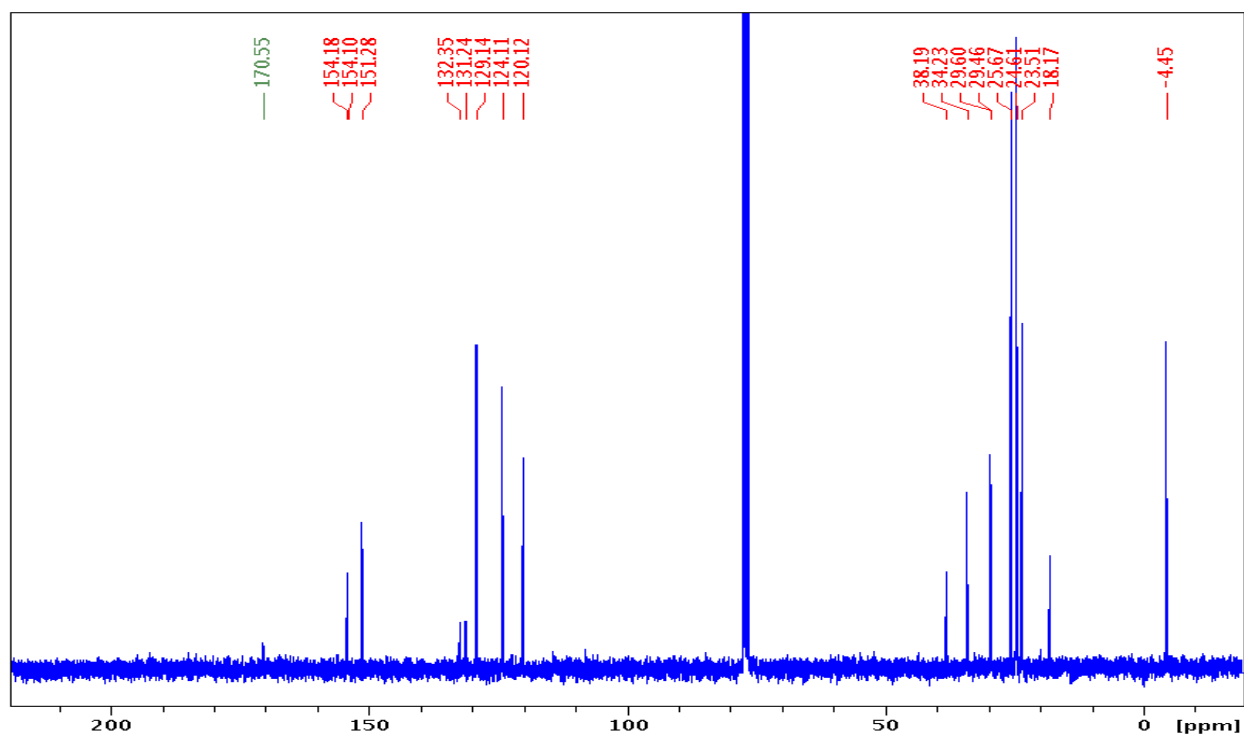


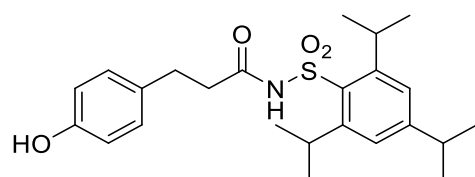
Compound 3.9f: 0.13 g (79% yield) from 0.1 g of **3.8**, white solid, m.p.: 136-137°C. **IR:** 3231 (broad), 2962, 1723, 1692. **¹H:** 7.20 (s, 2H), 6.95 (d, 2H, *J* = 8.4), 6.73 (d, 2H, *J* = 8.4), 4.16 (p, 3H, *J* = 5.4), 2.93 (m, 2H), 2.83 (t, 2H, *J* = 7.8), 2.53 (t, 2H, *J* = 7.8), 1.29 (s, 12H), 1.27 (s, 6H), 0.99 (s, 9H), 0.19 (s, 6H). **¹³C:** 170.6, 154.2, 154.1, 151.3, 132.4, 131.2, 129.1, 124.1, 120.1, 38.2, 34.2, 29.6, 29.5, 25.7, 24.6, 23.5, 18.2, -4.45. **HRMS:** calcd for C₃₀H₄₈NO₄SSi [M+H]⁺: 546.3073; found: 546.3073.

^1H NMR spectrum of **3.9f** (300 MHz, CDCl_3)



^{13}C NMR spectrum of **3.9f** (75 MHz, CDCl_3)

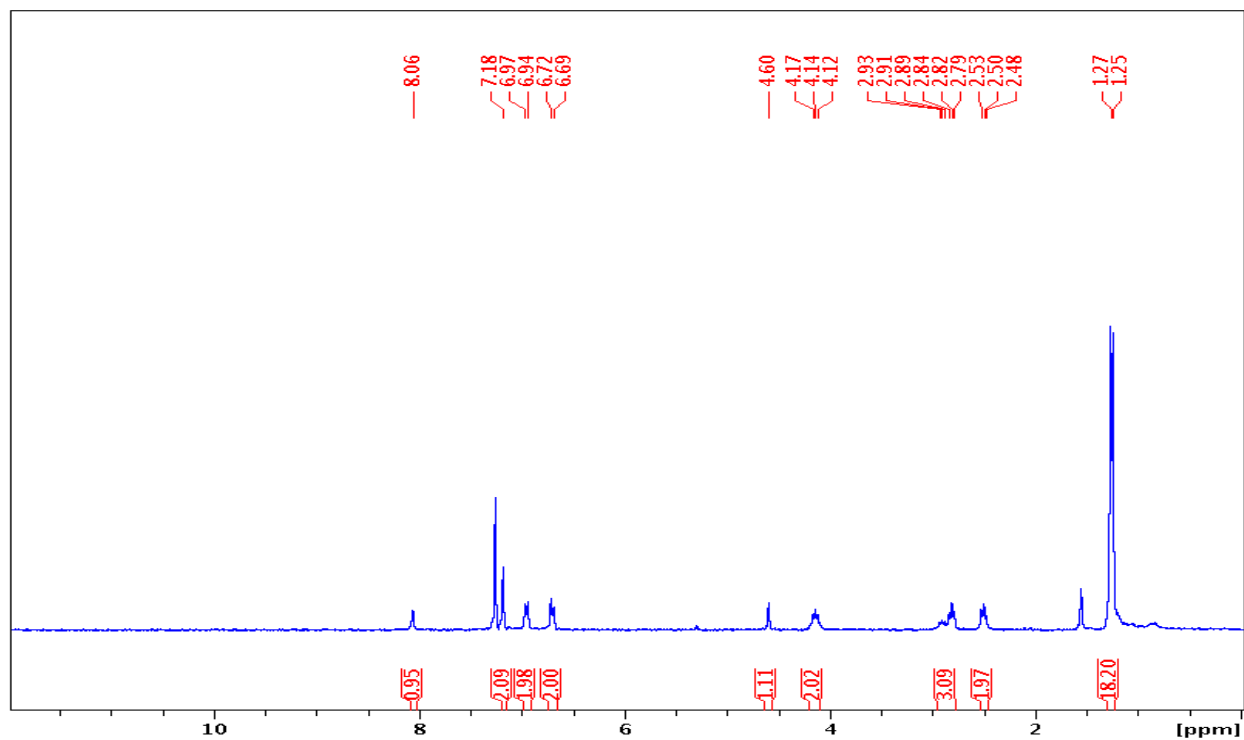




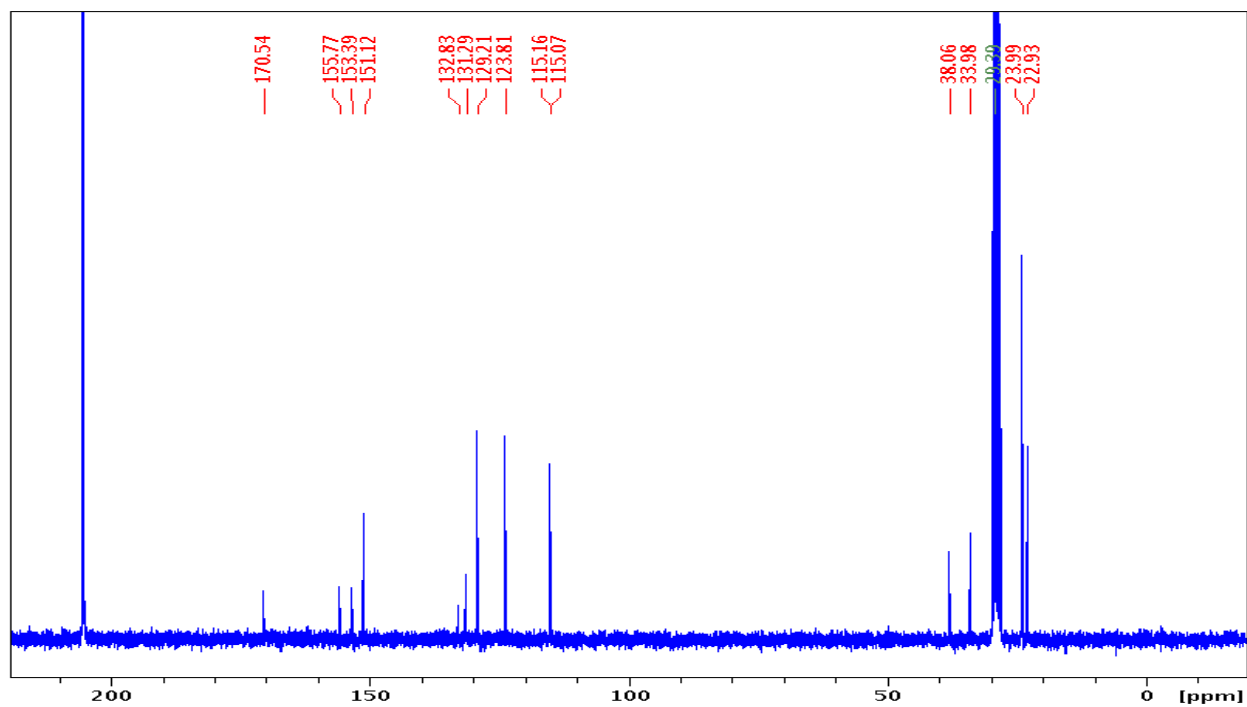
3.10f

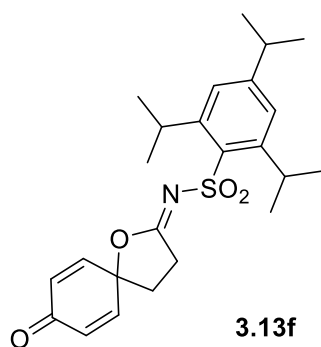
Compound 3.10f: 89 mg (91% yield) from 121 mg of **6a**, white solid, m.p.: 183-184°C. **IR:** 3417 (broad), 3240 (broad), 2962, 1692. **¹H:** 8.06 (s, broad, 1H), 7.18 (s, 2H), 6.95 (d, 2H, *J* = 8.4), 6.73 (d, 2H, *J* = 8.4), 4.16 (p, 3H, *J* = 5.4), 2.93 (m, 2H), 2.83 (t, 2H, *J* = 7.8), 2.53 (t, 2H, *J* = 7.8), 1.29 (s, 12H), 1.27 (s, 6H), 0.99 (s, 9H), 0.19 (s, 6H). **¹³C(acetone-*d*₆):** 170.5, 155.8, 153.4, 151.1, 132.8, 131.3, 129.2, 123.8, 115.2, 115.1, 38.1, 34.0, 29.4, 24.0, 23.0. **HRMS:** calcd for C₂₄H₃₂NO₄S [M-H]⁺: 430.2052; found: 430.2044.

^1H NMR spectrum of **3.10f** (300 MHz, CDCl_3)



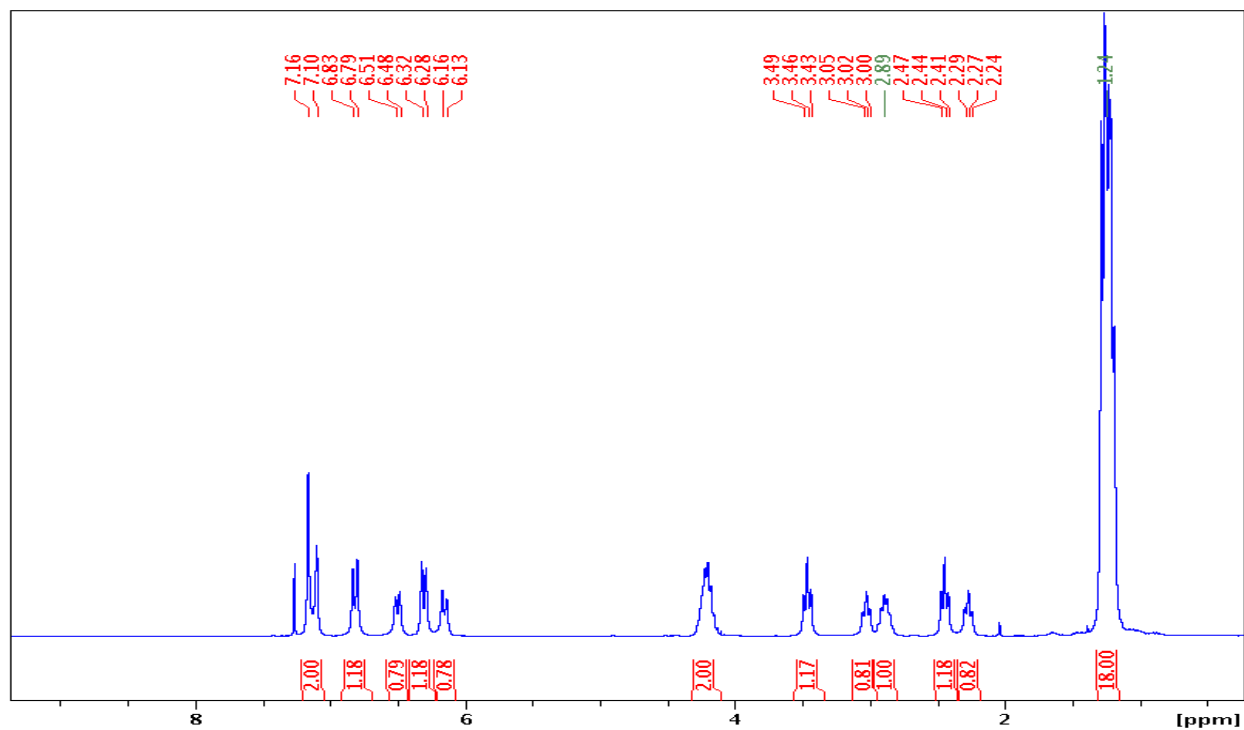
^{13}C NMR spectrum of **3.10f** (75 MHz, $\text{acetone-}d_6$)



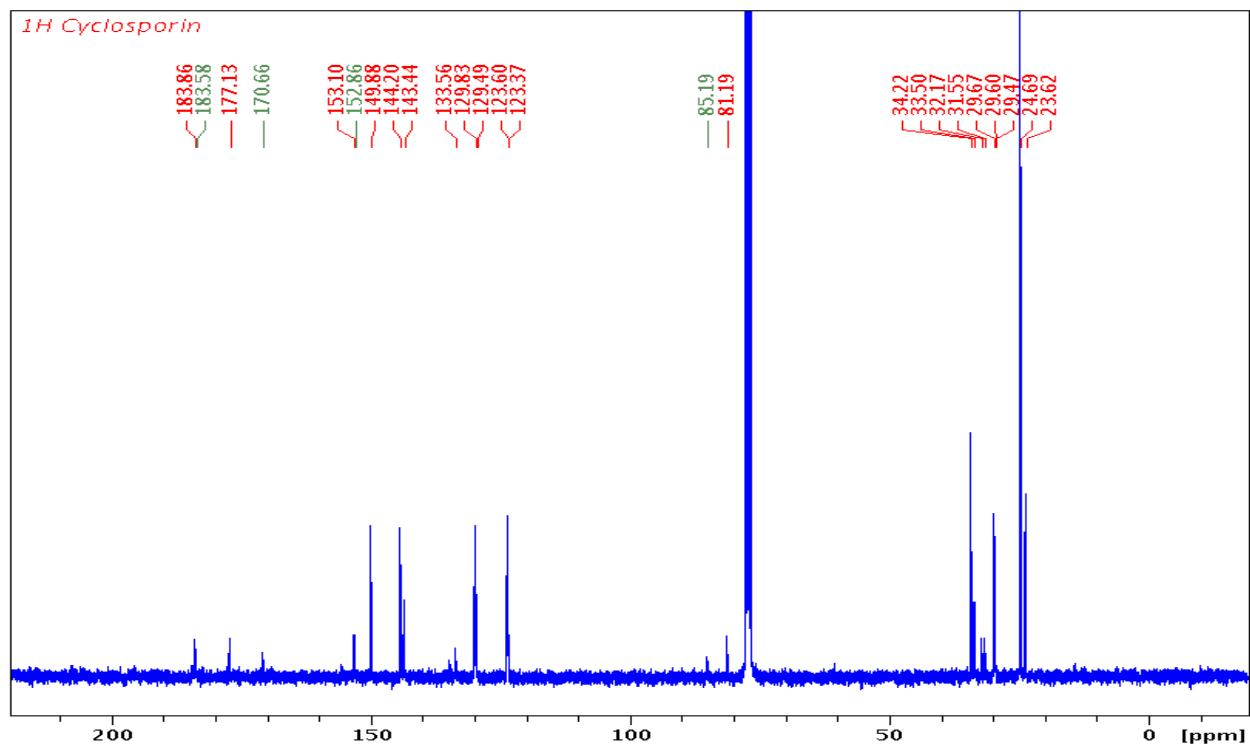


Compound 3.13f: 12 mg (59% yield) from 20 mg of **5a**, off-white solid, m.p.: 78-81°C. **IR:** 2960, 1675, 1633. **¹H (1.6:1 rotamer ratio, asterisks denote minor rotamer peaks, CDCl₃):** 7.16 (s, 2H), 7.10* (s, 2H), 6.81 (d, 2H, *J* = 9.7), 6.50* (d, 2H, *J* = 9.7), 6.32 (d, 2H, *J* = 9.7), 6.16* (d, 2H, *J* = 9.7), 6.81 (m, 2H), 4.21 (m, 2H), 3.47 (d, 2H, *J* = 8.2), 3.02* (d, 2H, *J* = 8.2), 2.89 (m, 1H), 2.44 (d, 2H, *J* = 8.2), 2.27* (d, 2H, *J* = 8.2), 1.24 (m, 18H). **¹³C (1.6:1 rotamer ratio, asterisks denote minor rotamer peaks, CDCl₃):** 183.9, 183.6*, 177.1, 170.7*, 153.1, 152.9*, 149.9, 144.2, 143.4*, 133.6, 129.8, 129.5*, 123.6, 123.4*, 85.2*, 81.2, 34.2, 33.5, 32.2*, 31.5*, 29.7, 29.6, 29.5*, 24.7, 23.6. **¹H (DMSO-*d*₆, 105°C):** 7.19 (s, 2H), 6.91 (d, 2H, *J* = 9.2), 6.29 (d, 2H, *J* = 10.0), 4.23 (m, 2H), 3.26 (d, 2H, *J* = 8.0), 2.94 (m, 1H), 2.39 (d, 2H, *J* = 8.2), 1.23 (d, 6H, *J* = 6.9), 1.20 (d, 12H, *J* = 6.8). **HRMS:** calcd for C₂₄H₃₂NO₄S [M+H]⁺: 430.2052; found: 430.2064.

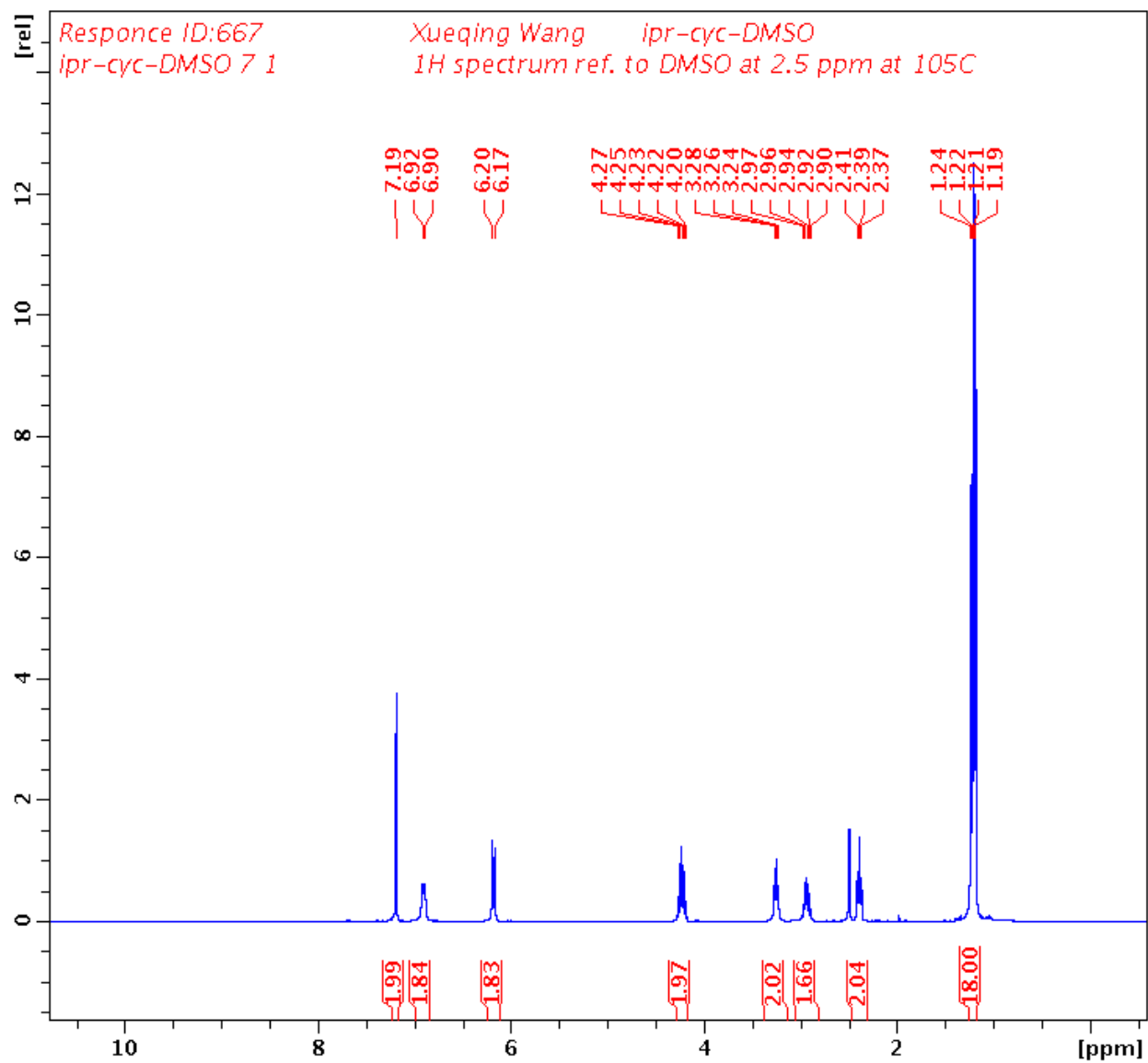
^1H NMR spectrum of **3.13f** (300 MHz, CDCl_3)



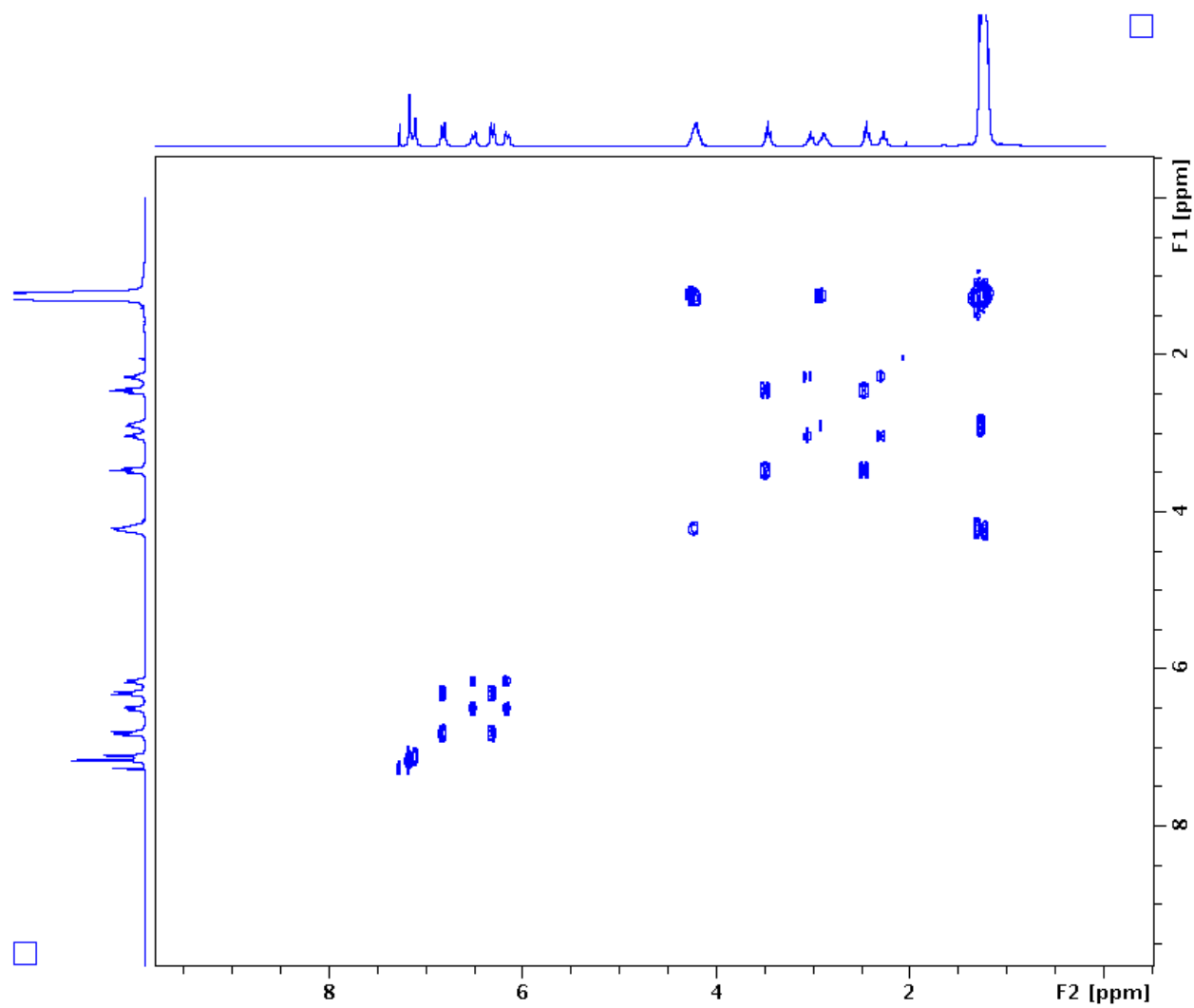
^{13}C NMR spectrum of **3.13f** (75 MHz, CDCl_3)



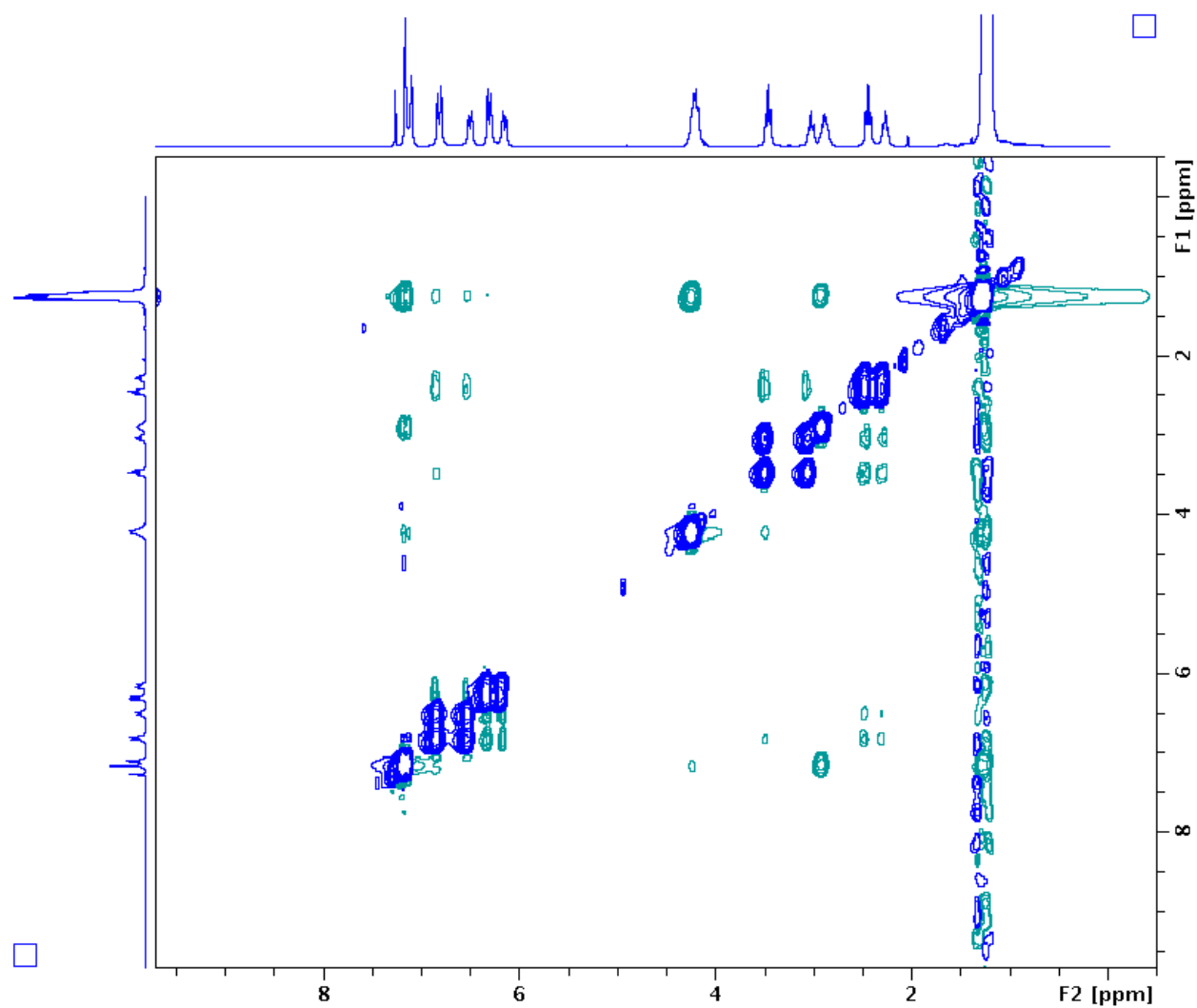
^1H NMR spectrum of **3.13f** (400 MHz, DMSO- d_6 , 105°C):



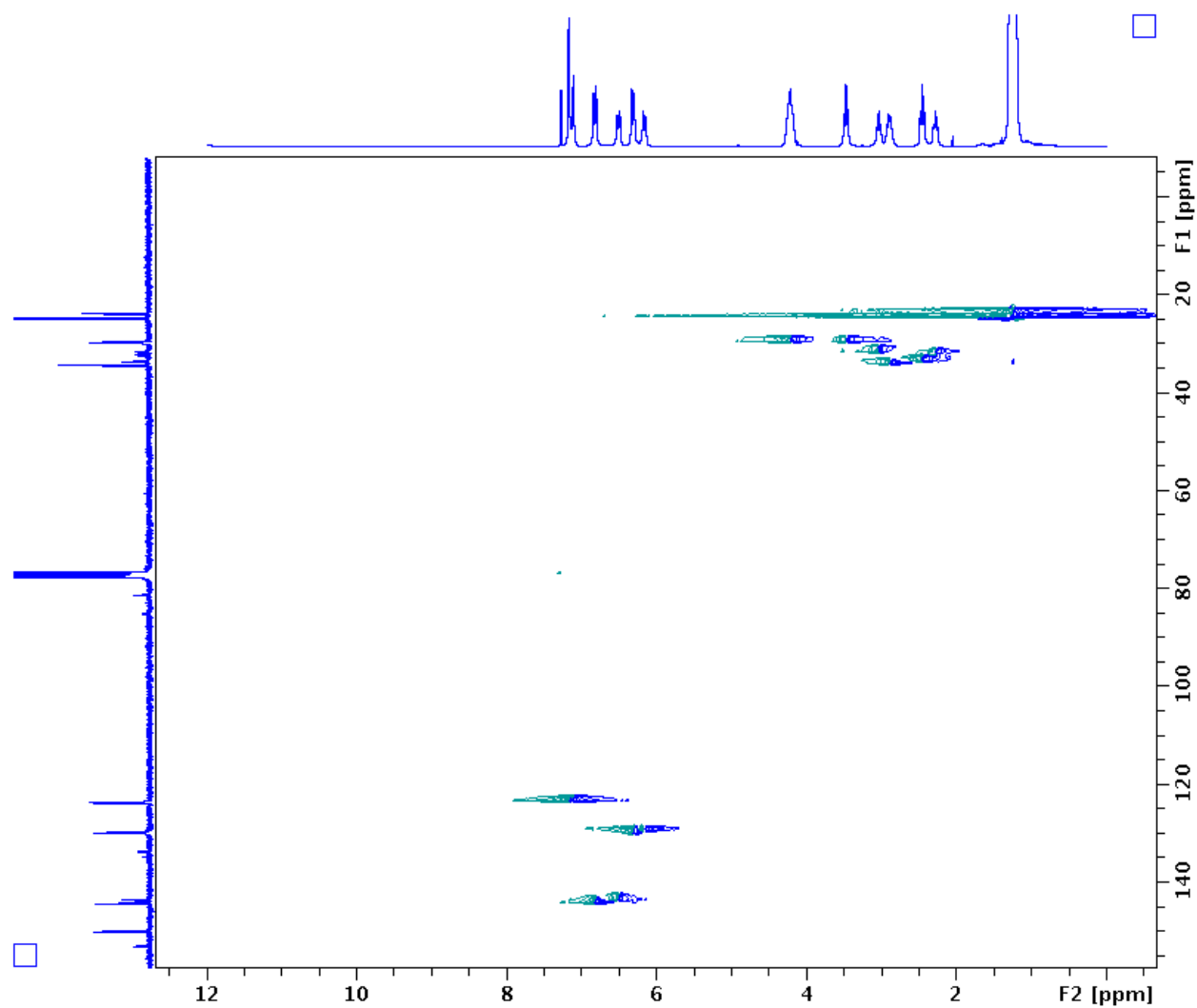
COSY spectrum of **3.13f** (300 MHz, CDCl₃)



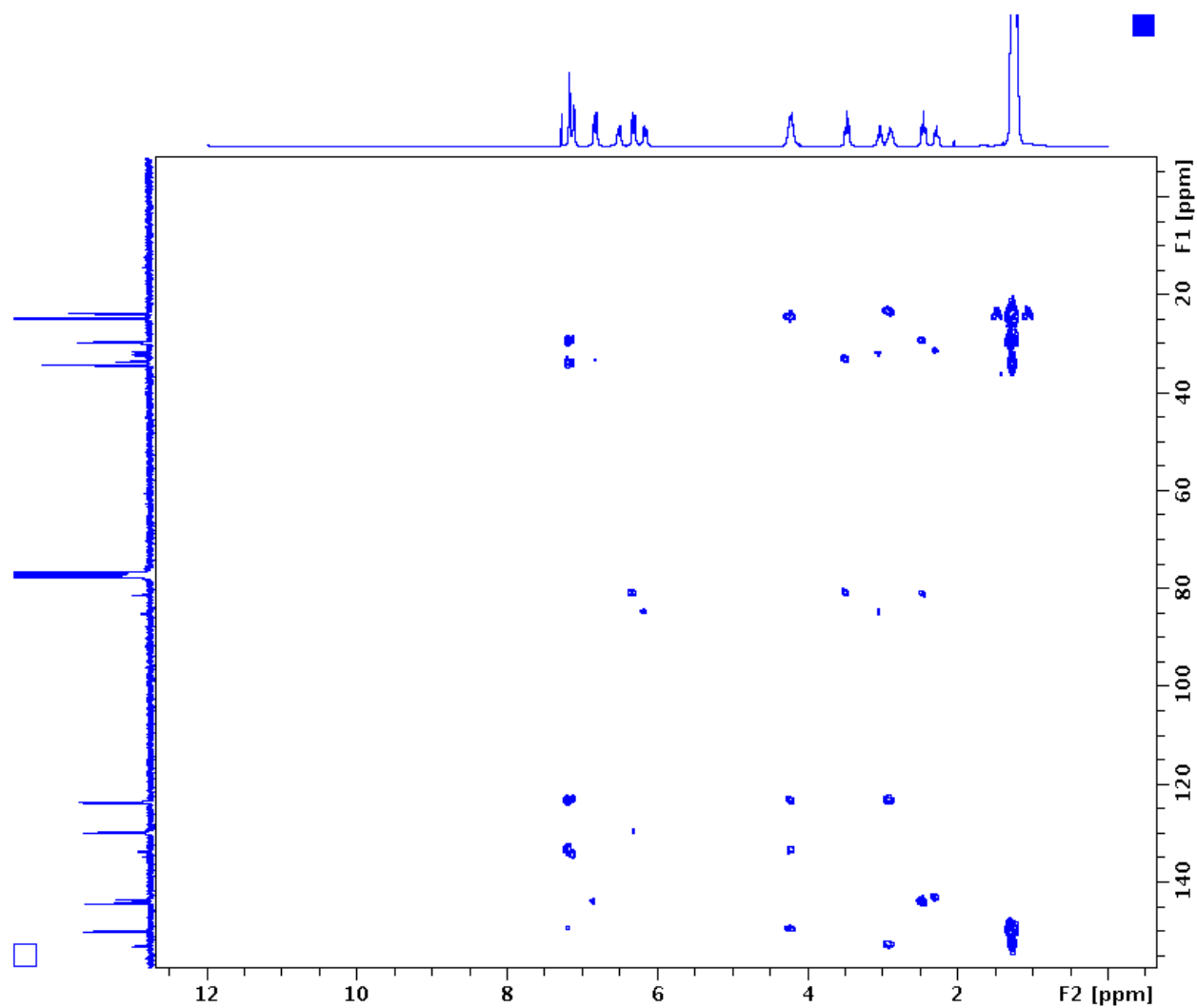
NOESY spectrum of **3.13f** (300 MHz, CDCl₃)



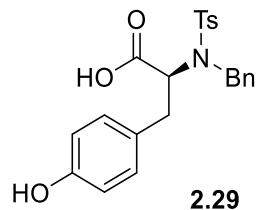
HSQC spectrum of **3.13f** (CDCl₃)



HMBC spectrum of **3.13f** (CDCl₃)

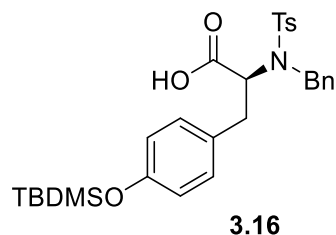


B.2. Experimental Data of Tyrosine-Derivatives for Rearrangement



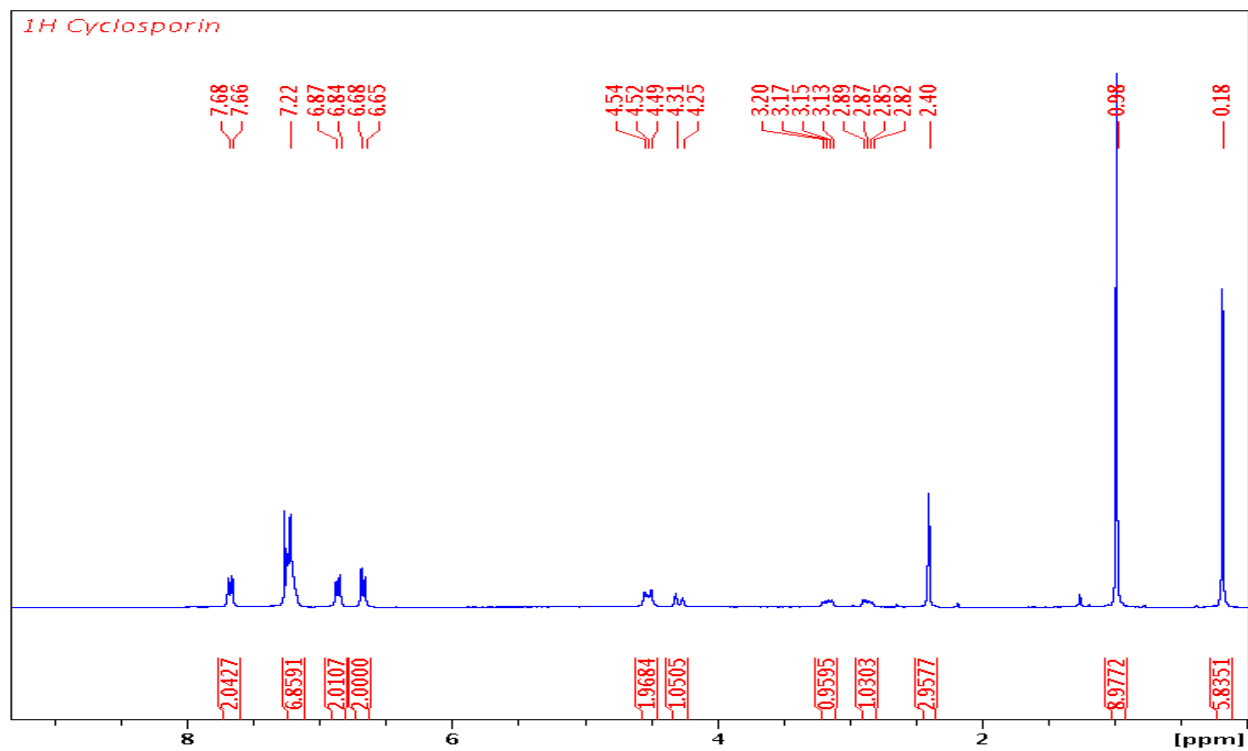
Compound 2.29: 12.5 g, 29.4 mmol (64 % yield), colorless crystals from refluxing DCM; m.p.: 154-156 °C. **IR:** 3455-3065 (broad), 1719, 1153. **¹H (acetone-**d**₆):** 8.20 (brs, 1H), 7.73 (d, 2H, *J* = 8.3), 7.35 (d, 2H, *J* = 8.3), 7.35-7.23 (m, 5H), 6.90 (d, 2H, *J* = 8.5), 6.69 (d, 2H, *J* = 8.5), 4.65 (d, 1H, *J* = 16.1), 4.64 (m, 1H), 4.43 (d, 1H, *J* = 16.1), 3.07 (dd, 1H, *J* = 13.9, 8.3), 2.72 (dd, 1H, *J* = 13.9, 6.5), 2.41 (s, 3H). **¹³C: (acetone-**d**₆):** 171.43, 156.93, 144.23, 138.66, 138.46, 131.03, 130.29, 129.21, 128.92, 128.85, 128.46, 128.09, 115.92, 62.36, 50.20, 36.99, 21.40. **HRMS** calcd for C₂₃H₂₃NO₅Na [M+Na]⁺: 448.1195; found: 448.1209. (*cf.* ref 26).

[α]_D²⁴ -8.9 (c 0.56, acetone).

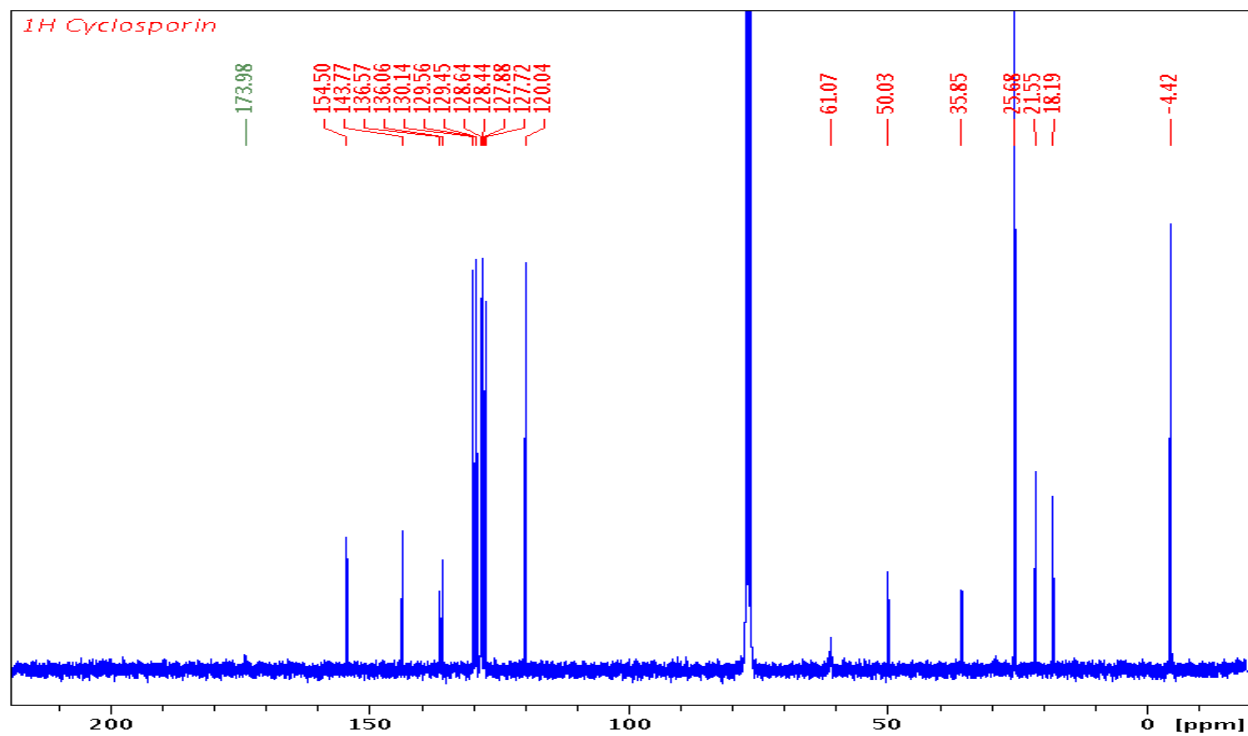


Compound 3.16: 60% yield over two steps from **2.29**, pale yellow solid; m.p.: 58-60°C. **IR:** 2930 (broad), 1720. **¹H:** 7.67 (d, 2H, J = 8.3), 7.17-7.25 (m, 7H), 6.86 (d, 2H, J = 8.2), 6.67 (d, 2H, J = 8.2), 4.51 (d, 1H, J = 15.7), 4.52 (s, 1H), 4.28 (d, 1H, J = 16.1), 3.16 (dd, 1H, J = 14.1, 7.2), 2.86 (dd, 1H, J = 14.1, 7.2), 2.40 (s, 3H), 0.98 (s, 9H), 0.18 (s, 6H). **¹³C:** 174.0, 154.5, 143.8, 136.6, 136.1, 130.1, 129.6, 129.5, 128.6, 128.4, 127.9, 127.7, 120.0, 61.1, 50.0, 35.9, 25.7, 21.5, 18.2, -4.4. **HRMS:** calcd for C₂₉H₃₈NO₅SSi [M+H]⁺: 540.2240; found: 540.2244. [α]_D²³ +9.8 (c 0.26, acetone).

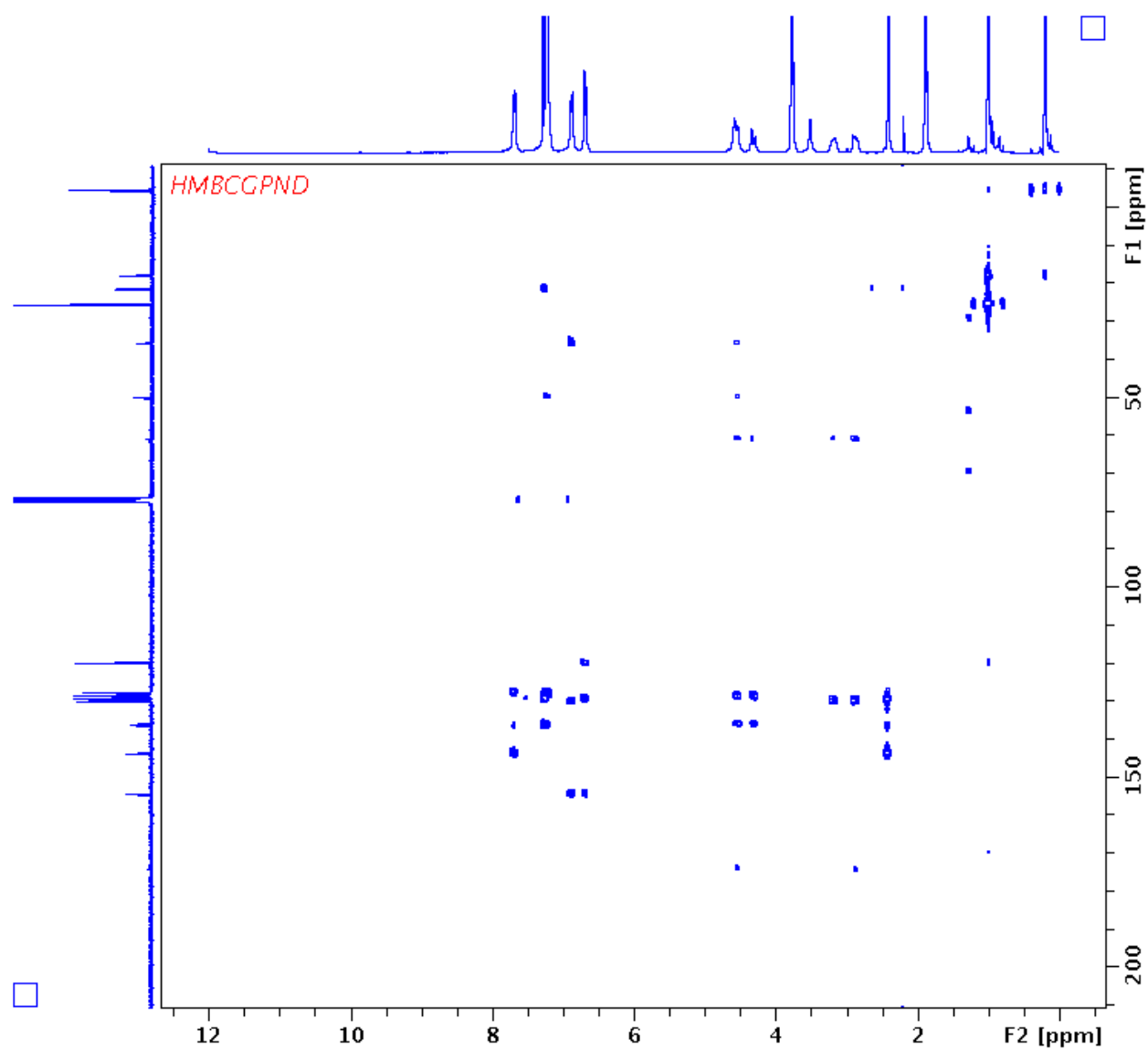
^1H NMR spectrum of **3.16** (300 MHz, CDCl_3)

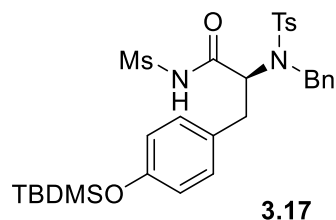


^{13}C NMR spectrum of **3.16** (75 MHz, CDCl_3)



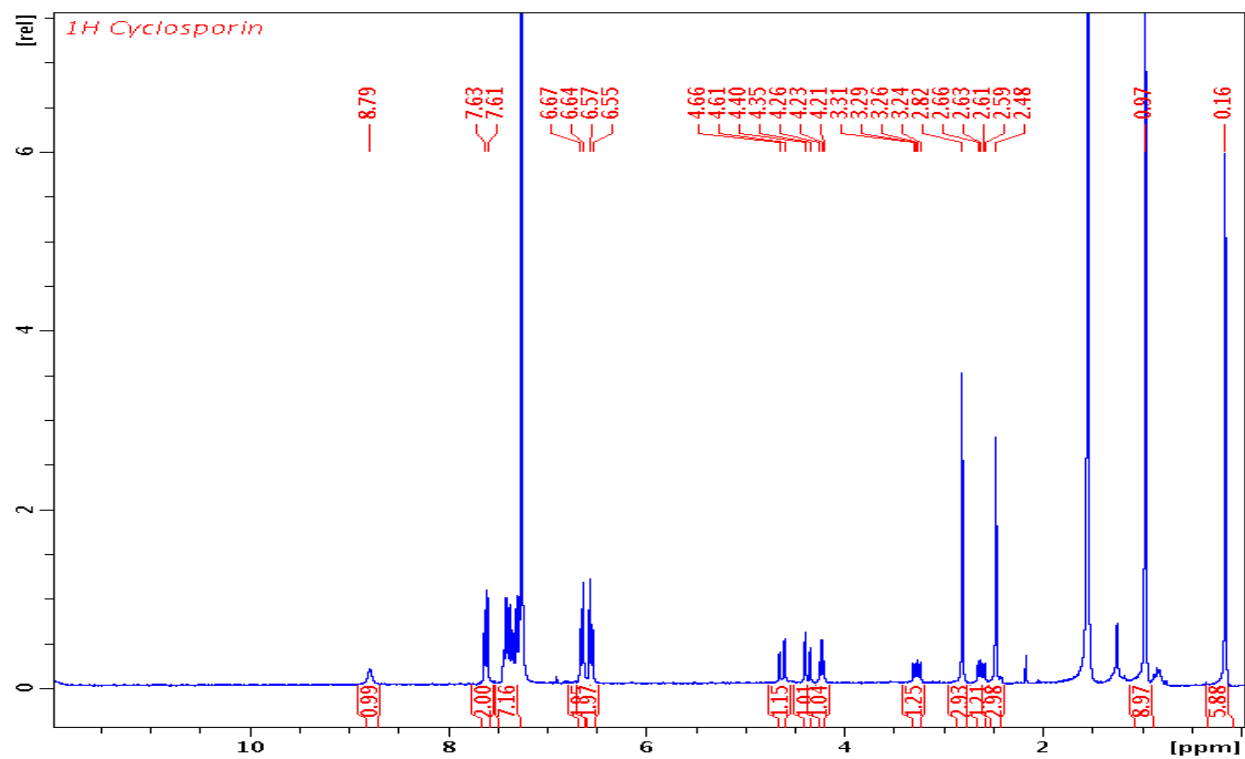
HMBC spectrum of **3.16** (CDCl₃)



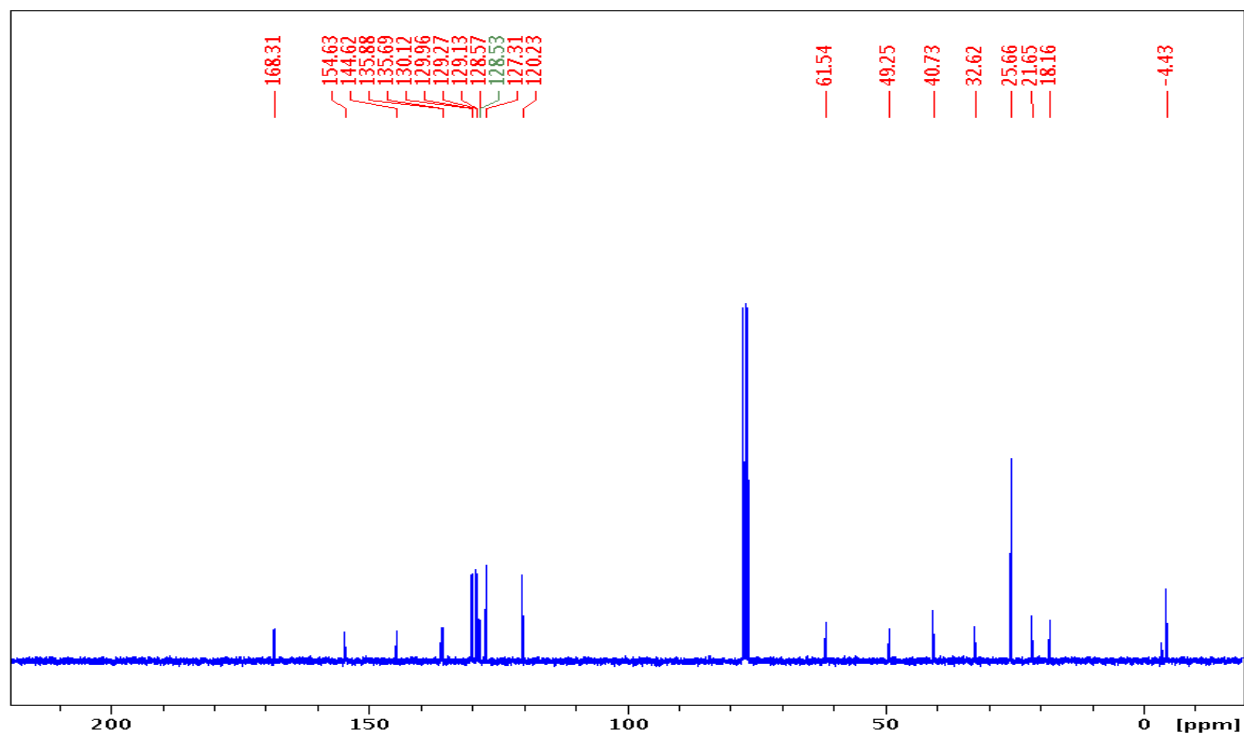


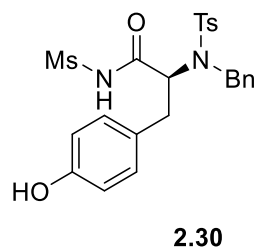
Compound 3.17: 0.18 g (60% yield) from 0.27 g of **12**, light yellow solid, m.p.: 69°C. **IR:** 3245, 1724. **¹H:** 8.79 (br, s, 1H), 7.62 (d, 2H, *J* = 8.3), 7.36 (m, 7H), 6.66 (d, 2H, *J* = 8.4), 6.56 (d, 2H, *J* = 8.4), 4.64, 4.38 (ABq, 2H, JAB = 77.5), 4.25 (t, 1H, *J* = 7.0), 3.28 (dd, 1H, *J* = 5.4), 2.82 (s, 3H), 2.62 (dd, 1H, *J* = 5.2), 2.48 (s, 3H), 0.97 (s, 9H), 0.16 (s, 6H). **¹³C:** 168.3, 154.6, 144.6, 135.9, 135.7, 130.1, 129.9, 129.3, 129.1, 128.6, 128.5, 127.3, 120.2, 61.5, 49.3, 40.7, 32.6, 25.7, 21.7, 18.1, -4.4. **HRMS:** calcd for C₃₀H₄₀N₂O₆S₂SiNa [M+Na]⁺: 639.1995; found: 639.1990. **[α]_D²³** -13 (c 0.50, acetone).

^1H NMR spectrum of **3.17** (300 MHz, CDCl_3)



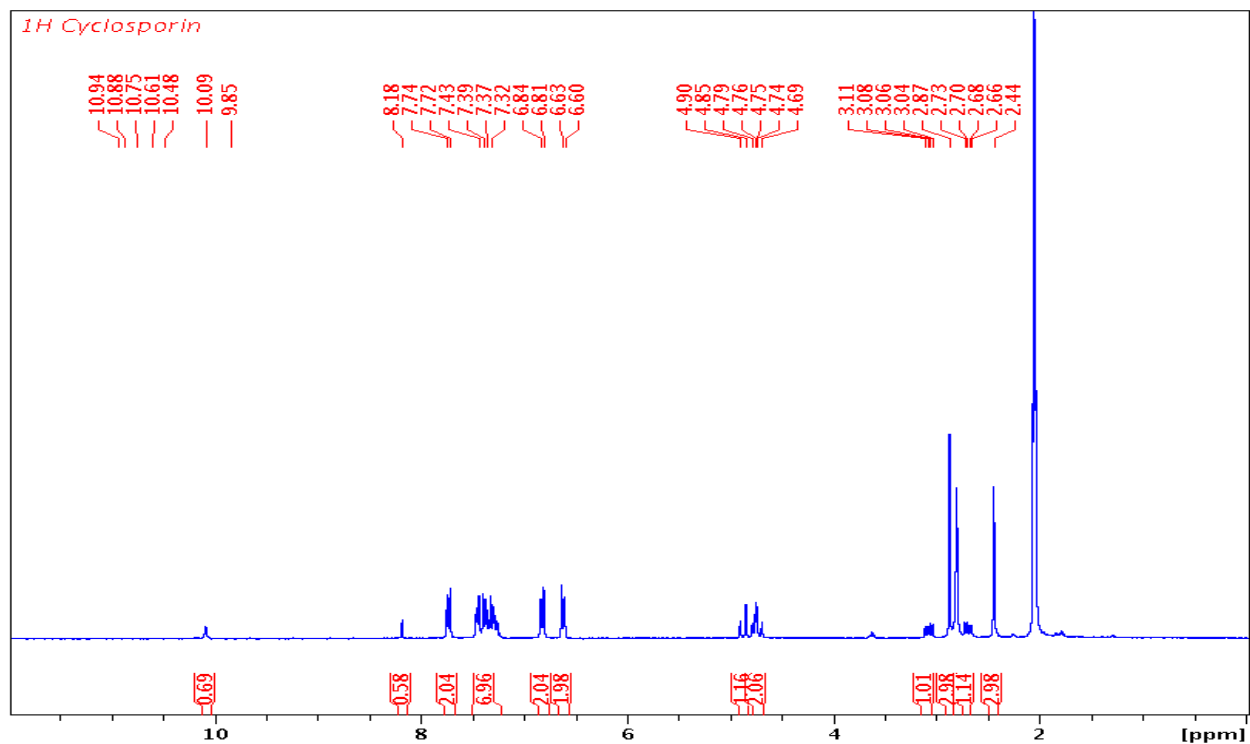
^{13}C NMR spectrum of **3.17** (75 MHz, CDCl_3)



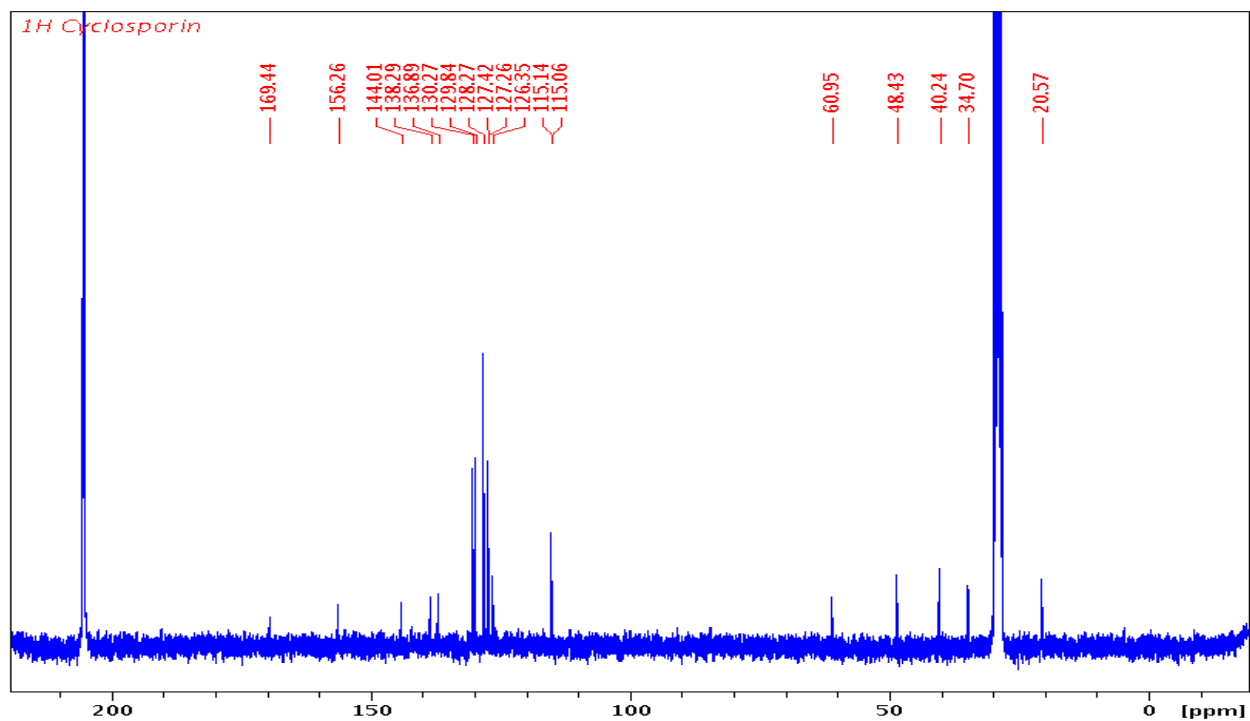


Compound 2.30: 74 mg (80% yield) from 113 mg of **13**, white solid, m.p.: 206-207°C. **IR:** 3461 (broad), 3205 (broad), 1725. **¹H (acetone-*d*₆):** 10.09 (br, s, 1H), 8.18 (br, s, 1H), 7.73 (d, 2H, *J* = 8.3), 7.36 (m, 7H), 6.83 (d, 2H, *J* = 8.5), 6.62 (d, 2H, *J* = 8.5), 4.88, 4.37 (ABq, 2H, *J*_{AB} = 46.8), 4.76 (t, 1H, *J* = 7.5), 3.07 (dd, 1H, *J* = 14.0, 8.3), 2.87 (s, 3H), 2.69 (dd, 1H, *J* = 14.0, 8.3), 2.44 (s, 3H). **¹³C(acetone-*d*₆):** 169.4, 156.3, 144.0, 138.3, 136.9, 130.3, 129.8, 128.3, 127.4, 127.3, 126.4, 115.1, 115.0, 61.0, 48.4, 40.2, 34.7, 20.6. **¹H:** 8.80 (br, s, 1H), 7.63 (d, 2H, *J* = 8.1), 7.36 (m, 7H), 6.67 (d, 2H, *J* = 8.3), 6.56 (d, 2H, *J* = 8.3), 4.67, 4.37 (ABq, 2H, *J*_{AB} = 92.2), 4.61 (br, s, 1H), 4.23 (t, 1H, *J* = 6.9), 3.30 (dd, 1H, *J* = 5.4), 2.83 (s, 3H), 2.63 (dd, 1H, *J* = 5.2), 2.50 (s, 3H). **HRMS:** calcd for C₂₄H₂₆N₂O₆S₂Na [M+Na]⁺: 525.1130; found: 525.1136. [**α**]_D²³ -7.0 (c 0.20, acetone).

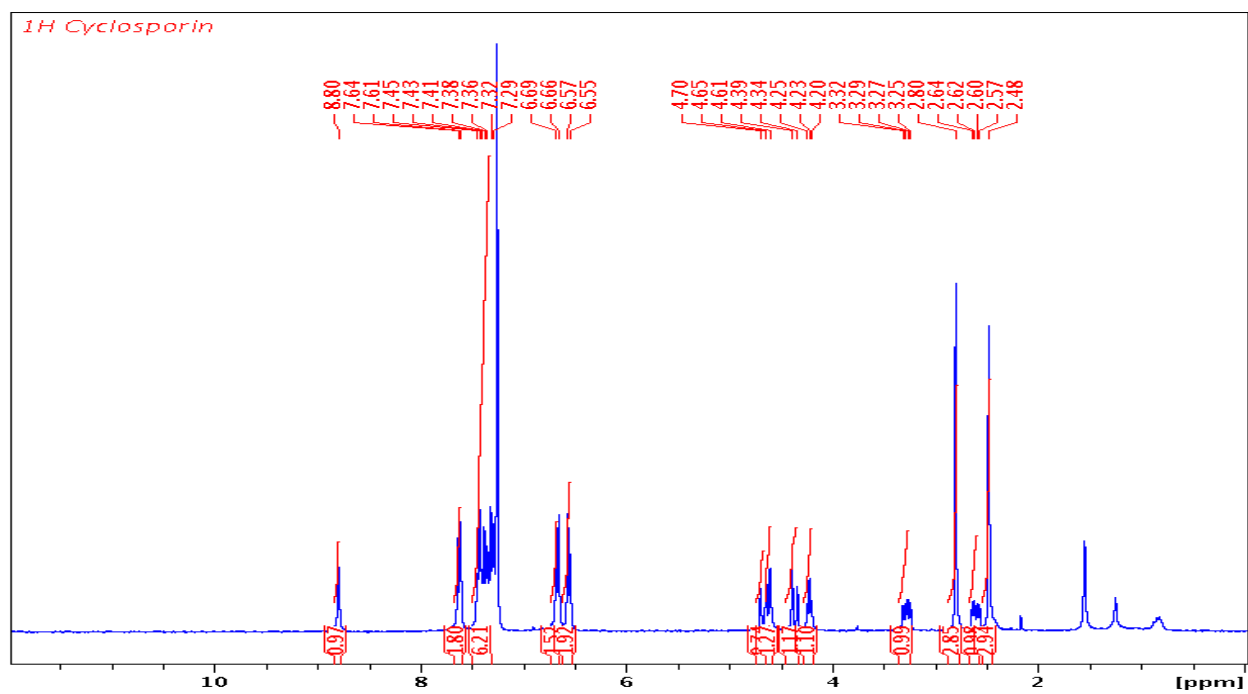
^1H NMR spectrum of **2.30** (300 MHz, acetone- d_6)

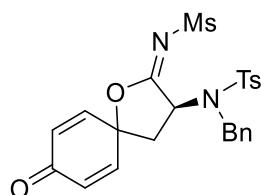


^{13}C NMR spectrum of **2.30** (75 MHz, acetone- d_6)



^1H NMR spectrum of **2.30** (300 MHz, CDCl_3)

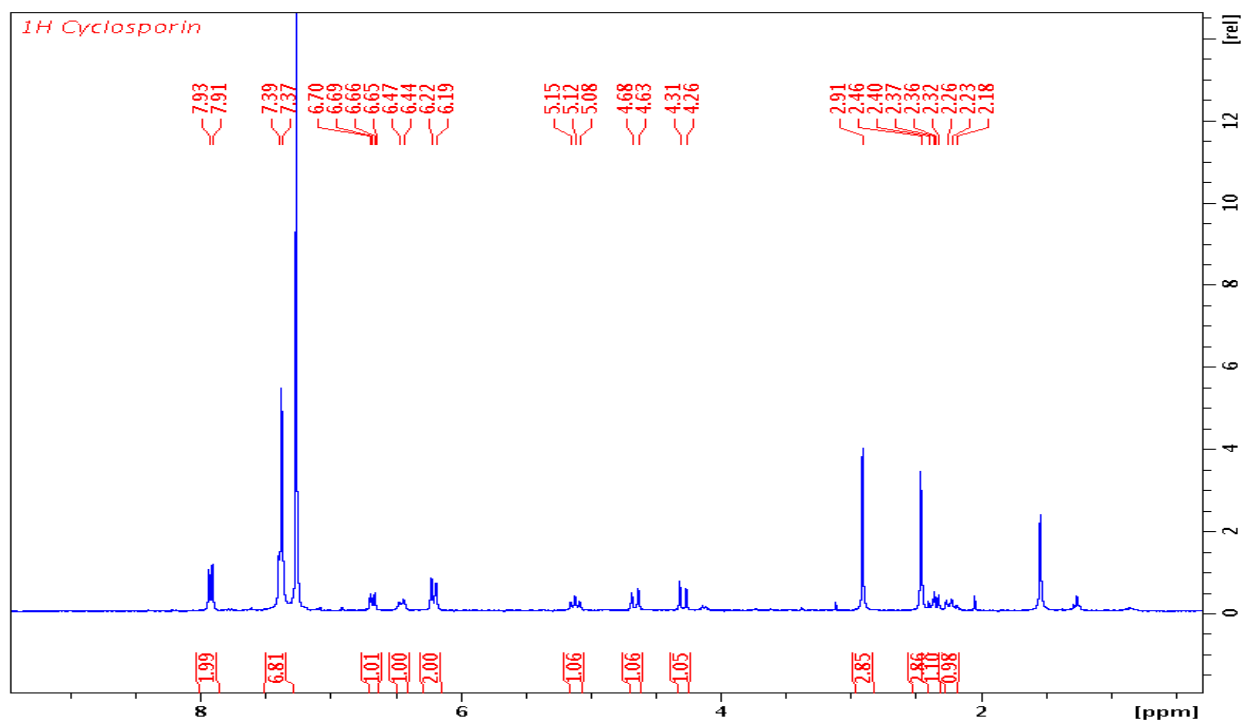




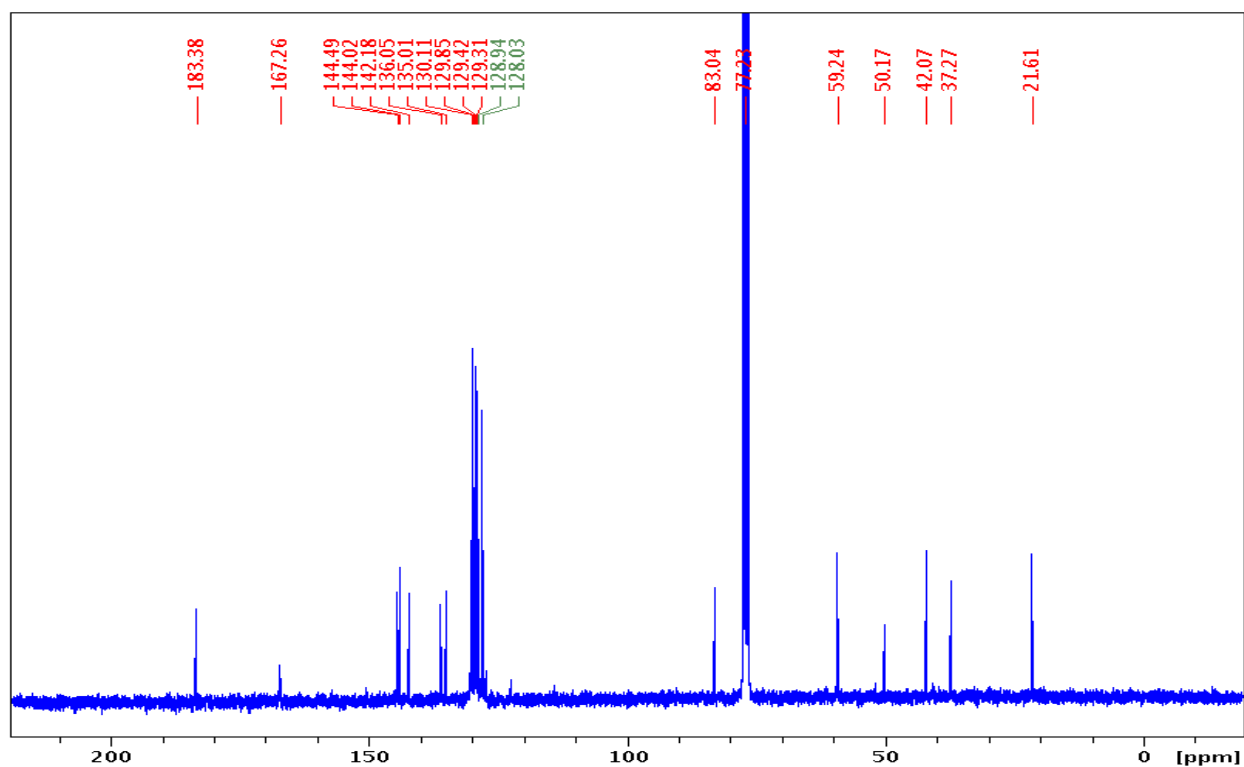
3.19

Compound 3.19: 0.37 g (88% yield) from 0.41 g of **14**, light yellow solid, m.p.: 105°C. **IR:** 3067, 3032, 1674, 1636. **¹H:** 7.92 (d, 2H, $J = 8.2$), 7.37 (m, 7H), 6.69 (dd, 1H, $J_{AB} = 10.2$), 6.46 (dd, 1H, $J_{AB} = 10.2$), 6.20 (d, 2H, $J = 10.2$), 5.13 (t, 1H, $J = 10.2$), 4.65, 4.29 (ABq, 2H, $J_{AB} = 110.0$), 2.90 (s, 3H), 2.46 (s, 3H), 2.26 (m, 2H). **¹³C:** 183.4, 167.3, 144.5, 144.0, 142.2, 136.1, 135.0, 130.1, 129.9, 129.4, 129.3, 128.9, 128.0, 83.0, 59.2, 50.2, 42.1, 37.3, 21.6. **HRMS:** calcd for C₂₄H₂₄N₂O₆S₂Na [M+Na]⁺: 523.0974; found: 523.0966. **[α]_D²³** +14 (c 0.18, acetone).

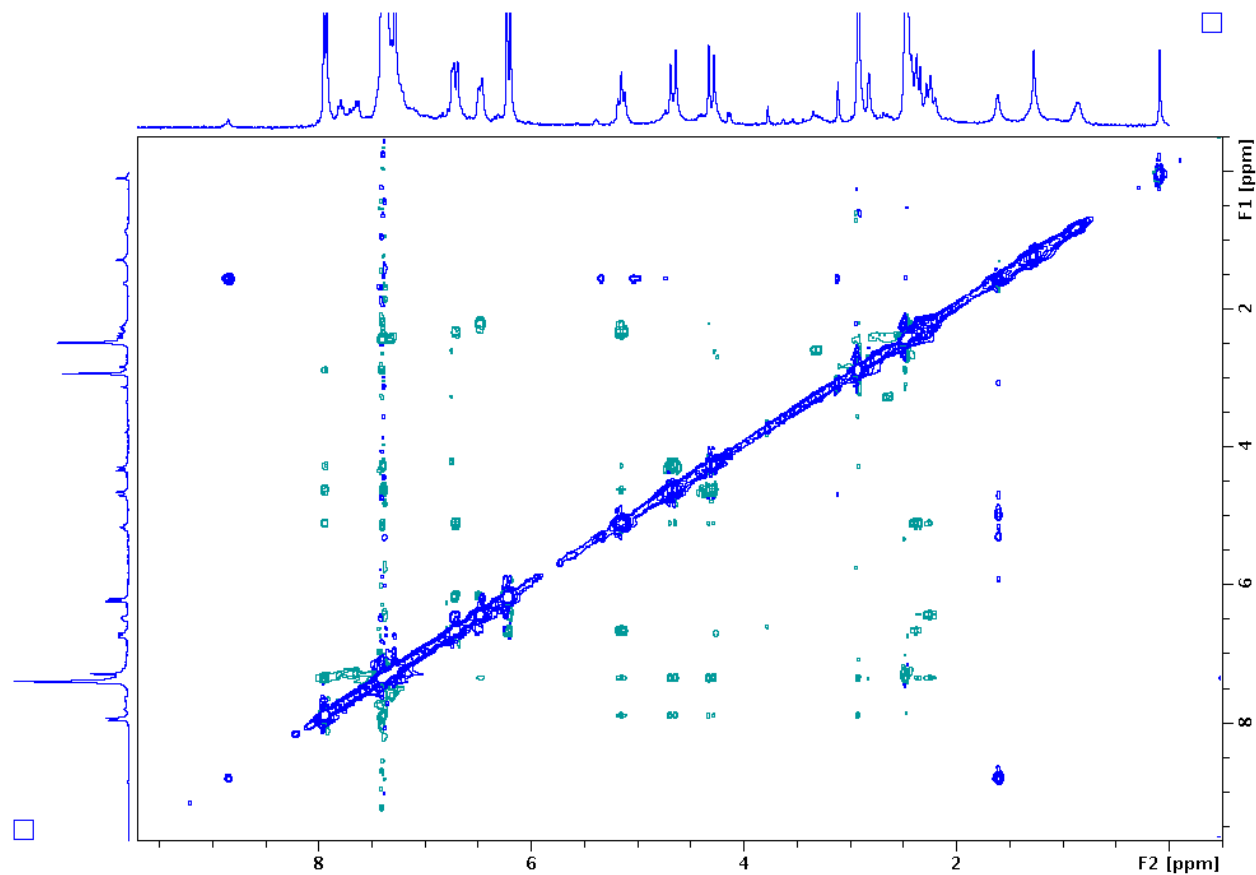
^1H NMR spectrum of **3.19** (300 MHz, CDCl_3)



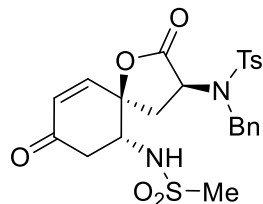
^{13}C NMR spectrum of **3.19** (75 MHz, CDCl_3)



NOESY spectrum of **3.19** (CDCl₃)



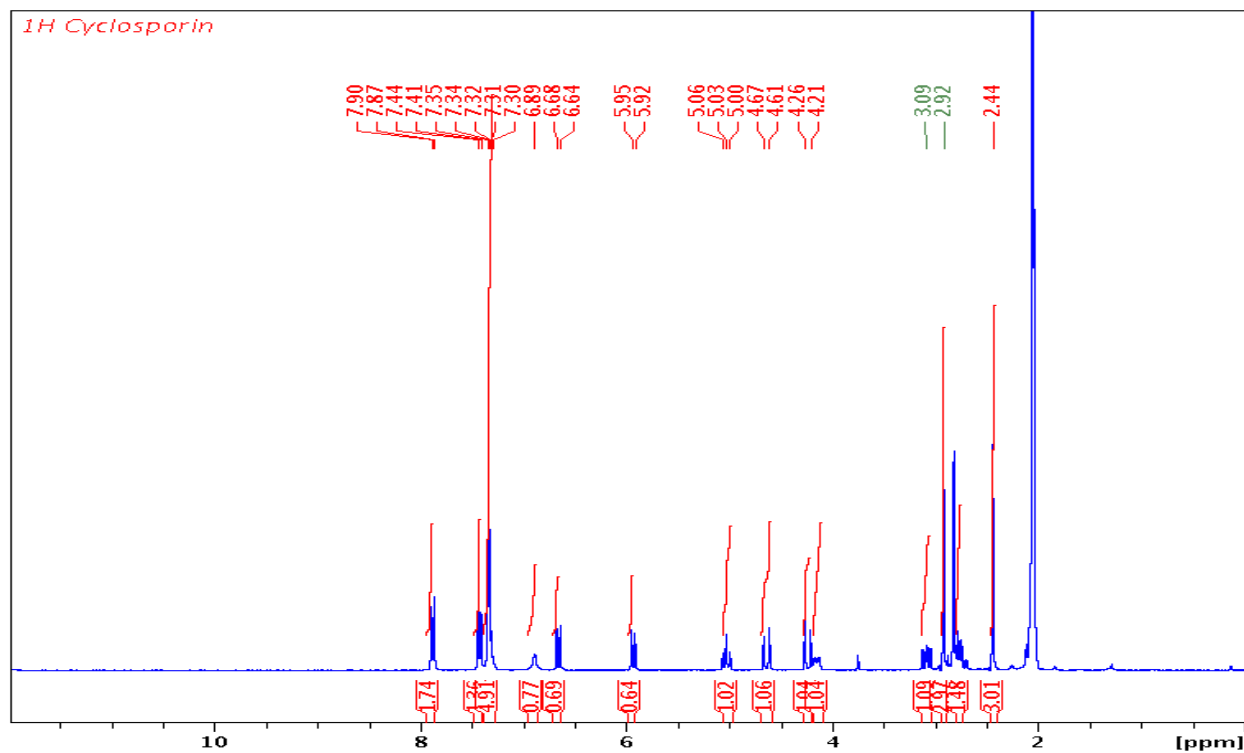
The NOESY-2D correlation between the protons at 2.92 ppm (the methyl group of the methanesulfonyl segment) with 7.94 ppm (the tosyl unit), strongly suggests that the mesyl CH₃ is in close proximity to the tosyl group. However, no correlation is apparent between the methanesulfonyl group and the hydrogens of the dienone, even though a correlation would be expected.



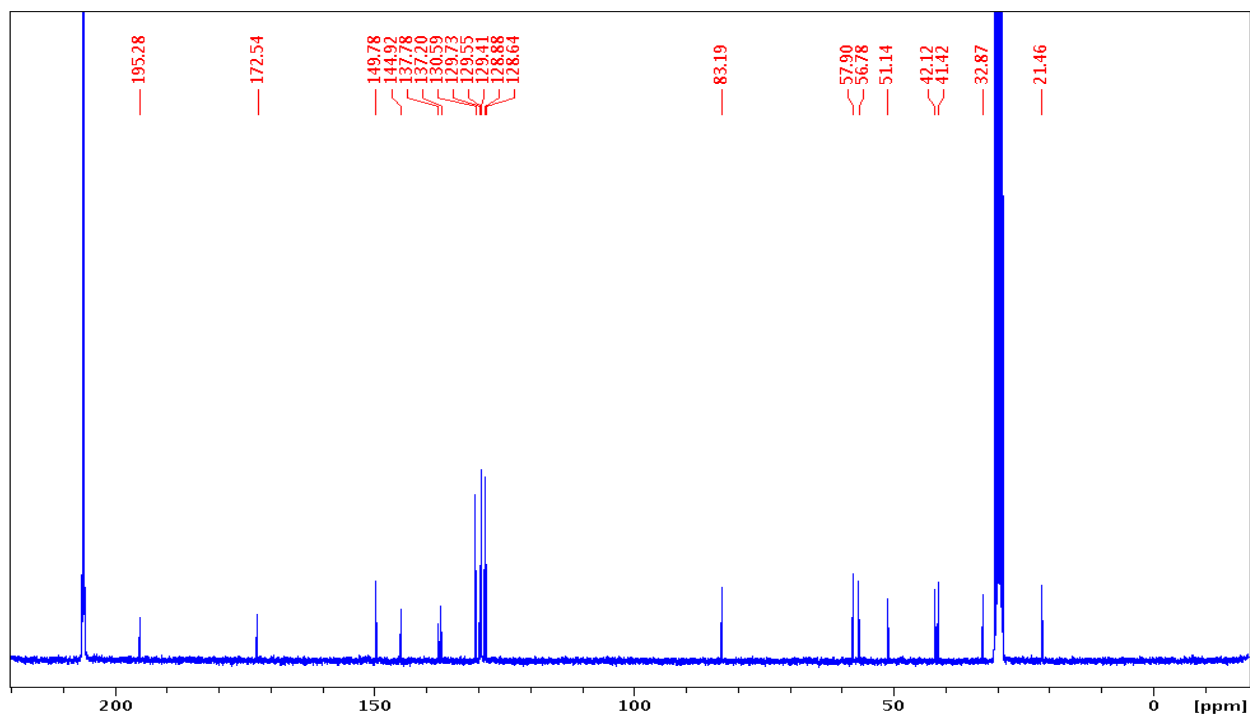
rac-**3.18**

Compound 3.18 and the corresponding enantiomer: 0.08 g (77% yield) from 0.10 g of **15**, white solid, m.p.: 134-136°C.. **IR:** 3258 (broad), 3068, 1787, 1692. **¹H (acetone-*d*₆):** 7.88 (d, 2H, *J* = 8.2), 7.43 (d, 2H, *J* = 8.2), 7.33 (m, 5H), 6.90 (d, 1H, *J* = 9.1), 6.66 (d, 1H, *J* = 10.2), 5.93 (d, 2H, *J* = 10.2), 5.03 (t, 1H, *J* = 10.2), 4.64, 4.24 (ABq, 2H, *J*_{AB} = 121.4), 4.16 (m, 1H), 3.09 (dd, 1H, *J*_{AB} = 14.2), 2.93 (s, 3H), 2.10 (m, 2H), 2.45 (s, 3H). **¹³C (acetone-*d*₆):** 195.3, 172.5, 149.8, 144.9, 137.8, 137.2, 130.6, 129.7, 129.6, 129.4, 128.9, 128.6, 83.2, 57.9, 56.8, 51.1, 42.1, 41.4, 32.9, 21.5. **HRMS:** calcd for C₂₄H₂₆N₂O₇S₂Na [M+Na]⁺: 541.1079; found: 541.1085. **[α]_D²³** -4.3 (c 0.1, acetone).

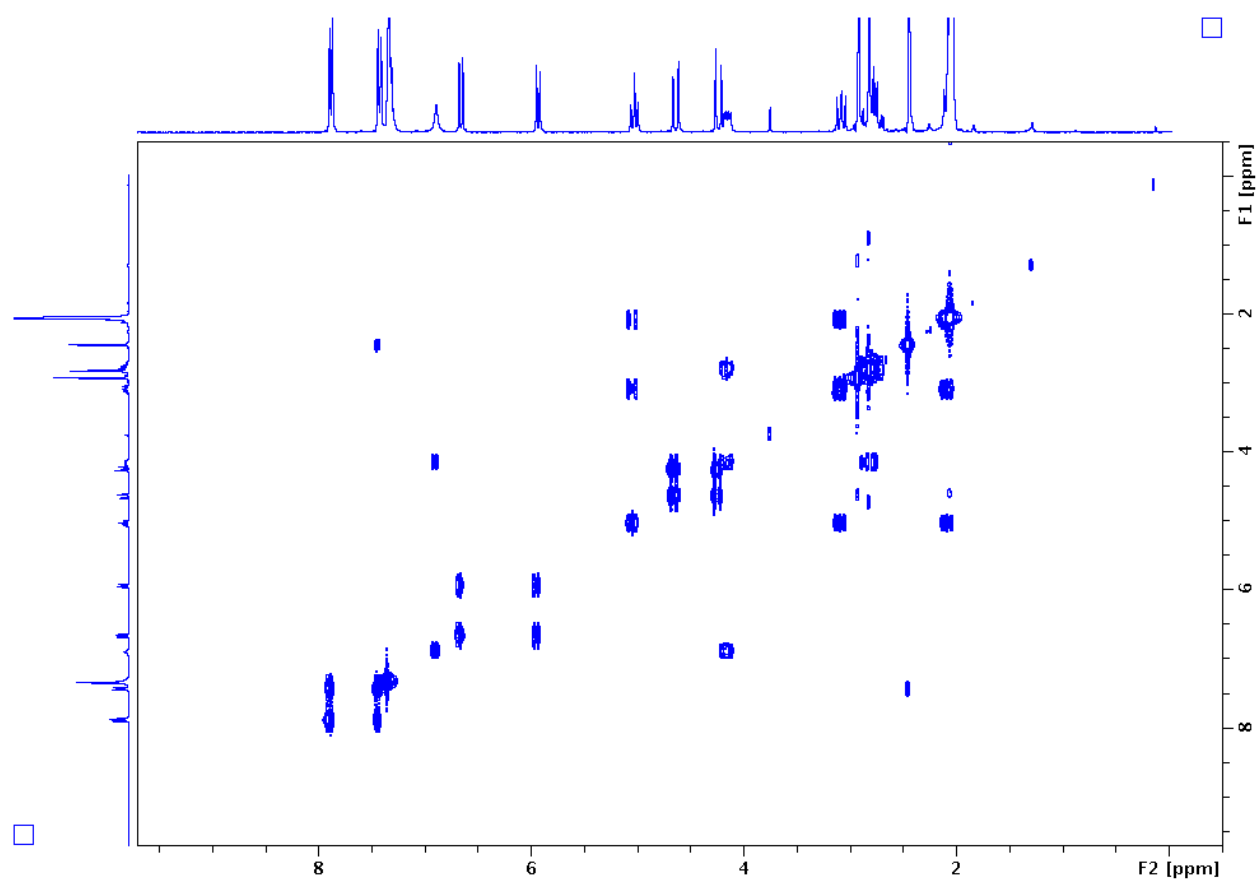
^1H NMR spectrum of **3.18** (300 MHz, acetone- d_6)



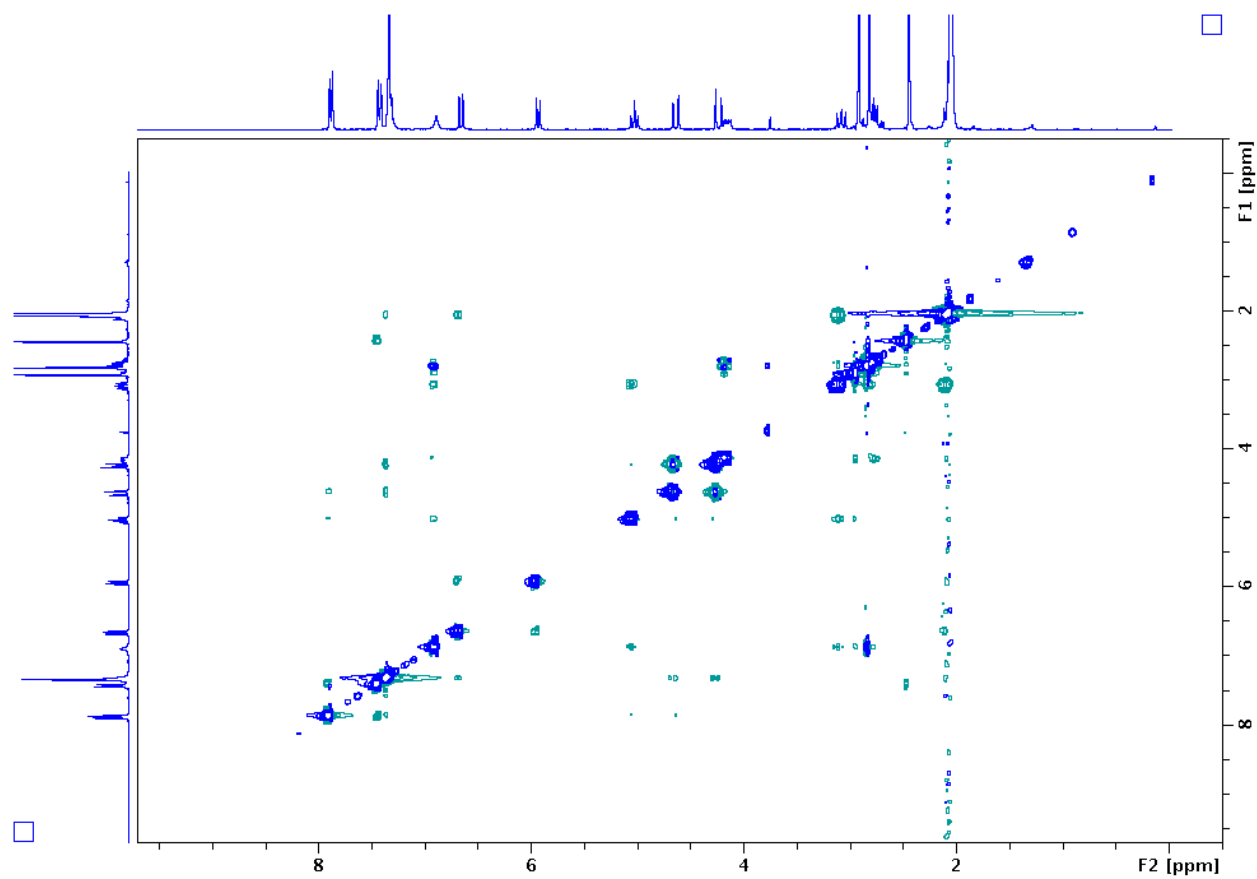
^{13}C NMR spectrum of **3.18** (75 MHz, acetone- d_6)



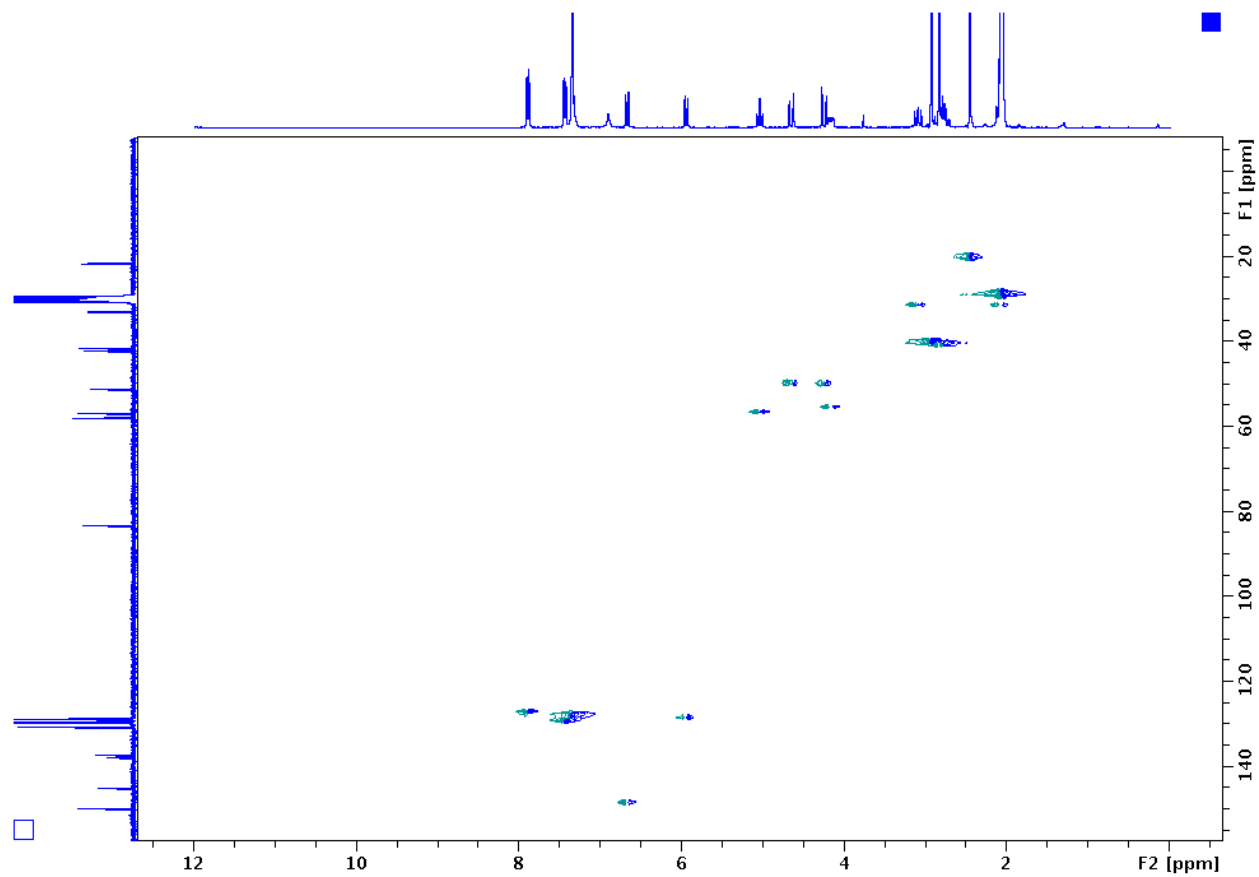
COSY spectrum of **3.18** (acetone- d_6)



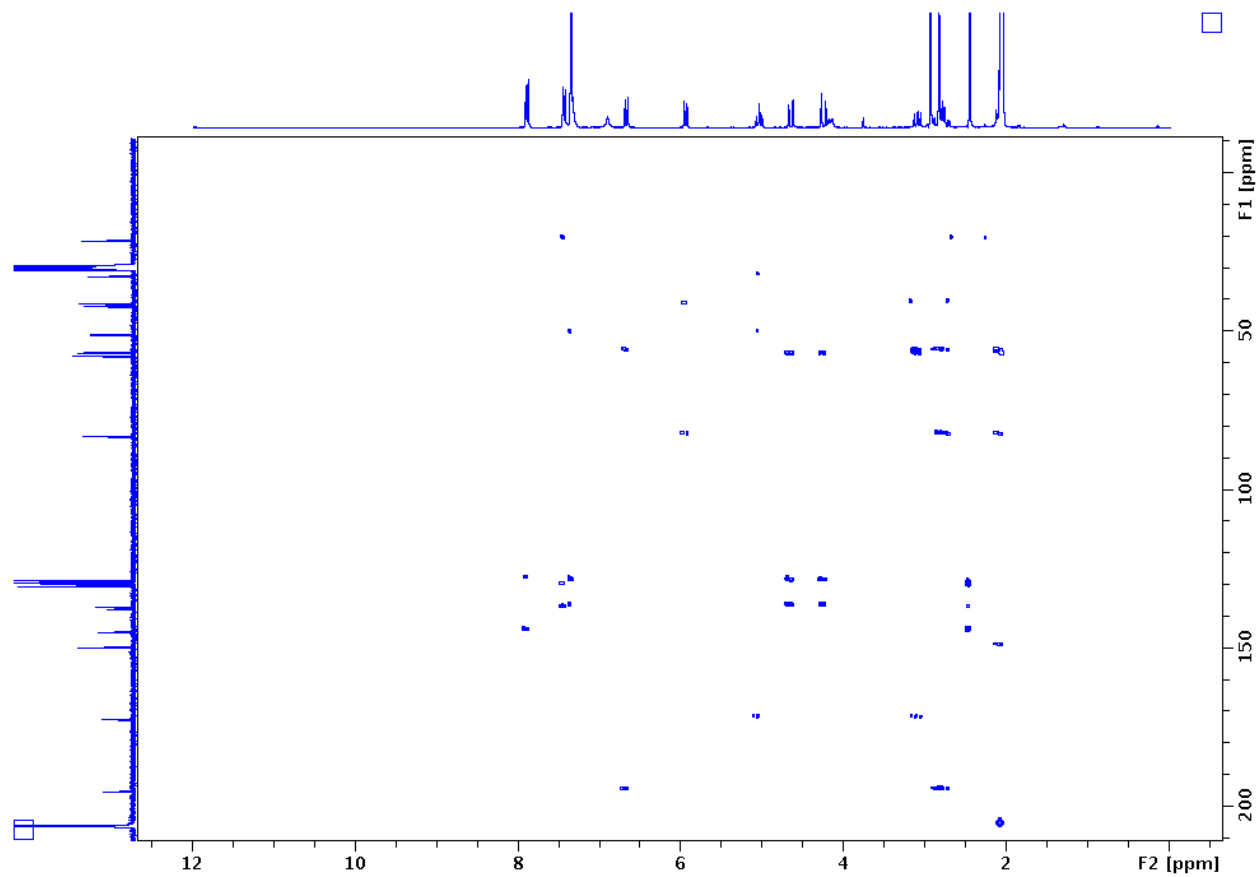
NOESY spectrum of **3.18** (acetone- d_6)



HSQC spectrum of **3.18** (acetone- d_6)

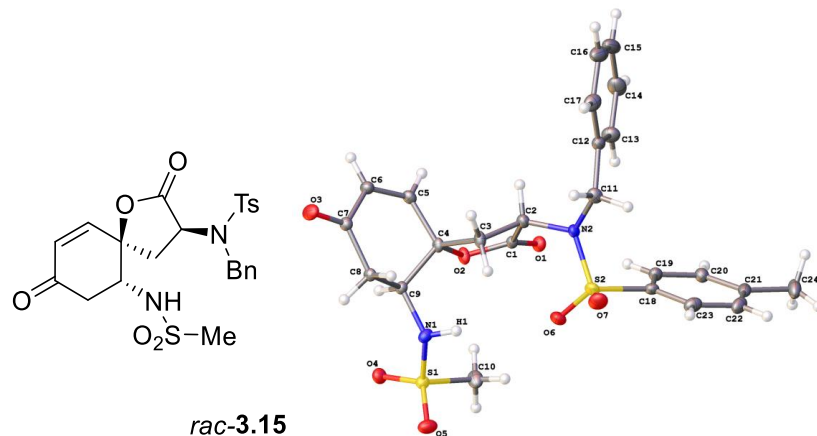


HMBC spectrum of **3.18** (acetone- d_6)



Appendix C: X-ray Diffractory Data

C.1. X-ray data for compound **3.18**



EXPERIMENTAL DETAILS

A. Crystal Data

| | |
|-----------------------|---|
| Empirical Formula | C ₂₄ H ₂₆ N ₂ O ₇ S ₂ |
| Formula Weight | 518.59 |
| Crystal Colour, Habit | colourless, tablet |
| Crystal Dimensions | 0.20 x 0.26 x 0.53 mm |
| Crystal System | monoclinic |
| Lattice Type | Primitive |
| Lattice Parameters | $a = 10.7280(7) \text{ \AA}$ $b = 22.4745(16) \text{ \AA}$ $c = 10.6430(7) \text{ \AA}$ |

| | |
|--------------------------|-------------------------------|
| | $\alpha = 90^{\circ}$ |
| | $\beta = 111.33(1)^{\circ}$ |
| | $\gamma = 90^{\circ}$ |
| | $V = 2390.4(3) \text{ \AA}^3$ |
| Space Group | $P 2_1/c$ (#14) |
| Z value | 4 |
| D_{calc} | 1.441 g/cm ³ |
| F000 | 1088.00 |
| $\mu(\text{Mo-K}\alpha)$ | 2.72 cm ⁻¹ |

Data Block

Bond precision: C-C = 0.0032 Å Wavelength=0.71073

Cell: a=10.7280(7) b=22.4745(16) c=10.6430(7) alpha=90 beta=111.327(1)
 gamma=90

Temperature: 90 K

| | Calculated | Reported |
|-------------|------------|---------------|
| Volume | 2390.4(3) | 2390.4(3) |
| Space group | $P 2_1/c$ | $P 1 2_1/c 1$ |
| Hall group | -P 2ybc | -P 2ybc |

| | | |
|------------------------|------------------|------------------|
| Moiety formula | C24 H26 N2 O7 S2 | C24 H26 N2 O7 S2 |
| Sum formula | C24 H26 N2 O7 S2 | C24 H26 N2 O7 S2 |
| Mr | 518.59 | 518.59 |
| Dx,g cm ⁻³ | 1.441 | 1.441 |
| Z | 4 | 4 |
| Mu (mm ⁻¹) | 0.272 | 0.272 |
| F000 | 1088.0 | 1088.0 |
| F000' | 1089.52 | |
| h,k,lmax | 15,31,14 | 15,31,14 |
| Nref | 6983 | 6978 |
| Tmin,Tmax | 0.919,0.947 | 0.874,0.947 |
| Tmin' | 0.866 | |

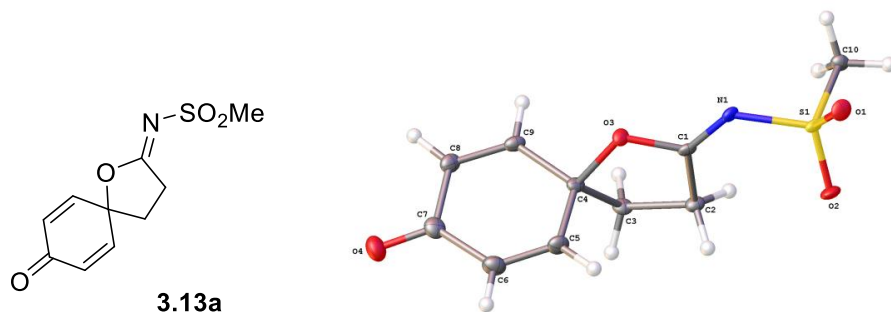
Correction method= # Reported T Limits: Tmin=0.874 Tmax=0.947 AbsCorr = MULTI-SCAN

Data completeness= 0.999 Theta(max)= 30.042

R(reflections)= 0.0605(6467) wR2(reflections)= 0.1479(6978)

S = 1.173 Npar= 322

C.2. X-ray data for compound 3.13a



EXPERIMENTAL DETAILS

Crystal Data

| | |
|-----------------------|--|
| Empirical Formula | C ₁₀ H ₁₁ NO ₄ S |
| Formula Weight | 241.26 |
| Crystal Colour, Habit | colourless, plate |
| Crystal Dimensions | 0.02 x 0.25 x 0.30 mm |
| Crystal System | monoclinic |
| Lattice Type | primitive |
| Lattice Parameters | $a = 19.330(5) \text{ \AA}$ $b = 5.2843(12) \text{ \AA}$ $c = 10.401(2) \text{ \AA}$ $\alpha = 90^\circ$ $\beta = 99.839(5)^\circ$ $\gamma = 90^\circ$ $V = 1046.8(4) \text{ \AA}^3$ |

| | |
|--------------------------|-------------------------|
| Space Group | $P 2_1/c$ (#14) |
| Z value | 4 |
| D _{calc} | 1.531 g/cm ³ |
| F ₀₀₀ | 504.00 |
| $\mu(\text{Mo-K}\alpha)$ | 3.07 cm ⁻¹ |

Data Block

| | | |
|-------------------------------------|---|----------------|
| Bond precision: C-C = 0.0038 Å | Wavelength=0.71073 | |
| Cell: a=19.330(5) beta=99.839(5) | b=5.2843(12) c=10.401(2) alpha=90 gamma=90 | |
| Temperature: 90 K | | |
| | Calculated | Reported |
| Volume | 1046.8(4) | 1046.8(4) |
| Space group | P 21/c | P 1 21/c 1 |
| Hall group | -P 2ybc | -P 2ybc |
| Moiety formula | C10 H11 N O4 S | C10 H11 N O4 S |
| Sum formula | C10 H11 N O4 S | C10 H11 N O4 S |
| Mr | 241.26 | 241.26 |
| D _x , g cm ⁻³ | 1.531 | 1.531 |
| Z | 4 | 4 |
| Mu (mm ⁻¹) | 0.307 | 0.307 |

| | | |
|-----------|-------------|-------------|
| F000 | 504.0 | 504.0 |
| F000' | 504.76 | |
| h,k,lmax | 27,7,14 | 27,7,14 |
| Nref | 3087 | 2969 |
| Tmin,Tmax | 0.912,0.994 | 0.623,0.994 |
| Tmin' | 0.912 | |

Correction method= # Reported T Limits: Tmin=0.623 Tmax=0.994 AbsCorr =MULTI-SCAN

Data completeness= 0.962

Theta(max)= 30.082

R(reflections)= 0.0489(2674)

wR2(reflections)= 0.1273(2969)

S = 1.045

Npar= 147